

Diss. ETH No. 15635

Optimal Utilization of a Non-Renewable Transboundary Groundwater Resource – Methodology, Case Study and Policy Implications

A dissertation submitted to the
SWISS FEDERAL INSTITUTE OF TECHNOLOGY
ZÜRICH

for the degree of
Doctor of Natural Sciences

presented by

Tobias Ulrich Siegfried

Dipl. Natw. ETH, MSc
born on September, 16 1970
citizen of Zürich

accepted on the recommendation of

Prof. Dr. Wolfgang Kinzelbach, examiner
Prof. Dr. Rolf Kappel, co-examiner

2004

Acknowledgement

First and foremost, I would like to thank my supervisor, Wolfgang Kinzelbach, for giving me the opportunity to work for four years on such an exciting project at the Institute of Hydromechanics and Water Resources Management (IHW), ETHZ. The many inspirations he gave me were invaluable. Furthermore, his generosity enabled me to travel extensively in Northern Africa so as to gain first hand experience in the region, of its problems, its people and culture. I would also like to thank Rolf Kappel for his willingness to be my co-supervisor. His ability to formulate succinct questions helped me to focus on the relevant topics. I am grateful to the Alliance for Global Sustainability (AGS) for partial funding of this work.

All of this could never have materialized without the help of a multitude of people. Most importantly, I would like to mention our North African partners. They enabled us access to important data, critically reviewed our work from their perspective of much greater experience with regard to local resource knowledge and management problems and always welcomed us with great hospitality. Above all, I would like to thank Mounira Zammouri from whom I could learn a great deal about the North–West Sahara Aquifer system as well as the Nefzawa oases. Also, she convinced me that the best Couscous in the world is prepared by her. Together with her student, Samiha Kriaa and Tobias El Fahem, an excellent Diploma student at our Institute, we were able to solve parts of the groundwater salination riddle of the Nefzawa oases.

The professional experience from the people of the Tunisian DGRE – General Director D. El Batti, Mr. Ben Baccar, Madame Y. Ben Salah, Madame F. Horriche and Mr. R. Khanfir – was of utmost importance to my research. Similarly, the many discussions with the staff from the SASS/OSS organization in Tunis, i.e. General Director Chedli Fezzani, Mr. D. Latrech, Mr. A. Mamou, inspired me a lot. The same holds true with regard to our Algerian and Libyan partners, General Director R. Taibi, Madame F. Biout, Mr. A. Larbez all from the ANRH in Algier and General Director O. Salem, Mr. A. Douma, Mr. L. Madi from the GWH in Tripolis. I would also like to thank Mr. M. Matoussi and his colleague Mr. M. Belloumi as well as Mr. F. Meddeb for their help in the setup of the socio-economic questionnaires, the time-consuming data collection all over the Nefzawa oases and the critical reviewing of the obtained econometric results. Finally, I learned from Pierre Combes and Philippe Pallas that one should spend a lifetime traveling in the Sahara.

During my work at the IHW, I supervised three Diploma and five semester work students. C. Abegglen, L. Beck (twice), T. El Fahem, S. Haag, F. Meddeb, D. Rutz and C. Schoch all contributed to a greater or lesser extent to this work. I am grateful for their assistance.

Chunmiao Zheng was the first to bring me into contact with single-objective evolutionary algorithms. It was for Eckart Zitzler, Marco Laumanns and Stefan Bleuler from the Computer Engineering and Networks Laboratory at ETHZ to introduce me to the exiting field of multi-objective evolutionary algorithms. Without all their help on this topic, this work would never have become what it is now.

Special thanks go to Harrie–Jan Hendriks Franssen for reading through the first, truly messy draft of this thesis. The critical comments by Peter Bauer were immensely helpful. Heiko Specking was kind enough to provide additional feedback. One thing for sure, all of their remarks helped to greatly improve the quality of this work.

Last but not least, I am indebted to all present and former members of the IHW who I know and with whom I could spend a truly inspiring time.

Contents

Acknowledgement	I
Glossary	V
Abstract	VII
1 Introduction	1
1.1 General Overview	1
1.2 Aspects of Transboundary Groundwater Management	5
1.3 Motivation for the Study	10
2 Case Study: The Nefzawa Oases	13
2.1 Introduction	13
2.2 Agricultural Production in the Nefzawa Oases	16
2.2.1 Data Collection	16
2.2.2 Descriptive Data Analysis	18
2.2.3 Estimation of a Stochastic Frontier Production Function - Empirical Model Formulation	19
2.2.4 Empirical Results	21
2.3 Salination as a Threat to Agricultural Production	23
2.3.1 Introduction	23
2.3.2 Geology of the Nefzawa Oases	24
2.3.3 The Terminal Complex Hydrochemistry and its Evolution in the Nefzawa Oases	26
2.3.4 Determination of the Salination Origins	32
2.3.5 Groundwater Flow Model	36
2.3.6 Transport Model	38
2.3.7 Future Development	41
2.4 Conclusion	43
3 Regional-Scale Simulation Optimization Approach	45
3.1 Introduction	45
3.2 NWSAS Finite-Difference Aquifer Model	46
3.3 Optimization Formulation and Methodology	50
3.4 Sensitivity Analysis	52
3.5 Results	54
4 Multi-Objective Groundwater Management Model	57
4.1 Introduction	57
4.2 Determinants of Spatial Allocation Patterns	60

4.3	Model Formulation	65
4.4	Optimization Method	67
4.5	Model Components	70
4.5.1	General Algorithmic Structure	70
4.5.2	Network Clustering	70
4.5.3	Cost Calculation	79
4.5.4	Variation - Mutation	81
4.5.5	Variation - Crossing Over	82
4.5.6	Adaptive Pumping Heuristics	83
5	Optimization Results	87
5.1	Sample Optimization Run	87
5.2	NWSAS Allocation Optimization	93
5.2.1	Description of Strategies	93
5.2.2	Optimization results	94
5.3	Areas of Future Research	103
6	Conclusions	105
A	Stochastic Frontier Production Function Estimation	109
A.1	FRONTIER 4.1c Input Data File	109
A.2	FRONTIER 4.1c Output File	115
	Bibliography	121
	Curriculum vitae	129

Glossary

Abbreviations

ANRH	National Hydraulic Resources Agency, Algeria
CRDA	Regional Commissariat for Agricultural Development, Tunisia
DGRE	General Direction of Water Resources, Tunisia
FAO	Food and Agricultural Organization
GIC	Irrigation collectif of farmers
GWA	General Water Authority, Libya
IAH	International Association of Hydrogeologists
IC	Intercalary Continental Aquifer
ISARM	Internationally Shared Aquifer Resources Management
NWSAS	North–West Sahara Aquifer System
OSS	Sahara and Sahel Observatory
SASS	NWSAS subdivision of the Sahara and Sahel Observatory
TC	Terminal Complex Aquifer
UNECE	United Nations Economic Commission for Europe
UNESCO	United Nations Educational, Scientific and Cultural Organization

Abstract

The North-West Sahara Aquifer System (NWSAS) is one of the largest groundwater systems of the world. It consists of two main aquifers, the Terminal Complex (TC) and the underlying Intercalary Continental (IC), and covers in total an area of more than 10^6 km². Present day recharge is approximately 30 m³/s and only of local importance in the Saharan Atlas. The natural system is draining into the topographic lows of the endorheic basin, the Chotts. It is used as a resource by three countries, Algeria, Tunisia and Libya. The bulk of the water pumped from the system is utilized for the irrigation of approximately 14'000 km² of agricultural land. The present situation can be characterized as fossil groundwater mining, the total abstraction being 80 m³/s.

While the stored amount of water would be able to sustain this abstraction for another 10'000 years, the water comes at a price. On one hand there is the cost of pumping and the investment for wells and pipelines. On the other hand the cones of depression created by the pumping lead to a deterioration of the water quality due to attraction of saline waters from different sources such as the brine of the Chotts, the saline water of the underlying Turonian and the seawater of the Mediterranean. In order to avert excessive prices for water and deterioration of the resource on the whole, a common management scheme for the three countries has to be found. In an effort towards such a scheme, a mathematical model of the NWSAS was developed. It is a groundwater flow model on the basis of a finite difference method. The model demonstrates that with the required total pumping rate by 2050 large areas of the presently strongly pumped regions will face a piezometric decline with economically infeasible drawdowns of more than 200 m below ground level.

A redistribution of the pumped quantity so as to minimize water provision costs seems interesting to explore. For that purpose, the groundwater model was coupled with optimization algorithms to find allocation patterns that conform to demand, drawdown and quality constraints in time while minimizing overall provision costs. The wells in an optimal scheme spread out over the area to equilibrate distribution cost with pumping cost, which depends on drawdown. They further spread to the IC from the TC and the pumping scheduling is characterized by oscillation between wellfields. The results demonstrate among other things that cooperating in devising internationally coordinated pumping schemes is advantageous for the three countries.

Besides the global management task for the whole basin a number of subproblems on a more local scale arise. For that purpose, the Nefzawa oases region is studied. Over the last fifty years, the pumped quantity in the Nefzawa has been increased six-fold while the irrigated area tripled. As a consequence, the salinity of pumped water has increased locally to unacceptable values. An econometric estimation of the farm-level technical inefficiencies in agricultural production revealed that the farmers in

the Nefzawa produce well below their potential agricultural output. Governmentally induced educational measures could allow to increase production without further increasing the amount of irrigation water applied.

To study salination, a detailed flow and transport model embedded in the regional NWSAS model has been developed. It was shown, that agricultural drainage waters that are highly enriched in TDS pollute the TC aquifer by leaching in cases where the confining unit of the TC shows structural weakness. Such drainage typically is channeled from the oases to nearby local terrain depressions. It seems crucial to improve the management of this drainage network so as to prevent further salination of the TC aquifer.

Kurzfassung

Die vorliegende Dissertationsarbeit untersucht Aspekte der optimalen Nutzung nicht-erneuerbarer Grundwasserressourcen am Beispiel des Nord-West Sahara Aquifer Systems (NWSAS). Die zwei dazugehörigen Grundwasserleiter, i.e. der Complexe Terminal (TC) und der unterliegende Continental Intercalaire (IC), bedecken eine Fläche von mehr als 10^6 km² und werden von Algerien, Tunesien und Libyen genutzt. Das geförderte Wasser wird grösstenteils zur Bewässerung der Oasen verwendet. In den drei Ländern wurden im Jahre 2000 auf einer Fläche von 14'000 km² Landwirtschaft betrieben. Aufgrund der grossen Menge an gespeichertem Grundwasser kann selbst unter stark steigender Nachfrage in den kommenden Jahrhunderten fossiles Wasser gepumpt werden. Jedoch werden dessen Gesteungskosten ständig steigen. Dafür verantwortlich ist einerseits die stetig steigende Fördertiefe, aus welcher das Grundwasser gepumpt werden muss. Andererseits kann das Abpumpen lokal zur Mobilisierung von Salzquellen führen und dadurch das gepumpte Grundwasser verschmutzt werden. Die Untersuchung von optimalen Strategien der künftigen Nutzung zur Verhinderung einer extensiven Preisentwicklung ist Gegenstand dieser Forschungsarbeit.

Zum besseren Verständnis der mit der Übernutzung einhergehenden Probleme wurden die Tunesischen Nefzauoa Oasen in einer Fallstudie untersucht. In diesem Gebiet wurde im Verlauf der letzten 20 Jahre ein starker Anstieg der Salinität des Grundwassers festgestellt. Die Quellen der Versalzung, salzführende Schichten sowie landwirtschaftliche Drainagewässer, konnten mittels Traceranalyse identifiziert werden. Die Ursache der Verschmutzung liegt in der Absenkung des Grundwasserspiegels. Diese wird durch Überlagerung der Auswirkungen lokaler sowie regionaler Bepumpung verursacht. Die Plausibilität dieser Erkenntnisse wurde durch Strömungs- und Transportmodellierung bestätigt. Eine maximale Absenktiefe sowie ein Gradientenkriterium gegenüber Salzquellen wurde als lokale Nutzungsrestriktion einer zukünftig erfolgreichen Grundwasserallokation eruiert. Ferner konnte mittels ökonomischen Untersuchungen der landwirtschaftlichen Produktivität gezeigt werden, dass die private, unregulierte Grundwassernutzung nur bedingt zu diesem Zweck beitragen kann. Optimale Allokationsstrategien sollten auf einer Koordination der Pumpaktivität, lokal sowie regional resp. international, beruhen.

Ein regionales Finite-Differenzen-Modell des NWSAS wurde zur Untersuchung dieser Strategien erstellt. Das Modell wurde mittels verfügbaren Zeitreihen von Piezometerhöhen sowie Quellschüttungen geeicht. Eine spezielle downscaling Methode wurde verwendet, um die eigentlichen Piezometerhöhen in den Absenktrichtern zu approximieren. Dieses räumliche Ressourcenmodell wurde im Folgenden mit Optimierungsalgorithmen gekoppelt. Unter der Annahme einer vorgeschriebenen Nachfrage der drei Länder, wurde die mit einer Allokation verbundene, diskontierte Kostensumme als Gütekriterium verwendet. Die Kosten ergeben sich aus der räum-

lichen und zeitlichen Erstellung der Pump- und Überlandleitungsinfrastruktur und hängen zudem von Fördertiefe und Energiepreisen ab. Lineare Optimierung bei vorgegebenen Pumpstellen und exogener Gesamtnachfrage wurde zur Identifikation einer eindeutigen, optimalen Strategie verwendet. Diese Lösung des Managementproblems ist jedoch nur beschränkt den drei Ländern kommunizierbar, da kein Raum für Verhandlungen besteht. Zudem sind die Annahmen, welche zur erfolgreichen linearen Optimierung getroffen werden müssen, übermäßig restriktiv.

Um diese Mängel zu beheben, wurde in einem zweiten Schritt eine neuartige, stochastische Mehrziel-Optimierungsmethode verwendet. Somit konnte eine Strategie als Zeitreihe von Pumpraten an räumlich unterschiedlichen Orten definiert werden. Zudem wurde eine Heuristik entwickelt, die Ort, Anzahl und Fördermenge der Pumpstellen regelt, so dass räumlich verteilten Absenk- sowie Gradientenkriterien nicht verletzt werden. Im Gegensatz zur gradienten-basierten Optimierung, wird bei der verwendeten Methode eine Familie von Lösungen iterativ ermittelt, für welche keine besseren Lösungen im Pareto-Sinne gefunden werden. Als stochastische Operatoren wurden Rekombinations- und Mutationsalgorithmen entwickelt.

Die Optimierungsmethode wurde in einem ersten Schritt anhand eines synthetischen Managementproblems getestet. Dessen Lösung zeigt, dass rationale Entscheidungsträger im nicht-kooperativen Fall Anreiz haben, egoistische Strategien der Grundwassernutzung zu verfolgen und sich Altruismus nicht auszahlt. Wendet man die Optimierung jedoch auf den institutionell-kooperativen Fall an, kann gezeigt werden, dass sich kooperative Strategien durch generell geringere Kostenfolgen auszeichnen. Jeder rationale Entscheidungsträger sollte folglich Anreiz haben, internationale Kooperation einer Politik der individuellen Ressourcenausbeutung vorzuziehen.

Die Methode wurde schlussendlich auf das Problem des NWSAS angewandt. Als Zeithorizont der Optimierung wurde 50 Jahre gewählt. Die ermittelten optimalen Strategien zeichnen sich durch verschiedene Merkmale aus. Erstens erscheint internationaler Wassertransfer über den erwähnten Zeithorizont nicht als Notwendigkeit. Zweitens, im Falle des NWSAS bedeutet Kooperation im eigentlichen Sinne Koordination der regionalen, basinweiten Nutzung. Dies erscheint plausibel, wenn man berücksichtigt, dass die einzelnen Länder aufgrund der grossen räumlichen Ausdehnung der Ressource mittels intelligenter Bepumpung über genügend eigene Versorgungsoptionen verfügen. Drittens steht intelligente Bepumpung für eine zeitlich und räumlich oszillierende Belastung der ständig wachsenden Anzahl von Bohrlöchern. Die Identifikation einer solchen Anzahl von Pareto-optimalen Strategien eröffnet den Ländern die Möglichkeit, Verhandlungslösungen zu finden, die - unter Einbehaltung der Nebenbedingungen - kostenminimal sind.

Chapter 1

Introduction

1.1 General Overview

Of the 4'300'000 km² that Algeria, Tunisia and Libya cover together, only 2% receive enough rainfall to sustain agriculture without irrigation. They are located along the coast line which is subject to a moderate Mediterranean climate. More than 80% of the 48.2 million inhabitants of the three countries live within this so-called *green belt*. The remaining, sparsely populated area is under the influence of the arid to hyper-arid Saharan climate which is characterized by very hot summers, extreme diurnal temperature variations and highly irregular precipitation both in time and space. In the desert and on its fringes, economic activity solely relies on production from irrigated agriculture (World Bank, 2002).

All three countries have seen a considerable growth of their economy since independence in the fifties and sixties. Algeria and Libya largely profited from hydrocarbon revenues. In Algeria, oil price fluctuations led to regular political instabilities. Although political struggle is ongoing with respect to Berber unrest and islamic fundamentalism and unemployment remains high (27% of active workforce in 2001), the country has seen accelerated economic performance over the last years. From 1999 to 2003, real GDP grew by 3.8% a year, on average, essentially led by the oil sector performance, which grew by 4.3% during the same period. The non—hydrocarbon / non-agricultural sector grew by 3.3%, led by a strong 5% real growth in value added from private manufacturing industries. In 2003 alone, GDP growth reached 6.8%, the highest rate in the last five years, on account of higher oil production and an extraordinarily good agricultural output performance related to good weather (US Federal Research Division, Library of Congress, 1993; World Bank, 2002; CIA, 2003).

When Col. Qadhafi took power in a 1969 military coup, he established his own political system in Libya – a combination of socialism and Islam – which he calls the Third International Theory. Viewing himself as a revolutionary leader, he used oil funds during the 1970s and 1980s to promote his ideology outside Libya. Libya nowadays is moving through a variety of economic reforms and a reduction in the state's direct role in the economy. In June 2003, President Qadhafi said that the country's public sector had failed and should be abolished, and called for privatization of the country's oil sector, in addition to other areas of the economy. Oil export revenues, which account for over 95% of Libya's hard currency earnings, were hurt severely by the dramatic decline in oil prices during 1998, as well as by reduced oil exports and production as a result of US and UN sanctions. Those sanctions were imposed on Libya in 1992 due to the country's support for terrorism. UN sanctions

were suspended in 1999 whereas the US stopped sanctioning the country as of 2004. With higher oil prices since 1999, oil export revenues have helped to improve Libya's fiscal situation significantly. Although infrastructure remains generally poor in the country, oil revenues helped to finance huge public works programmes such as the *Great Man made River*-project, which provides the coast with fossil groundwater used for irrigation, industrial and municipal purposes. Similarly to Algeria, the country remains vulnerable to oil price fluctuations (US Federal Research Division, 1986; World Bank, 2002; CIA, 2003).

Since independence in 1956, Tunisia has seen political stability under its first elected president, Habib Bourguiba. Bourguiba maintained a pro-Western foreign policy trying to eradicate Islamic fundamentalist movements. In 1987, the aged Bourguiba was removed from power in a bloodless coup and was succeeded by General Zine al-Abidine Ben Ali. Tunisia's economy continued to improve throughout the nineties, making the country one of the most attractive in Africa for foreign investors and tourism. Tunisia has pursued a strategy of equitable development and has registered steady long-term development progress. From 1970–2001, real per capita income grew from 700\$ to 2070\$, while poverty has declined from 40% to 10% for Tunisia's 2001 population of 9.7 million. Over the same time horizon, life expectancy jumped from 50 to 72 years. As of 2001, 98 % of children were enrolled in primary school. In addition, the status of women has improved considerably, and today women comprise one-third of the labor force. Unemployment, however, has remained relatively high at about 15% of the labor force and is generally more pronounced in rural areas. The four year drought which ended in 2003, has brought agricultural production to a record low and greatly affected the export sector's performance (World Bank, 2002; CIA, 2003).

Agricultural policy in Algeria, Tunisia and Libya, in the last fifty years was largely determined by considerations of food security, self-sufficiency and import substitution practices (Pérennès, 1993). Due to ongoing border disputes with the neighboring countries, special consideration was given to the desert population. Irrigated agriculture as backbone of the population living in the countries vast desert stretches, was governmentally promoted. From 1950 to 2000 in the three countries, the irrigated area in the Saharan environment has tripled proportionally to the development of the population. In the year 2000, it extended over an area of more than 14'000km². This extension was made possible by technological transition, i.e. the gradual progression from traditional groundwater abstraction by hand dug wells or springs to high volume abstraction by motor pumps and deep artesian wells.

Water for desert irrigation is pumped from two aquifers, the Intercalary Continental (IC) and the Terminal Complex (TC), that constitute together one of the largest groundwater systems in the world – the North West Sahara Aquifer System (NWSAS). Extensive knowledge of the Algerian and Tunisian part of the system was obtained for the first time 1972 within the scope of an international resource assessment study coordinated by the UNESCO (UNESCO, 1972). Figure 1.1 shows a map outlining the aquifer system boundaries. A cross section through the system



Figure 1.1: Extension of the NWSAS (red line). The water budget as of the year 2000 is indicated by the estimated fluxes. The dashed line shows the location of the cross section as portrayed by Figure 1.2.

is provided in Figure 1.2. Water abstraction has increased more than fivefold over the last 50 years, from an estimated $15 \text{ m}^3/\text{s}$ in 1950 to approximately $80 \text{ m}^3/\text{s}$ in the year 2000 ($48 \text{ m}^3/\text{s}$ in Algeria, $17 \text{ m}^3/\text{s}$ in Tunisia and $15 \text{ m}^3/\text{s}$ in Libya). More than 90% of that quantity pumped is consumptively used for irrigation. Mainly due to these measures, Algeria and Tunisia increased their share of total agricultural output as percentage of total GDP from a marginal 2% in the sixties to more than 15% at the turn of the century. In Libya, it accounted for 5% of the total GDP during the nineties (FAOSTAT, 2004).

The TC and IC aquifers of the NWSAS are sedimentary aquifers separated by a complex sequence of clay-rich, semi-pervious layers of the Cenomanian. The structures were formed by clastic and then carbonate depositions that occurred throughout the Cretaceous over much of central North Africa. Both subterranean reservoirs were filled with freshwater during the wet Quaternary Period. The IC and the TC are continuous between Algeria, Libya and Tunisia covering an area of more than 10^6 km^2 (Mamou & Hlaimi, 1999). Recent recharge to the system has been recognized in both aquifers, the bulk of it taking place south of the Saharan Atlas in Algeria

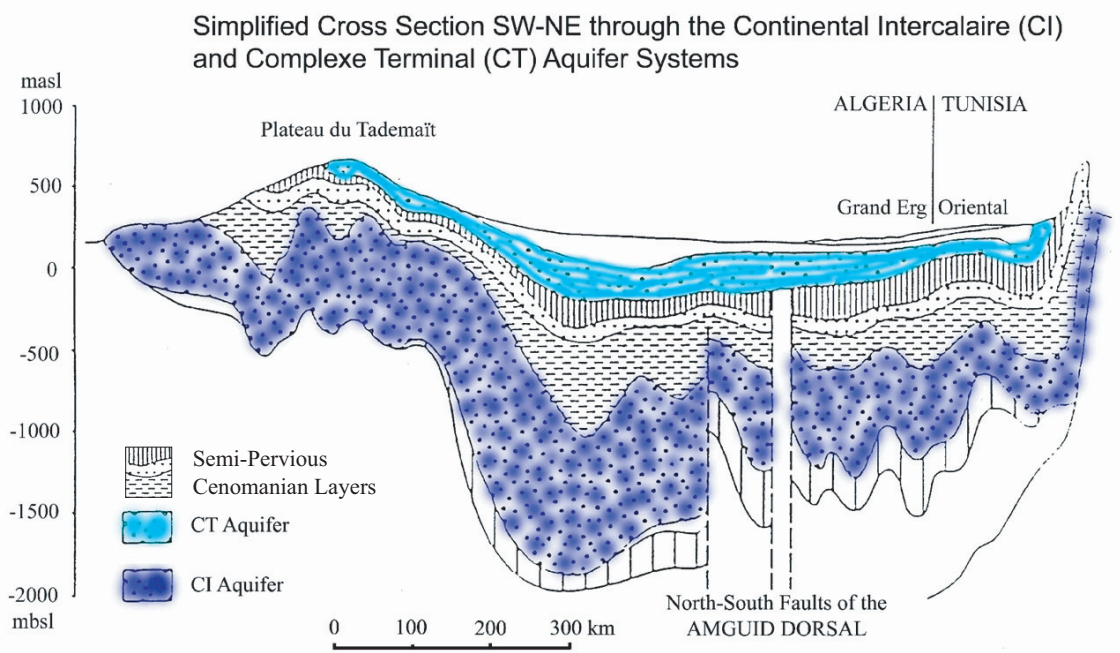


Figure 1.2: North–West to South–East cross section through the NWSAS (Sahara and Sahel Observatory, 2000).

as well as in the Dahar Mountains in Tunisia (Edmunds *et al.*, 1997). Those fluxes, estimated at approximately $30 \text{ m}^3/\text{s}$, are of some importance in the recharge areas with regard to local resource management. However, they are negligible on a basin wide scale considering the enormous size of the resources stored in relation to the limited spatial extension of the recharge zones.

The NWSAS is mined, its stock is being run down, by an abstraction which is much larger than recharge. Yet, a simple *back of the envelope* calculation shows that the NWSAS constitutes a resource for exploitative use for many centuries to come. Under the assumption that 10% of the estimated 10^5 km^3 water stored in the NWSAS can be extracted in a technically and economically feasible way, reserves will last for more than half a millennium assuming a further six-fold increase of abstraction up to a total of $500 \text{ m}^3/\text{s}$. On quantitative grounds, the reliance of irrigated agriculture on NWSAS groundwater is not threatened. However, pursuing for this reason purely exploitative strategies is a fallacy, since the rise of marginal extraction costs above an economic limit will cause economic exhaustion long before physical exhaustion. This decrease of the ratio of resource to capital employed is mainly due to the end of artesian conditions over parts of the basin. Furthermore, a steady increase of salinity has been observed since the 1970s in highly exploited regions such as in the region of El Oued and the Djerid and Nefzawa Oases. Where boreholes deliver saline groundwater which is no longer suitable for irrigation purposes, a relocation of the pumping sites will be necessary (Sahara and Sahel Observatory, 2002). There exists thus a clear incentive for the countries to explore management

strategies that prevent local resource degradation.

Water related legislation in Algeria and Tunisia is largely based on laws introduced by the colonial forces in the first half of the twentieth century and has been continuously developed in response to emerging needs and dangers of growing exploitation. Contrary to that, the colonial legislative heritage in Libya was renounced with the 1969 revolution and a new legislation based on the islamic law, the *Shari'ah*, was established. In the three countries, groundwater is state owned. Up to a maximum depth of 50 m, private resource utilization is legal in Tunisia and does not require any formal approval. Otherwise, authorization by the responsible agencies for utilization is necessary (ElBatti, 1996; Salem, 1996; Adoum, 1996).

No trilateral efforts with regard to joint resource management, taking into consideration the transboundary nature of the NWSAS, existed until 1999. A joint NWSAS management program was launched that year under the auspices of the international organization *Observatoire du Sahara et du Sahel* (OSS). The program was supported by all three countries and was one of the first of its kind world-wide. One of the achievements of the program was the compilation of a basin-wide database related to pumping and hydrodynamical data that was made available to all three states. Furthermore, a mathematical model of the system was developed that lets the countries explore different future allocation scenarios and assess their implication upon the state of the resource. Although no binding trilateral treaty on the future management of the common-property resource resulted, the established consultation mechanism may facilitate cooperative and commonly agreed upon management strategies in the time to come.

1.2 Aspects of Transboundary Groundwater Management

With global population growth, world water demand has tripled over the last half-century. In many countries, the sustainable yield of aquifers is exceeded, i.e. abstraction exceeds recharge to groundwater. This leads to falling water tables on a world-wide scale as was observed by Gleick (2002). As an example for such a process, Figure 1.3 shows the vanishing yield of springs in Southern Tunisia (Nezawa and Djerid Oases) which were fed by artesian groundwater of the TC aquifer. Yield decreased to zero vanished in the mid-eighties from whereon, water harvesting for free was no longer possible.

Warnings of groundwater shortages due to falling groundwater tables and polluted aquifers have periodically led to calls for urgent management responses. One of the first such attempts was the UN report on "Large Scale Groundwater Development" (United Nations, 1960). The report was a response to the rapidly growing importance and exploitation of groundwater in a period of post-war reconstruction and expansion of irrigated agriculture. More recently, many reports appeared by members of the World Watch and Earth Policy Institute, discussing the problem related to unsustainable aquifer utilization by collecting more anecdotal evidence than hard facts (see for example Brown *et al.* (1998); Postel (1999) and Sampat &

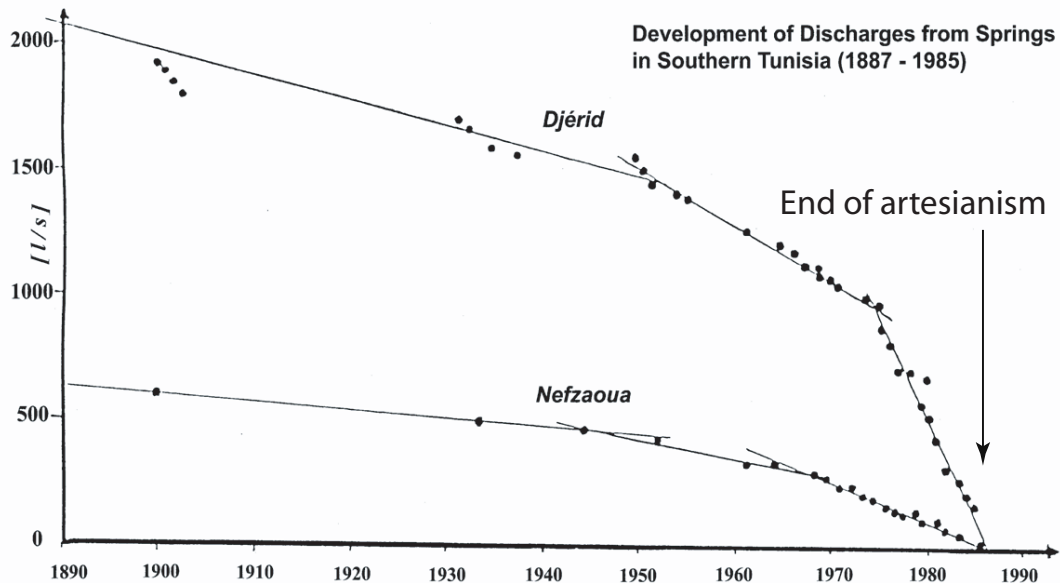


Figure 1.3: During the last century, the yield of springs by the artesian TC groundwater has steadily declined in the Nefzaoua and Djérid Oases in Southern Tunisia due to unsustainable abstraction (Mamou, 1990).

Peterson (2000)). Their main claim is that effectively, governments are satisfying the growing demand for food by overpumping groundwater. This measure virtually assures a drop in food production when the aquifer is depleted. Knowingly or not, governments are creating a *food bubble*–economy, that at some point in the future will burst, unless stabilizing factors help to avert such development. Such factors include an increase in production efficiency by technical change, the recourse to economies of scale and product as well as factor substitution (Stiglitz, 1974).

Studies carried out by the World Bank highlight the importance of the link between resource and management. They promote the engagement in broad-field studies that, apart from the purely technical issues, encompass socio-economic and political aspects as well (see World Bank (1998, 1999)). According to their reasoning, the cause of groundwater resource depletion and degradation is a simple one. Often, development initiatives related to water provision in arid countries have been based on incomplete knowledge of the groundwater resource characteristics and its sustainable yield. The steady supply with groundwater led to a decoupling of the end user from the apparent risk of adequate supply faced under the natural conditions of scarcity in the arid environment. The reliability of storage and conveyance infrastructure and the relative cheapness and flexibility of groundwater exploitation offered by mechanized drilling and pumping has protected the end user and society as a whole from the risk of crop failure due to natural hydrological variability.

Unanimously, the studies mentioned here point to an important fact, namely

that sound management in many countries is not possible due to lacking data and resource knowledge. Most often in a development context, aquifer properties as well as data on pumping history are not known or subject to considerable uncertainty. The difficulties related to the compilation of a trinational database on hydrogeological and pumping data of the NWSAS basin serves as a prime example (Sahara and Sahel Observatory, 2001). The FAO (2003) advocates both, "more informed assessments of the implications of groundwater conditions for food security" and "scientifically found courses of action for managing the resource base". For their advice is generally vague, they point to the need of flexible management that is capable to adaption with the availability of new data or technologies in order to "improve livelihoods while increasing the sustainability of basic groundwater resources". Whatever the improved livelihoods and sustainability *of* basic groundwater resources in this context precisely encompass remains, however, unclear.

Economic theory emphasizes that high rates of non-renewable resource exploitation may be part of a welfare-maximizing program. They are not necessarily incompatible with a development process that is characterized by a sustainable, i.e. non-declining consumption flow. At least, this is so under the assumption of sufficient substitutability between the resource and capital assets (Heal, 1998). In the absence of well defined property-rights however, high rates of resource exploitation may also be related to the presence of externalities and thus reflect economic inefficiency which is generally referred to as allocative inefficiency.

An abundant literature exists that explores such inefficiencies related to groundwater exploitation under differing property regimes - the regulated and unregulated common property (see Koundouri (2004) for an excellent overview). A common-property resource is characterized by the fact, that the *right of exclusion* is assigned to a well defined group (Baland & Platteau, 1996). Unlike in the case of open-access like marine fisheries, this group, e.g. Algeria, Tunisia and Libya in the case of the NWSAS, has the right to exclude non-members from the utilization of the resource. Under the unregulated private profit maximizing approach of common-property utilization, the marginal social user cost is not internalized. In this setting, the level of pumping is determined by the general economic efficiency condition

$$\frac{\partial f_{i,j}(\cdot)}{\partial q_{i,j}} = \frac{\partial g_{i,j}(\cdot)}{\partial q_{i,j}} \quad (1.1)$$

In Equation 1.1, $q_{i,j}$ refers to the pumping rate of the j th user in the i th country. Furthermore, $f_{i,j}(\cdot)$ is a production function that relates factor input, e.g. irrigation water $q_{i,j}$ applied, to return. $g_{i,j}(\cdot)$ the cost function of the (i,j) th user and depends among other things on factor prices as well as the piezometric level $h(t)$ that determines the pumping depth. Contrary to that, the social planner tries to maximize the present value of the net stream of aggregated profits

$$\int_0^{T_{end}} \exp^{-\delta t} \left(\hat{f}(\cdot) - \hat{g}(\cdot) \right) dt \quad (1.2)$$

over the planning horizon T_{end} to achieve an economically efficient outcome of the allocation. The difference $f_{i,j}(\cdot) - g_{i,j}(\cdot)$ is the (i, j) th users net current benefit. $\hat{f}(\cdot)$ and $\hat{g}(\cdot)$ are aggregated benefit and costs functions. Finally, δ is the social discount rate.

Paths of extraction are determined by the prices for that extraction. The ignorance of the additional external social cost in the case of private optimization means that the price for groundwater is too low and abstraction therefore consequently too high. Gisser & Sanchez (1980) for the first time quantified these costs using a bath-tub aquifer for analytical tractability, with transmissivity T being infinite and homogeneous domain properties as well as linear benefit and cost functions.

Gisser & Sanchez (1980) showed that the difference between benefits incurring when the social costs are internalized compared to the competitive approach, where these costs are not fully accounted for, is so small, that it can be ignored for all practical purposes. The authors concluded that this effect will persist if the storage capacity of the aquifer, i.e. the aquifer's area times its storativity, is large and the slope of the demand curve is inelastic. The latter generally holds true for commodities that are essential in production such as water in irrigation. Therefore, the inefficiency of private exploitation cannot be a sole motivation for public intervention. It even seems very likely, that the costs of such intervention would exceed the benefits of the corrective policy and welfare gains effectively become welfare losses.

Similar findings within the framework of Game Theory have been obtained (see Negri (1989); Provencher & Burt (1993); Dockner (2000); Rubio & Casino (2003)). Out of a feasible set of admissible strategies, equilibria strategies are investigated. Such strategies are characterized by the fact that none of the n users has an incentive to deviate from them, given the $n-1$ strategies of the other players. Two kinds of equilibrium strategies exist, i.e. the non-cooperative open-loop Nash equilibrium strategies and the Markov perfect Nash equilibrium strategies. Under the former, each player follows precommitment strategies throughout the game, his pumping $q_i(t)$ solely being time-dependent. The latter implies feedback because each player chooses a strategy that specifies $q_i(h(t), t)$ at time t as a function of piezometric level $h(t)$ and of t itself. Again with the simplifying assumption of the bath-tub aquifer, it was shown that the extraction paths generated by an open-loop Nash equilibrium coincides with the cooperative extraction paths. Contrary to that, players exploiting a common property by following Markov perfect Nash equilibrium strategies are faced with a strategic externality. That is, each player knows that trying to be more conservationist encourages others to extract more. This implies that there is little incentive to be conservationist within such setting. In other words, strategic behavior plays against the efficient exploitation. The basic results of Gisser & Sanchez (1980) of only minor welfare gains over the benchmark solution are recovered since the same physical structure of groundwater has been assumed.

Empirical estimations of the increase of net benefits that result from optimal control policies on aquifers have emerged as response to the work of Gisser & Sanchez (1980). They seemed to confirm the above basic findings (for example Noel *et al.*

(1980); Lee *et al.* (1981); Feinerman & Knapp (1983) and Nieswiadomy (1985)). Estimates ranged between 0.28% to a maximum of 10%.

Worthington *et al.* (1985) were applying the method of dynamic programming to devise an optimal inter-seasonal pattern of groundwater allocation. There, it was first noted that the difference between the two property rights regimes might not be trivial indeed when the lowering of the piezometric head was no longer assumed to be linearly dependent on pumped quantity, the nonlinearity of the provision cost function was introduced and the producers were assumed to have asymmetric demand. The authors of the study computed considerable welfare gains of approximately 30% from regulation compared to the unregulated situation.

Similarly, utilizing a more realistic aquifer model, Brill & Burness (1994) found significant differences between the property regimes once demand is time-dependent and the possibility of a low social discount-rate exists. They too showed that successive refinements of the overly simplistic Gisser-Sanchez model weakens the findings that regulation possesses only minor advantages over non-regulation.

All of the above authors made strong assumptions about the underlying aquifer properties as well as the structure of groundwater demand. Additionally, Gisser & Sanchez (1980) left the terminal value of the piezometric level $h(T_{end})$ free so that the aquifer was essentially bottomless (Brozovic, 2002). Furthermore, all of the approaches discussed above implicitly assume that the spatial placement of wells is irrelevant with regard to mutual influence and that the history of past extractions does not affect present and future extraction decisions. Yet, in reality, the hydraulics of groundwater flow in a confined aquifer is governed by the following equation

$$\frac{\partial}{\partial x} \left(T \frac{\partial h(t)}{\partial x} \right) + \frac{\partial}{\partial y} \left(T \frac{\partial h(t)}{\partial y} \right) + \frac{\partial}{\partial z} \left(T \frac{\partial h(t)}{\partial z} \right) = S \frac{\partial h(t)}{\partial t} \quad (1.3)$$

where $T = f(x, y, z)$, a function in space, is the transmissivity. S is the spatially variable storage coefficient and $h(t)$ the piezometric level at a certain time t and location. Ongoing pumping from a well in an aquifer induces a horizontal hydraulic gradient towards the well. Because of this gradient, a localized cone of depression develops around the well. The dimensions of a cone of depression will depend not only on the pumping rate through time, but also on the hydrogeological variables T and S by which the aquifer is characterized. With ongoing pumping, the drawdown cone expands over the domain and well interference is observed in case of multiple wells.

These effects of well interference and the logarithmic shape of drawdown cones cannot be portrayed by the models discussed above. It seems to be a self-evident result that gains from optimal management are minimal in low transmissivity, high storativity aquifers since these are close to private property to begin with (Figure 1.4). On top of that, such an aquifer least resembles the bath-tub aquifer utilized in standard economic analysis. Figure 1.4 shows schematically the idiosyncratic effects that two groundwater utilisers place upon each other using the Theis-solution to compute drawdowns. In the example, Player 1 is pumping a constant quantity over

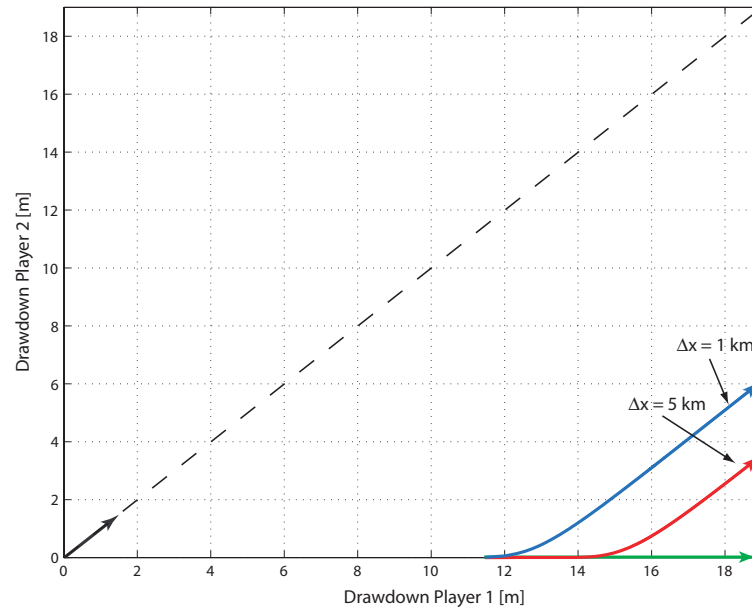


Figure 1.4: Influence of 2 users on each other shown for 2 different configurations of well spacing Δx (red and blue arrowed line). Player 1 is pumping a constant quantity over a certain time horizon. The abscissa shows the aquifer response for player 1 and the ordinate aquifer response for player 2 respectively. Black arrow: aquifer response in high transmissivity T , low storativity S aquifer; green arrow: aquifer response in low transmissivity T , high storativity S aquifer.

a certain time horizon. The time-lag for Player 2 feeling the effect of Player 1 pumping depends on the distance Δx between the two users. This effect vanishes in the case of the bath-tub aquifer since the pressure signal is transmitted over the whole of the basin instantaneously.

1.3 Motivation for the Study

The transboundary aquifer as an unregulated common property does not give the individuals proper incentives to act in an efficient way since such a property system generates externalities. These inefficiencies can be dealt in two ways – either by the establishment of clearly defined private property rights or by regulation. Standard economic theory shows that by the establishment of perfect markets, externalities are internalized. The proposition rests upon strong assumptions, namely that a) enforcement costs of the establishment of these markets are nil, b) the rights are well defined and privatization is complete, c) that the markets are competitive and d) perfect (Baland & Platteau, 1996). International property rights, as in the case of the NWSAS, are clearly established by the nations territory. However, the first two assumptions would also necessitate the division of the resource down to the individual farmer. Clearly, the enforcement costs of such undertaking would be

prohibitive. Assumption c) is problematic too, since wells in arid countries are strategically located from which the owners could conceivably prevent herders or nomadic people gaining access to water and thus create a monopoly. This would again be a classical cause of inefficiency. Finally, the proposition of the presence of perfect water markets rests on the assumption, that they are embedded in an economic environment with perfect markets, anything but far from what actually is found in most of the world's economies.

Independent of the above discussion, there exists at least one strong argument for the planners approach in the allocation of non-renewable groundwater resources. Namely, in the absence of recharge, the resource stock cannot increase. This implies that information obtained over time cannot affect decisions prior to the occurrence of an undesirable, irreversible event (Tsur & Zemel, 1995). Uncertainty in the occurrence of such event therefore has a profound effect on optimal allocation policies.

Imagine, for example, due to coastal proximity, a risk of salination of the groundwater resources exists. The myopic perspective of the individual profit maximizing groundwater user would lead him to achieve a spatial configuration of his wells that does not take into consideration the possible threat from intrusion of saline water. Such a behavior naturally results from incomplete knowledge about possible pollution mechanisms and the resource. Contrary to that, a planner aware of the resource and about the physical processes that possible threaten its productive potential would - most probably - pump groundwater from the hinterland and distribute it to the farmers by charging adequate prices.

The scale of the NWSAS and its properties suggest that undesirable events such as salination threaten the resource locally as well as regionally, but never its entire productive potential. It is for the spatial resource characteristics as well as aspects of distribution and location of economic activity to determine the nature of any optimal allocation pattern. In other words, the success or failure of public or private sector agricultural water provision facilities depends crucially on the locations chosen for those facilities.

In an ideal decision-making process of resource utilization, decisions on regional, national or even supranational scales have to be based on local resource characteristics and the aggregate knowledge about the resource. Quite obvious in the case of the NWSAS, this would imply cooperation of Algeria, Tunisia and Libya. In a second step, such knowledge then is determining the local decisions on the distribution of economic activity. Cooperation and regulation thus seems a prerequisite of groundwater management of a transboundary resource.

So far, transboundary groundwater resources have largely been ignored by international water law that would frame international cooperation within a set of laws and institutional approaches. The 1977 United Nations Water conference recommended the application of the *precautionary principle* in the absence of bilateral or multilateral agreements with regard to the development and management of shared water resources (United Nations, 1977). The *precautionary principle* is codified in international environmental law and includes the obligation not to cause appreciable

harm to the resource. It promotes equitable and reasonable use of the resource and includes a prior notice obligation and the duty to negotiate as well as the polluter pays principle (Freestone & Hey, 1996). In the year 2000, the IAH, UNESCO, FAO and the UNECE launched an international initiative, *ISARM*, to promote the transboundary management of internationally shared groundwater resources and to overcome this apparent neglect in international law. It aims at promoting basin-wide cooperation with regard to transboundary groundwater management. Especially, it should "encourage policy and decision-makers to incorporate appropriate international management practices" based on specific lessons learnt from case studies (Puri *et al.*, 2000).

This thesis aims at the development of a quantitative decision-making tool that evaluates transboundary management practices. If it can be shown that such cooperative management is beneficiary for each of the participants involved, a chance for mutual consent and therefore implementation exists. The structure of the work is as follows. In Chapter 2, inefficiencies of irrigated agriculture are assessed and typical problems related to groundwater abstraction in the Saharan environment discussed. From these findings, principles and constraints of optimal transboundary aquifer management are derived. A finite difference resource model of the NWSAS is consequently developed. It is utilized in a simply constrained linear simulation-optimization approach in Chapter 3 to minimize groundwater provision costs. The resulting unique, globally optimal allocation pattern however leaves no room for negotiation between the stakeholders involved. In fact, for a given *status quo* allocation, there exist many feasible allocation strategies that improve welfare by reducing provision costs of at least one stakeholder involved without harming anyone else. Such strategies are members of the set of *Pareto*-optimal solutions. Furthermore, the options from which decision-makers can choose include the location and relocation as well as the magnitude of pumping in response to water demand, aquifer properties and the development of the piezometric head over time. The costs of such strategies include costs of infrastructure, conveyance and pumping costs in time. The complexity of the aquifer together with existing resource constraints as well as the manifold of management options make it difficult to identify *Pareto*-optimal solutions.

Recent optimization techniques are able to approximate this *Pareto*-optimal set by stochastic sampling of the search space. For this purpose, an advanced simulation-optimization model is presented in Chapter 4. It couples a multi-objective evolutionary algorithm with the aquifer model and a decision-makers heuristics that mimics well relocation in response to constraints. With that, potential benefits from optimal transboundary groundwater management can be assessed. Model results and policy recommendations are finally discussed in Chapter 5.

Chapter 2

Case Study: The Nefzawa Oases

2.1 Introduction

Historically, desert agriculture was only possible in oases where natural spring flow occurred. These oases were the way points of the trading routes for the caravans crossing the Saharan desert (see for example Barth (1986)). One such oasis region are the Nefzawa oases located in Southern Tunisia. Their location within the NWSAS is indicated in Figure 1.1. A detailed map of the region is found in Figure 2.6. These oases are somewhat representative for the whole of the Sahara with regard to agricultural production and emerging problems related to such practice.

The Nefzawa region is famous for the production of the high quality Deglet Nour date. At the turn of the century, Tunisia was selling more than 20'000 metric tons on the world market which accounted for more than half of the total dates export of Africa or 10% of the total Tunisian agricultural export market value (FAO, 2004a). Apart from tourism, agriculture provides the main source of income for the inhabitants of the Tunisian oases.

Agricultural production in the Saharan Oases takes place on three levels (see Figure 2.1). Apart from providing the dates, the palm trees at the top most level give shade that creates a special oasis microclimate. This is characterized by a higher relative humidity and a lower average temperature than the surrounding desert. Not only do the palms reduce solar radiation, they also act as wind breakers (Dollé & Toutain, 1990). On the secondary level, fruit plants such as vines, pomegranates, apricots, olives, etc. are grown. On the primary level, i.e. the ground level, the farmer plants grain, potatoes as well as vegetables (tomatoes, melons, water melons, ...) and animal food such as alfalfa (Meddeb, 2003).

Two forms of oases management exist, communal and private. Communal farmers participate in so called *Groupements d'intérêt collectif* or GIC. They get water and land allocated based on a communal agreement upon the distribution of the resources (see Figure 2.2). Responsibility is handed over to the individuals with regard to the maintenance of the conveying system as well as the periodic cleaning of the drainage channels. The government supports the GICs for example by subsidizing the introduction of recent irrigation technology such as PVC supply tubes or sprinkler irrigation. These GIC were implemented at the beginning of 1990 in order to give farmers more responsibility by enabling low level decentralized decision making within those organizations. By 2000, approximately 100 GICs were operating in the Nefzawa Oases. Contrary to that, private farmers are not served by GIC water. The *Commissariat Régional du Développement Agricole* (CRDA) does not formally approve the drilling of private boreholes nor in any way support these farms.



Figure 2.1: Deglet Nour palm trees in the Douz Oasis. Shortly before their harvest in late October, the dates are protected against potential rainfall.

The bulk of the pumped groundwater from the TC and IC aquifers is used for irrigation. Until 1907, exploitation of the TC was accomplished by utilizing discharge from natural springs to be found in the area of the Nefzawa (see map in Figure 2.6). These springs were fed by artesian water from the TC. The first deep well with artesian outflow was drilled in 1907. From the 1950s onward, the flow from the natural springs diminished because of the continuous lowering of the piezometric level by the installed artesian wells. To prevent shortages in irrigation water, exploitation by pumping from deep wells got more and more common from 1970 on (Mamou & Hlaimi, 1999).

Figure 2.3 shows the water quantities extracted from the TC between 1950 and 2002. The total abstraction increased approximately sevenfold from 1.4 m³/s in 1950 to 10.5 m³/s in 2002. The natural outflow of the springs reached 0.47 m³/s in 1950 and had practically vanished in 1995. Exploitation through pumping was increased from 0.45 m³/s in 1976 to 2.7 m³/s in 2002. The installation of the so-called *illicit* deep wells brought another notable, yet governmentally not approved increase of exploitation. These wells belong to private farmers settling in the vicinity of existing oases. There, they reclaim land and extract water from privately funded wells. Nowadays, exploitation by illicit wells exceeds the officially approved one. It rose from only 25 l/s in 1981 to about 6'000 l/s in 2002.

Over time, the increase of pumping had negative consequences. First, pumped



Figure 2.2: A farmer opens up the furrow so as to water his field. The quantity of water he is allotted per irrigation turn is measured in hours.

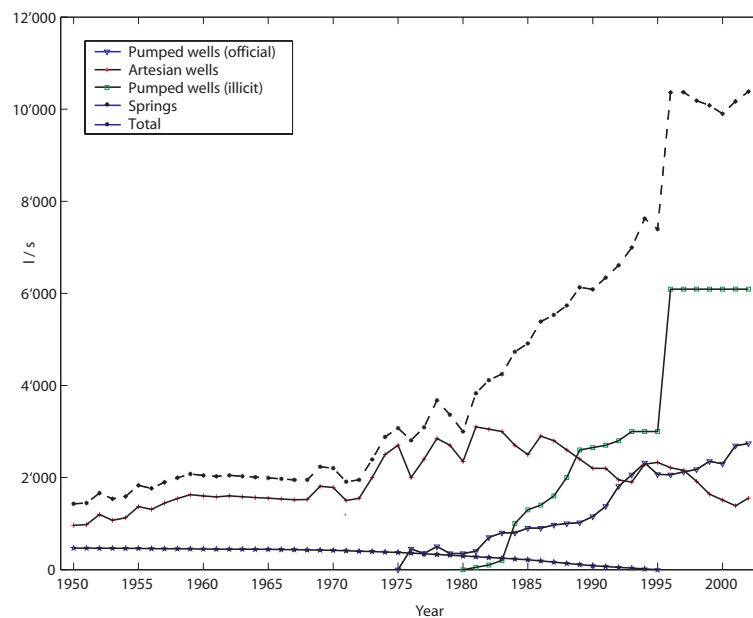


Figure 2.3: Development of TC water abstraction in the Nefzawa (Source: CRDA Kebili).



Figure 2.4: Soil salination at the southern fringe of El Hsay Oasis. The white crusts indicate salt precipitation caused by capillary rise of shallow groundwater.

groundwater quality started to deteriorate with ongoing resource mining. Second, irrigation led to an increase of the shallow groundwater table. In areas of inadequate drainage, capillary rise of groundwater resulted in salt accumulation in the top soil which reduced agricultural yield. The low terrain gradient makes adequate drainage particularly difficult (see Figure 2.4). The question arises whether land and groundwater resource degradation are inevitable consequences of such expansionist development or whether there exist ways to make oases production sustainable. An inquiry into the efficiency of the productive system and the causes of groundwater salination help to answer such questions.

2.2 Agricultural Production in the Nefzawa Oases

2.2.1 Data Collection

In irrigation, two sources of inefficiency can be identified. First, as introduced in Section 1.2 of Chapter 1, inefficiency may arise when farmers do not equalize marginal returns with true factor market prices. The presence of imperfect markets and externalities leads to wrong individual allocation decisions where the input factor mix is not consistent with cost minimization. Applying an insufficient amount of water

is an obvious waste. Contrary to that, the application of too much water tends to impede aeration, leach nutrients, induce greater evaporation, raise the water-table, cause salination and greatly increases the need for and cost of drainage (Hillel, 1994). The second source of inefficiency is the failure of the farmer to produce the greatest possible output from a given set of input quantities. This deviation of the observed input-per-unit-of-output from a so-called unit isoquant is generally referred to as technical inefficiency. It is a measure for the farmers management capability given his resource and capital endowment (Battese, 1992). The unit isoquant defines the input-per-unit-of-output ratios associated with the most efficient output. Such a definition of inefficiency covers situations, where for example a recent sprinkler irrigation system provided to a farmer can be technically inefficient due to lacking knowledge about the handling of such technology.

Many empirical estimates of technical efficiency in irrigated agriculture have proved to be useful (see Battese (1992) for an extensive list). Obviously, for the water resources manager in the semi-arid and arid zones, it is interesting to know how far agricultural production can be expected to increase its output by simply increasing its productive efficiency, without absorbing further resources, given the level of technology involved.

To obtain farmer specific efficiency estimates, cross-sectional data from the Ne-zawa Oases have been collected by random sampling from different oasis during two field campaigns in autumn 2002 and winter 2003. Meddeb (2003) provides a detailed description of the questionnaires utilized in this study. Generally, quantitative data on agricultural production and input factors together with descriptive farmer data was surveyed. The criteria for the selection of the oases to be sampled were discussed with representatives of the DGRE in Tunis and the CRDA in Kebili. Distinction between farmers organized within GICs and private farmers was made.

For our study, a set of 13 irrigated oasis perimeters was chosen of which 5 are managed by GICs. The remaining 8 are owned by private farmers that are not served by GIC water but are organized within themselves.

- GIC Oases: El Hsay, Souk El Biaz, Tifout, Douz, Glea
- Private Oases: Blidet, Nouiel, Zaafrane, Gemna, Kebili, Kalouamen, Douz^{*}, Glea^{*}

Note that the private Oases of Douz^{*} and Glea^{*} are recent extensions on the fringes of the ancient oases.

A representative sampling of farmers within each oasis had to be ensured. For this purpose, based on the data provided by the CRDA, the farmers of a certain GIC oasis were grouped into three different farm categories according to farm size. Farmers to be sampled within a certain category were then randomly chosen out of the total set of farmers of a particular oasis. The farmer, identified by withdrawing a number from a basket, was accepted for interviewing if the area of his farmland was within a 10% margin of the category to be sampled. During this process, 40 farmers

Case Study: The Nefzawa Oases

Var.	Description	valid n	min	max	μ	σ
v_1	Irr. surface [acre]	137	1.50E-01	1.00E+03	8.91E+01	1.21E+02
v_2	Appl. water [m ³ /(a·acre)]	137	0.00E+00	1.62E+04	1.85E+03	1.71E+03
v_3	time in field [month/(a·acre)]	137	8.00E-02	1.50E+02	4.35E+00	1.53E+01
v_4	Agri. yield [t/(a·acre)]	137	3.20E+00	1.03E+03	3.90E+01	9.64E+01
v_5	Phosphate [kg/(a·acre)]	137	0.00E+00	8.00E+01	1.92E+00	7.34E+00
v_6	Manure [ton/(a·acre)]	137	0.00E+00	2.50E+00	7.07E-02	2.15E-01
v_7	water consumption [m ³ /(a·acre)]	137	0.00E+00	1.11E+02	4.36E+00	1.26E+01
v_8	Date yield per tree [kg/a]	137	2.38E+00	8.00E+01	2.45E+01	1.57E+01
v_9	Agri. practice [a]	137	1.00E+00	7.00E+01	2.97E+01	1.56E+01

Table 2.1: Descriptive statistics of the GIC oases. Minimal, maximal and mean values (μ) of the n observed values are shown as well as the standard-deviation (σ).

of each oasis were selected. In the end, 137 farmers were effectively interviewed. Such data were not available in the case of the private farmers. The 8 private oases were chosen randomly from the list of private oases and a total of 124 private farmers were interviewed.

2.2.2 Descriptive Data Analysis

Table 2.1 and 2.2 show the descriptive statistics of selected variables for the GIC and the privately owned oases. The irrigated surface of private farmers is on the average more than twice as big as for the GIC farmers (v_1 in acres). Apart from the better capital endowment of the private farmers, the tradition, that a farmer's land gets divided between the number of his sons, is responsible for this. v_2-v_7 are all standardized with regard to v_1 in order to mask the effect of the irrigated surface. As they have their own boreholes, private farmers can apply water when needed (v_2 in m³/acre). In contrast, GIC farmers get water according to the irrigation schedule. Without exception, all of the farmers use the flood irrigation method on their fields. One of the interviewed GIC farmers did not get water allocated since he practically abandoned his plot, hence $\min(v_2 = 0$ in month per acre). v_7 shows the water consumption per acre and yield. The private farmers in this case are more efficient with regard to their drop-per-crop ratio.

GIC farmers in general spend more time in the field than private ones (v_3 in month per year and per acre) and are more experienced (v_9 in years practicing agriculture). Contrary to that, private farmers are more time efficient due to a generally younger age and the employment of more recent agricultural techniques. One might expect private farmers to have higher per area yields than the GIC ones (v_4 in tons per acre and year). However, this is not the case. The lower per area yield is related to the fact, that private farmers have a more generous tree spacing. Certainly, this is one of the reason for the higher date yield per tree v_8 . For the private oases, v_8 is almost 50% higher than for the GIC farmers. The amount of fertilizer applied per irrigated agricultural area is comparable for both management types (v_5 is Phosphate in kg per acre and v_6 is biological fertilizer in ton per acre).

Var.	Description	valid n	min	max	μ	σ
v_1	Irr. surface [acre]	124	1.25E+01	7.00E+03	2.05E+02	6.37E+02
v_2	Appl. water [m ³ /(a·acre)]	124	3.00E+01	2.75E+03	3.35E+02	3.04E+02
v_3	time in field [month/(a·acre)]	124	2.80E-01	7.47E+00	1.68E+00	9.80E-01
v_4	Agri. yield [t/(a·acre)]	124	1.20E+00	1.21E+02	3.06E+01	1.90E+01
v_5	Phosphate [kg/(a·acre)]	124	0.00E+00	1.20E+01	1.60E+00	1.96E+00
v_6	Manure [ton/(a·acre)]	124	0.00E+00	1.67E-01	4.32E-02	3.25E-02
v_7	water consumption [m ³ /(a·acre)]	124	3.90E-04	3.44E+00	2.29E-01	4.10E-01
v_8	Date yield per tree [kg/a]	124	9.00E+00	8.17E+01	3.64E+01	1.48E+01
v_9	Agri. practice [a]	124	2.00E+00	2.80E+01	1.48E+01	4.78E+00

Table 2.2: Descriptive statistics of the private oases. Minimal, maximal and mean values (μ) of the n observed values are shown as well as the standard-deviation (σ).

2.2.3 Estimation of a Stochastic Frontier Production Function - Empirical Model Formulation

In microeconomic theory, an agricultural production function is defined in terms of the maximum output y that can be produced from a specific set of inputs \mathbf{x} , given the technology available to the farmers. In reality, the observed input–output values are below such a production frontier for various reasons. A inefficiency measure of the individual farmers would then be the deviation from his actual output relative to the maximum attainable, given technology and input factors. The estimation of a frontier production function provides useful insight into best-practice technology and measures by which the productive efficiency of different farmers may be compared. Since Farrell (1957) developed the notion of the production frontier, several different econometric models have emerged that allow the quantification of individual inefficiencies. For the purpose given, we adopt the definition proposed by Meeusen (1977) and Aigner *et al.* (1977) which defined the stochastic frontier production function as

$$y_i = f(\mathbf{x}_i; \boldsymbol{\alpha}) \cdot e^{v_i - u_i} \quad (2.1)$$

where y_i is the possible production level for the i th sample farmer ($i = 1, \dots, N$); $f(\mathbf{x}_i; \boldsymbol{\alpha})$ is a Cobb-Douglas production function

$$f(\mathbf{x}_i; \boldsymbol{\alpha}) = \alpha_0 \prod_{j=1}^m x_{i,j}^{\alpha_j} \quad (2.2)$$

with the $(1 \times m)$ vector \mathbf{x}_i of inputs to production for farmer i and a $((m+1) \times 1)$ vector $\boldsymbol{\alpha}$ of unknown parameters (Hexem & Heady, 1978), i.e. the corresponding production elasticities. v_i and u_i represent two economically distinguishable random disturbances with different characteristics. The v_i are assumed to be independently and identically distributed as $N(0, \sigma_v^2)$ signifying favorable resp. unfavorable exogenous events (i.e. climate, luck, errors of observation and measurement, ...). The model is such, that the possible production y_i is bounded above by the stochastic quantity $f(\mathbf{x}_i; \boldsymbol{\alpha}) \cdot e^{v_i}$, i.e. the stochastic frontier. The u_i are non-negative random variables associated with farmer’s-specific factors which contribute to the i th

farmer not attaining maximum efficiency of production. Following the model given by Battese & Coelli (1995), the u_i are specified as:

$$u_i = g(\mathbf{z}_i; \boldsymbol{\delta}) + \omega_i \quad (2.3)$$

with \mathbf{z}_i being a vector of variables which may influence the efficiency of farmer i , $\boldsymbol{\delta}$ is a vector of variables to be estimated and ω_i being derived from a non-negative truncation of the $N(0, \sigma^2)$ distribution. Note that $g(\mathbf{z}_i; \boldsymbol{\delta})$ is of the same form as $f(\mathbf{x}_i; \boldsymbol{\alpha})$. For $u_i > 0$, it is required that $\omega_i \geq -|g(\mathbf{z}_i; \boldsymbol{\delta})|$.

Given the model by the equations (2.1), (2.2) and (2.3), the maximum-likelihood estimation $\hat{\Gamma}$ of the unknown parameter set Γ requires solving the following system of equations

$$\nabla_{\Gamma}(\ln(\mathcal{L}(\Gamma|\{\mathbf{X}, \mathbf{y}\})))|_{\Gamma=\hat{\Gamma}} = 0 \quad (2.4)$$

where $\Gamma = (\boldsymbol{\alpha}, \boldsymbol{\delta}, \sigma^2, \gamma)$ denotes the parameter vector with $\sigma^2 = \sigma_v^2 + \sigma_u^2$ and $\gamma = \sigma_u^2/(\sigma_v^2 + \sigma_u^2)$ being the parametrization for the variance of the likelihood function, ∇_{Γ} is the gradient with regard to the parameter vector and $\ln(\mathcal{L}(\cdot))$ is the log-likelihood function given the distributional assumptions of the observed farmers data (\mathbf{X}, \mathbf{y}) . The log-likelihood function of this model is presented in the appendix of the working paper of Battese & Coelli (1993). γ is a measure of relative importance of the farm specific variance to the overall variability of farm outputs with $0 < \gamma < 1$.

Technical efficiency φ_i of farmer i then is defined as the ratio of the observed output to the corresponding frontier output, conditional on the levels of input used by that particular farmer. Thus, φ_i becomes

$$\varphi_i = f(\mathbf{x}_i; \boldsymbol{\alpha}) \cdot e^{v_i - u_i} / (f(\mathbf{x}_i; \boldsymbol{\alpha}) \cdot e^{v_i}) = e^{-u_i} \quad (2.5)$$

and is determined by the unobservable u_i being predicted given the model assumptions. Unfortunately, reliable data on factor prices were not available. Hence, the estimation of allocative efficiencies was not possible.

For the purpose of our modeling task, the following model variables were chosen. The dependent variable y_i is the total per farm date production (Deglet Nour and lesser quality dates) as of the year preceding the survey. The inputs to production are: $x_{i,1}$, irrigation water volume (m³/a); $x_{i,2}$, irrigated surface (ares); $x_{i,3}$, labor, i.e. time spent effectively in the field comprising of family, contract labor and hired staff (permanent or casual) measured in working days per year; $x_{i,4}$, fertilizer, i.e. manure and phosphate (kg/a); $x_{i,5}$, salinity of irrigation water (g/l). The explanatory variables of the model are the following: $z_{i,1}$, farmers experience in years; $z_{2,i}$, form of organization (dummy variable for GIC or private); $z_{i,3}$, level of education (dummy variable); $z_{i,4}$, family size (members). Table 2.3 collects the summary statistics of the model variables. The empirical analysis of the efficiency of production in the Nefzawa Oases was carried out with the computer program Frontier4 (Battese & Coelli, 1993). The input and resulting output files are provided in the Appendix.

Variable	unit	n	min	max	μ	σ
y	kg/a	261	20	231000	4381	15126
x ₁	m ³ /yr	261	0	311040	117047	285213
x ₂	ares	261	0.15	7000	144	451
x ₃	man-days/a	261	2	7600	227	580
x ₄	kg/a	261	0	71001	5572.77	9039.25
x ₅	g/l	261	1	7	3.23	1.67
z ₁	a	261	1.0	70.0	22.59	13.91
z ₂	[-]	261	1	2	1.48	0.5
z ₃	[-]	261	1	6	2.69	1.5
z ₄	[-]	260	1.0	23.0	7.09	2.85

Table 2.3: Summary statistics of variables used in the model (see text for a description of the variables).

Parameter	Value	$\sqrt{\hat{\sigma}_P^2}$	t-ratio
$\hat{\alpha}_0$	3.21E+00	4.42E-01	7.27E+00**
$\hat{\alpha}_1$	6.48E-02	3.65E-02	1.77E+00
$\hat{\alpha}_2$	5.25E-01	5.57E-02	9.43E+00**
$\hat{\alpha}_3$	3.93E-01	5.72E-02	6.87E+00**
$\hat{\alpha}_4$	3.20E-02	1.41E-02	2.27E+00**
$\hat{\alpha}_5$	-1.42E-01	3.44E-02	-4.13E+00**
$\hat{\delta}_1$	1.82E-02	1.32E-02	1.37E+00
$\hat{\delta}_2$	-1.55E+00	1.86E+00	-8.33E-01
$\hat{\delta}_3$	1.42E-01	1.11E-01	1.28E+00
$\hat{\delta}_4$	4.77E-03	5.34E-02	8.94E-02
$\hat{\sigma}^2$	1.47E+00	9.00E-01	1.64E+00
$\hat{\gamma}$	8.15E-01	1.09E-01	7.50E+00**

Table 2.4: Maximum-likelihood parameter estimates. $\sqrt{\hat{\sigma}_P^2}$ is the estimated standard error given to two significant digits. The t-ratio is the test of statistical significance. **: Significant at the 95% level.

2.2.4 Empirical Results

The estimates of the variables defined by the model defined in Equations 2.1 – 2.3 are presented in Table 2.4.

The signs of the parameters estimates are as expected in the case of α . The negative elasticity of α_4 indicates that yield decreases with increasing irrigation water salinity. Generally, a t -ratio of more than 2 is statistically significant at the 95% level. Thus, apart from α_1 , i.e. the applied irrigation water elasticity, all estimates are highly significant. This might be related to an inherent problem of such data survey. Farmers may have intentionally biased estimates of their allotted

water with the expectation that such study would enable them to get higher annual quota.

The estimated inefficiency parameters are all relatively small relative to their estimated standard error. From the t -ratio values of the δ_i one might conclude that the technical inefficiencies in production are, in fact, absent. However, the estimate of the variance parameter γ equals 0.815 and is highly significant which, in other words, indicates that inefficiency effects are likely to be highly significant in the analysis of the value of output of the farmers. The remainder of inefficiency effects are due to factors outside the control of the farmers such as weather, soil quality, etc.. The null hypothesis that the inefficiency effects are absent (i.e. $\delta_i = 0 \forall i$) or have simpler distributions, can be rejected at the 95% level (test statistic with mixed chi-square distribution: 12.21; $\chi_{0.95}^2 = 11.071$). Thus, the cumulative effect of the inefficiencies of production are significant although the individual variables may not be statistically significant.

The individual estimates of farmer's efficiencies are given in Appendix A. We calculate a mean efficiency of 63.8% as a mean over both, GIC and private farmers. Thus, with the present state of technology and unchanged input uses, production could be increased by 36.2% if the technical inefficiencies were to be removed completely. Figure 2.5 shows the histograms of the estimated efficiencies.

The communal form of management appears less efficient than private management. Mean technical inefficiency for the former is estimated to be 42.2% and 30.7% for the latter. This might be related to various factors. First, private farmers profit from economics of scale. That is, their plot sizes have not become affected by continuous inheritance parting. The generally better monetary situation allows those farmers to better substitute scarce input factors by capital. Second, most of them are educated in the application of recent agricultural techniques. This is not to say that the long standing traditions in oases management, the knowledge about land tilling and the spacing of irrigation intervals should be neglected. It rather might be an indication that this knowledge, which has been codified in historical water rights that are inherently tied to a particular plot of land of the GIC farmer, is no longer appropriate due to the growing population pressure.

As with any empirical analysis, our findings should be interpreted with caution. If one accepts the notion of maximality, i.e. that there exists a frontier defining maximal output-to-input ratio, it nevertheless seems worth to investigate failures of the individuals to produce at the frontier. The results indicate that significant inefficiencies in the case of the agricultural practice of the Nefzawa farmers exist. The increase of farm-level output would be a cost effective measure to improve the farmers income. Yet, despite the effect that higher efficiency levels have on output, holding input constant, productivity gains from technological innovations and change remain of critical importance. In our model, technological progress would cause the stochastic frontier to be shifted upwards. For example, more salt tolerant species can be planted in areas where soil salination has progressed. In addition, precision irrigation could reduce the return flow to the shallow aquifer

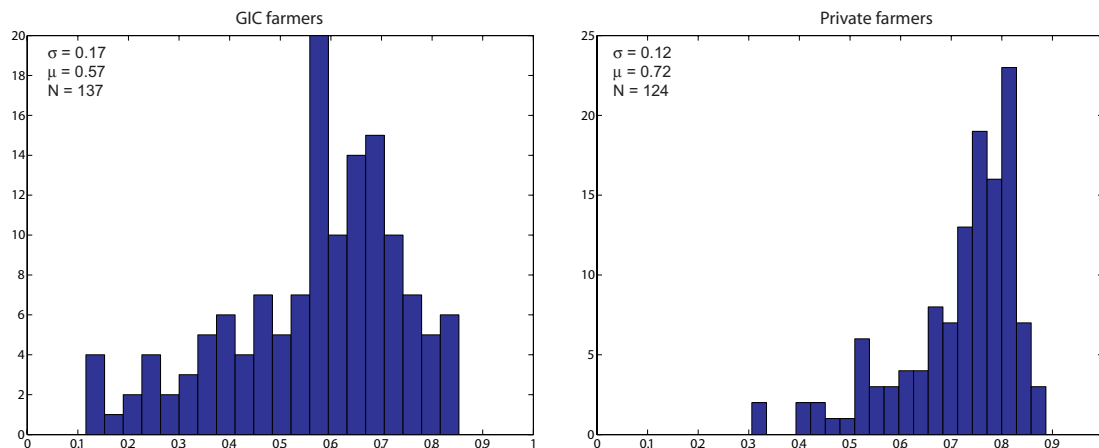


Figure 2.5: Histograms of estimated efficiencies for private and GIC farmers.

and thus prevent the rise of the water table beyond a critical level. The present governmentally supported substitution of furrow channels by PVC tubes is aiming in this direction. To this policy, measures for the reduction of the technical inefficiency effects could be added in order to gain productivity at the same or even at a lower factor input level.

2.3 Salination as a Threat to Agricultural Production

2.3.1 Introduction

Piezometric levels of the TC aquifer have been declining in the Nefzawa region at an average rate of 1 m/year over the last 30 years. Related to that, a deterioration of the pumped water quality from the TC aquifer has been observed locally. This threatens future agriculture in the region primarily due to the chronic input of an increasing salt load to the farmers fields. In some places such as the El Hsay Oasis, yields and quality of the dates are diminishing at an alarming rate already nowadays. So far, the sources of this contamination have not been identified and remain ambiguous. However, several possible causes for salination exist in the region. First, brine from the Chott El Djerid could pollute the TC. Second, the salinity of underlying aquifers, i.e. the Turonian and the IC as well as the lagoonal Senonian aquitard between TC and Turonian may threaten the productive potential of the TC. Third, agricultural drainage water may pollute the phreatic oasis aquifer from which water with an increased salt load can percolate into the TC.

Here, we seek to find an explanation for the deterioration of the TC water quality. The relevance of processes will be discussed with regard to their present and future impact on TC water. For this purpose, available data at the Tunisian agencies responsible for management of surface water and groundwater resources (CRDA, Kebili and DGRE, Tunis) have been collected and analyzed. During numerous field

trips in 2002, complementary water samples were taken and hydrochemical as well as isotopic analyses carried out. Based on this dataset, a numerical groundwater flow and contaminant transport model was developed.

In the following, the hydrogeology of the Nefzawa area is presented. Second, the problems with regard to groundwater quality deterioration are highlighted and different causes, responsible for such a development discussed. Third, results from the field campaigns are presented and, based on these, conclusions with regard to the origins of the salination are drawn. Finally, a predictive flow and transport model is introduced that may be used by local decision makers in order to assess different management strategies with regard to their future threat to the TC resource.

2.3.2 Geology of the Nefzawa Oases

Among the different aquifer systems that exist in the study area, the TC and IC formations are the two major ones with regard to extent and their relevance for yield. The term Terminal Complex describes a multi-layer aquifer which consists of the most recent formations in the northern Saharan basin: the Senonian, Eocene and Mio–Pliocene. Together, they form one single groundwater body. The diversity of geologic formations, the lithological heterogeneity and late sedimentation lead to the name Terminal Complex (UNESCO, 1972). In the Nefzawa, the Senonian limestones are the aquifer primarily exploited. The thickness of the TC varies between 100 m in the northeast and 400 m towards the southwest. The depth to the top of the Senonian limestones ranges from 50 m to 100 m. It is generally increasing from east to west and towards the Chott where the limestones dive under the quaternary and mio–pliocene Chott deposits. Over most of the Nefzawa region, the TC is confined by shales and marls of the Paleocene, evaporites of the middle Eocene. The most recent cover are sands as well as shales of the Mio–Pliocene and the quaternary alluvium.

Towards the east, the Senonian limestones are cropping out. The exposure to weathering has left them highly karstified. In these areas, the TC gets recharged by direct infiltration in wadis through floods descending from the Djebel Tebaga and Dahar mountain ranges located at the northern and eastern boundary of Nefzawa. Younger water ages at the fringes of the basin are an indication of this recharge (Edmunds *et al.*, 1997). However, recharge nowadays is strictly limited due to arid to hyper–arid conditions within the catchment. Ages dated by radiocarbon (C14) range from 5'000 to 28'000 years in the central basin. The bulk of it was recharged in the pluvial phases of the Pleistocene.

The underlying Turonian dolomites constitute a separate aquifer towards the central basin where the impermeable lagoonal Lower Senonian is present. At the eastern borders of the study area, where the dolomites are cropping out, and along the Kebili-Tozeur fault Turonian water mixes with water from the Senonian. Although this permeable dolomite potentially is an interesting aquifer in these regions, it is of little interest in the other parts of the Nefzawa due to its salinity with a TDS

of up to 7 g/l.

The IC, like the TC, is a multilayer aquifer. Generally, the IC includes the different aquifers between the bottom of the Triassic and the top of the Albian (UNESCO, 1972). The main aquifers in the Nefzawa are situated in the Lower Cretaceous from the Barremian to the Albian. Its confining unit is clearly defined as the Cenomanian shales which separate the IC from the Turonian. In the Nefzawa, the base is given by the shales of the Malm. The groundwater of the IC mainly derives from infiltration of waters during the pluvial ages in the Pleistocene. Recent recharge is possible at the periphery of the Sahara basins where the IC is outcropping. In the Nefzawa, the general flow of IC groundwater is directed from southeast towards northwest. IC groundwater quality in the study region is mediocre with TDS ranging from 2 g/l to 4 g/l.

Three types of phreatic aquifers can be distinguished in the study region: the oasis aquifers in the mio-plio-quaternary sediments, the wadi aquifers in the alluvial fillings of the wadis and the Chott El Djerid. With regard to exploitation, they are only of secondary importance because their water is usually highly charged with 2-10 g/l TDS (Mamou & Hlaimi, 1999; El-Fahem, 2003).

TDS observations in the Presqu'île de Kebili (PIK) in the 1960s showed salinity to range from 5 to 12 g/l (Pouget, 1966). These phreatic aquifers are mainly recharged by vertical percolation from the confined TC. Additionally, the oasis aquifers are recharged by excess irrigation water so that their piezometric level is elevated in the vicinity of the oasis and diminishing with rising distance from the irrigated perimeters. Measurements of the water table depth show an average depth below ground level in the oases from 1 m in the PIK to 5 m in Douz (DGRE, 2000).

Outside the oases, lower water table have been measured ranging from 9 m below ground in the PIK to 14 m in Douz. Water of the oasis aquifers generally flows towards the Chott El Djerid. In times of shortage during summer months, the oasis aquifers are used for irrigation to complement the official water allotment. However, their waters have to be diluted with TC water to lower total TDS. As of the year 2000, exploitation has been estimated as 0.05 m³/s of which more than 70% is utilized in Douz. The wadi aquifers of quaternary alluvium are situated in the eastern, western and southern part of the Nefzawa. They are mainly used by nomadic tribes to provide drinking water to their livestock. Similar to the outcropping TC, these aquifers are recharged by floods in the eastern mountains. Salinity ranges between 2-5 g/l.

The Chott El Djerid finally, covering an area of 5'400 km², is a playa system in a subsidence basin between the southern flank of the Djebel Tebaga mountain range and the North of the Sahara platform. In the undisturbed state, the Chott constituted the final sink of water from the TC and the phreatic aquifers. Groundwater is highly charged and often exceeding 100 g/l of dissolved salts (Gueddari, 1980). The hydrogeology of the Chott is not well known. There exists no well or piezometer inside the Chott. Silty sediments and crusts formed by salts cover the greatest part of it. The sedimentation of the Chott Djerid is evaporitic and lacustrine since the

late Pleistocene. Geological log samples taken in different areas in the Chott show layers of clays and salty materials (Gypsum) to a depth of around 60 m. This is the maximum thickness of the quaternary Chott sediments. Between 60 m and 125 m, there are sandy sediments from the Mio–Pliocene with clayish and salty intercalated layers (Meckelein, 1977). At the bottom, there are bedded marly sandstones or red shales to a depth of around 900 m in the center of the Chott. The groundwater table is relatively high ranging from 20 to 50 cm below the surface. Mainly in winter, floods from the surrounding mountain ranges can result in standing water in some areas of the Chott.

2.3.3 The Terminal Complex Hydrochemistry and its Evolution in the Nefzawa Oases

Hydrochemical investigations in the Nefzawa started in the late 1950s. However, systematic and continuous observations are only available from 1980 on. At this time, TDS values of the oases situated in the PIK were elevated (2 to 3.5 g/l) when compared to the rest of the Nefzawa oases (1 to 2 g/l in average). During the last 20 years, a rise in TDS of 1 up to 2 g/l was observed in the PIK, especially in Ras el Ain, Ziret Louhichi and Telmine, and in the southerly Douz region (Douz, El Hsay). The chemical N–S cross-section through the study region shown in Figure 2.6 depicts the situation in 2002. Oases situated in the central region as well as next to the Chott El Djerid (such as Negga and Gueliada) do not show any deterioration of water quality. The highest TDS rise of 4 g/l can be observed in the oasis of El Hsay at the southeastern limit of the Nefzawa where some of the pumped water is no longer suitable for irrigation purposes. Thus, the change in salinity is not homogeneously distributed within the affected regions, neither temporally nor spatially. Even inside the same oasis such as for example Ras el Ain, TC boreholes located next to each other show different behavior. Nevertheless, it can be generally stated that salinity in the northern Nefzawa, i.e. the PIK as well as to the southeast of the study region is elevated and raises concern about future groundwater utilization. Additionally, the TDS increases at generally lower speed in the PIK compared to the Douz region. Contrary to that, the central Nefzawa is not affected up to now by quality deterioration of its groundwater.

Due to the hydrogeological situation of the Nefzawa, three differing salination mechanisms are likely causes for such a development: infiltration of brine from the Chott El Djerid, upwelling of Turonian and IC water and finally, infiltration of agricultural drainage water from the oases aquifers. These will be discussed in the following.

The Chott El Djerid has to be viewed as a first source of salination. As already stated, it contains very saline groundwater within its tertiary and quaternary sediments. A pronounced density layering is present with TDS ranging from 10 g/l up to 350 g/l. In the undisturbed state, the elevated TC head relative to the shallow groundwater piezometry prevented any significant downward percolation of

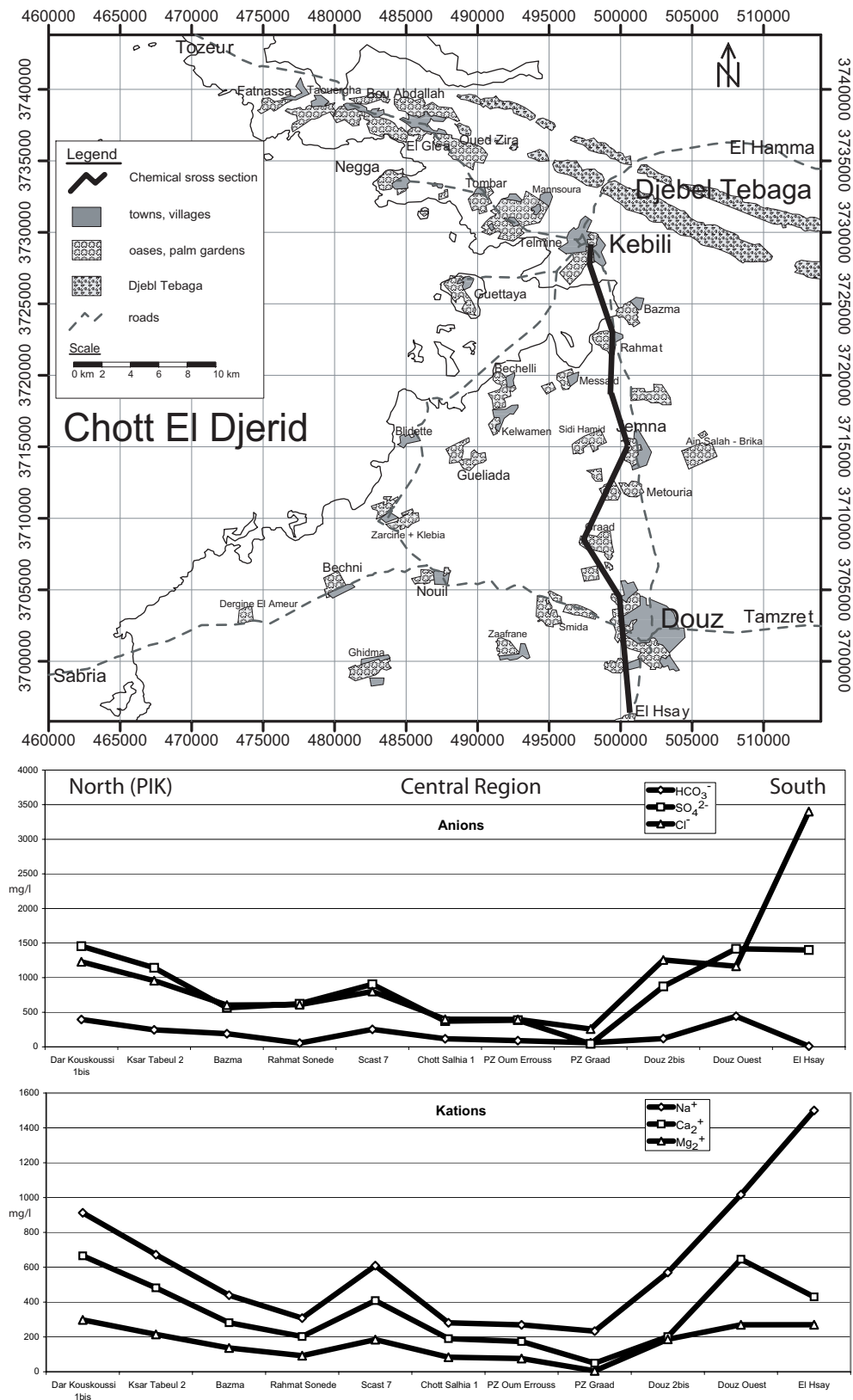


Figure 2.6: Map (Universal transverse Mercator coordinates, zone 32, northern hemisphere) of the region with chemical cross sections.

phreatic groundwater. Progressive groundwater mining lowered the TC head leading to an inversion of the hydraulic gradient in the TC. The schematic Figure 2.9 shows how an infiltration of Chott water into the TC may be caused by such a gradient inversion. The figure shows the piezometric level of the TC before and during exploitation. It is conceivable that Chott water infiltrates into the TC with the progression of the gradient inversion. In this case infiltrating water has to pass the semipermeable aquitards of the Pleistocene clays. Although these clays cover most of the Cretaceous in the Nefzawa region, their thickness varies. After sedimentation in the late Paleocene, these clays were exposed to erosion on the surface and partially attenuated. Hence, percolation through these strata further accentuated by density fingering of the Chott's brine might locally be possible. An interesting but still not clearly understood natural feature in this context are the spring mounds on the fringes of the Chott El Djerid in the Nefzawa Oases. Previous studies determined the discharge of these springs to be about $1.5 \text{ m}^3/\text{s}$ (Armines-ENIT, 1984). In the past, TC water evaporated in these spring mounds after having risen through preferential flow paths from the TC towards the quaternary surface (Meckelein, 1977). The lowering of the hydraulic heads of the TC in recent years caused a complete drying up of the springs.

Second, the water of the Turonian shows increased salinity in the Nefzawa. Measured TDS values range from 2.5 – 3.5 g/l in the PIK to 7 g/l in the southeastern part of the Nefzawa. This also holds true for the IC in the Nefzawa. Measured TDS in this aquifer increase from 2.5 – 3.5 g/l in the PIK to 4 g/l in Douz. It is likely that salination of the TC occurs where interactions between these aquifers exist. The higher pressure head of the Turonian allows its water to leach upward. With a lowered piezometric level of the TC and a still quite unchanged level of the Turonian, this upwelling might be increased leading to a density layering in the basal zone of the TC formation (see Figure 2.9). Under these circumstances, pumping possibly triggers upconing and thus leads to quality deterioration.

Third and finally, drainage water with an increased TDS collects in terrain depressions, so called Sebkhass, where it gets enriched due to strong evaporation (see Figures 2.7 and 2.8). The TDS of drainage water varies from 8 g/l in winter to 25 g/l in summer. In autumn 2001, the measured TDS in the Sebkhass of El Hsay reached 100 g/l (El-Fahem, 2003). Especially in summer months, drainage waters do not get flushed to the more distant Chott due to greatly reduced flow. These waters then collect in the Sebkhass within close proximity of the oases (see Figure 2.8). Consequently, they infiltrate to the underlying shallow aquifer (DGRE, 2000). The drawdown of the piezometric level of the TC around the oases itself can cause induced infiltration of enriched water from the upper shallow aquifers. As already stated, the confining clays of the Paleocene are not a continuous layer of equal thickness (Figure 2.9). They might be thinning and forming lenses thus containing preferential infiltration pathways. In case of a lowering of the TC head below the head of the oases aquifer, it is plausible that either drainage water from the oases or highly charged water from the Sebkhass leach into the TC.



Figure 2.7: The Sebkha of El Hsay Oasis in autumn 2002 (location indicated by red arrow in satellite pictures, Figure 2.8). A TDS of 100 g/l was measured during the field visit. Foam is blown from the brine by strong winds.

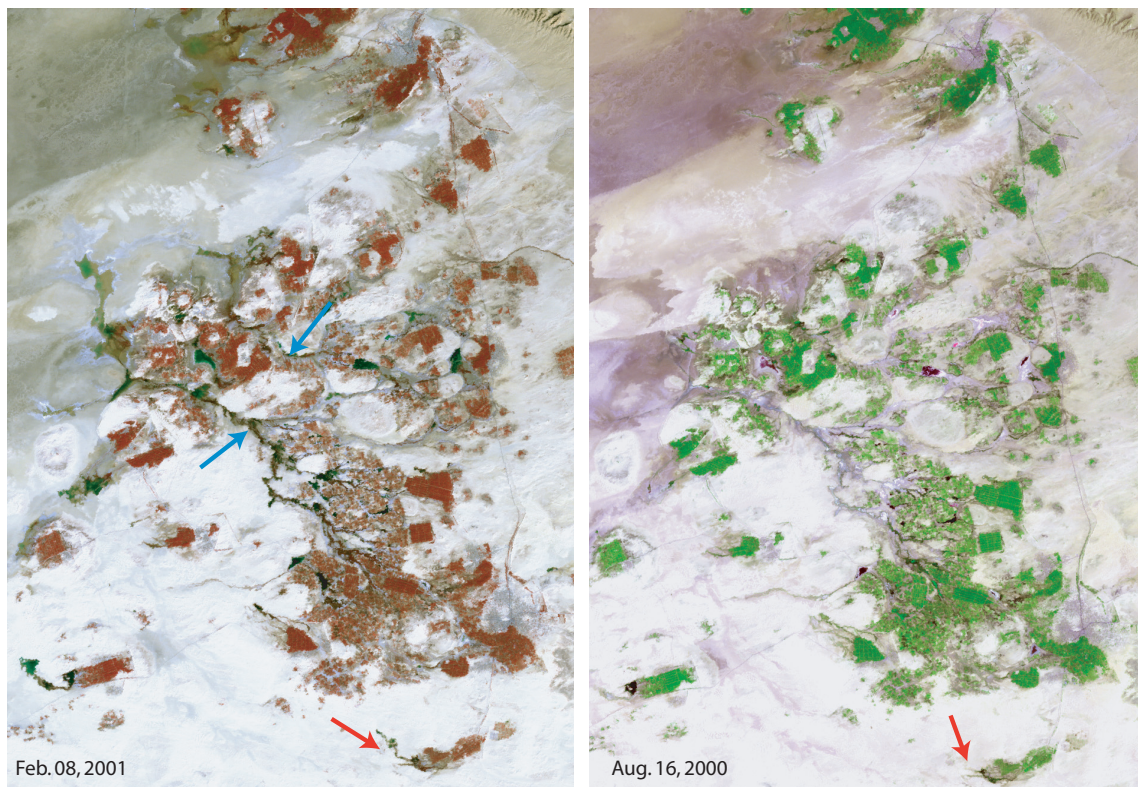


Figure 2.8: False color Landsat ETM+ images from the Nefzawa (not scaled). Left: Band combination 4,3,1. Winter image with agricultural drainage water (black to dark green color) being flushed to the Chott. Right: Band combination 3,4,1. Summer image with dried up drainage network. Drainage water collects in the vicinity of the oases (blue colored ponds). Note the drain of Oasis El Hsay (red arrow) is not connected to the larger drainage network (blue arrows).

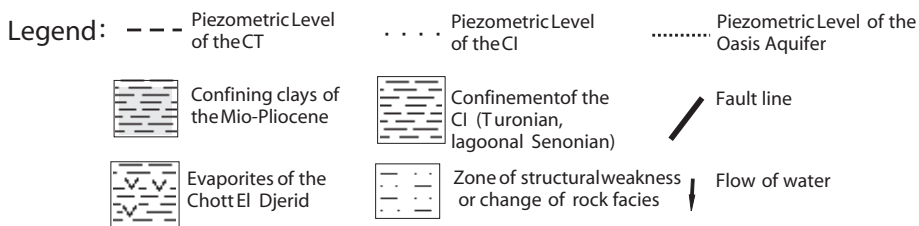
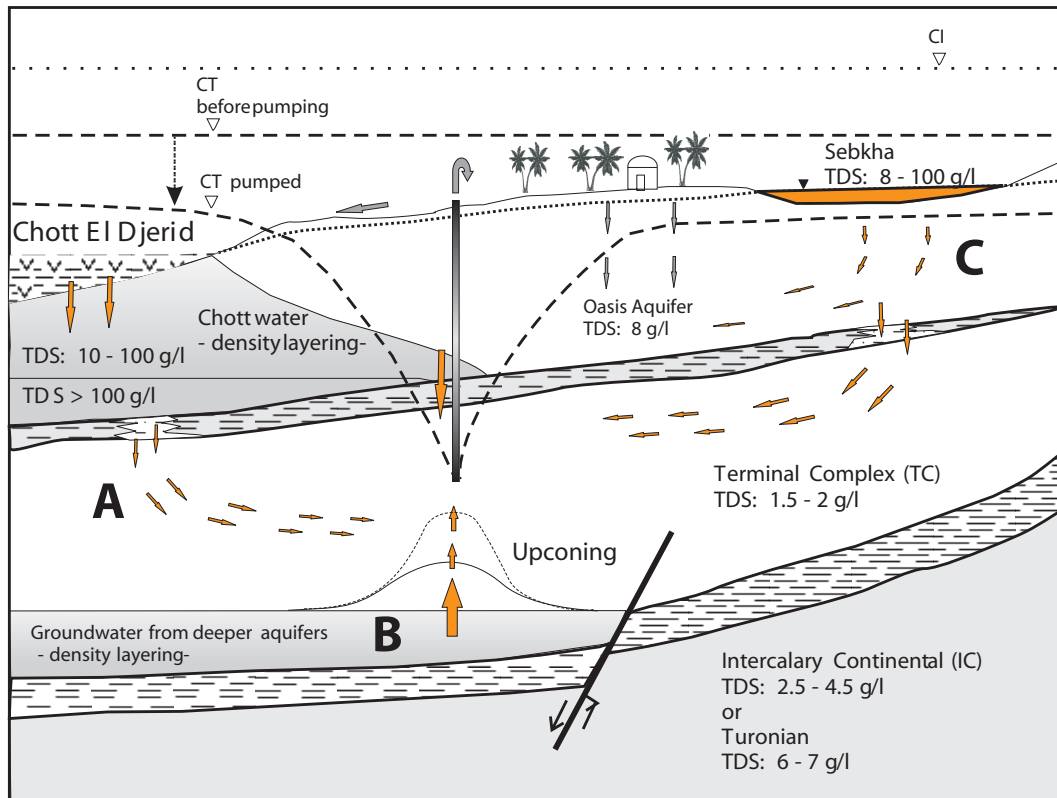


Figure 2.9: Conceptualization of the three differing salinization processes. A: Infiltration of brine from Chott; B: Upconing of IC/Turonian water; C: Pollution by agricultural drainage water (El-Fahem, 2003).

2.3.4 Determination of the Salination Origins

Geological, hydrogeological and geochemical information have to be combined in order to get an understanding of the complex salination phenomena observed in the Nefzawa oases. In a first step, correlations between the pointwise TC salinity increase and pumping, piezometry and structural properties were established. As a result, the pumped quantity alone cannot be considered to be a determining factor with regard to an increase of TDS. For example, the Gueliada oasis ($0.71 \text{ m}^3/\text{s}$ in 1998) or Smida oasis ($0.45 \text{ m}^3/\text{s}$ in 1997) which are strongly exploited since 1990 show no sign of increasing TDS. In contrast to that, the less exploited El Hsay oasis ($0.08 \text{ m}^3/\text{s}$ in 1997) shows the highest increase of TDS. However, this only confirms the strong local nature and relevance of the different origins of salination. A similar conclusion results from the correlation of drawdown and quality. TC aquifer drawdown (1950 until 2000) ranges between 20 m and 45 m. The highest drawdown value is located in the PIK region, e.g. the Telmine oases. Towards the south, in the Douz-El Hsay oases that are strongly affected by salination, drawdown is 34 m on average. Contrary to that, in the nearby oases of Negga where no salinity development is observed, it reaches 38 m. However, a strong relationship between the increase of the TDS and the depth of the TC top, that is generally coincident with the screen top for most of the boreholes, exists. Boreholes tapping the TC near to the surface show a pronounced increase of the TDS (Douz, El Hsay) whereas deeper TC boreholes do not show any sign of a deterioration of the pumped water quality (Figure 2.10).

This result indicates possible contamination by the third salination source, i.e. the phreatic aquifer where the shielding of the TC by its confining unit is less pronounced. It is well known, that the agricultural practice of excess irrigation greatly increases the salinity of the underlying phreatic aquifer (Meybeck & System, 1989). Clearly, a downward percolation of TDS enriched shallow groundwater can only occur if the piezometric head of the oases aquifer is locally higher than the TC head. By 1996, TC artesianism around Douz and El Hsay retreated to up to 10 km west of these oases in the direction of the Chott El Djerid. TC piezometric levels are up to 20 m below ground. Hence, conditions conducive for percolation prevail in this southerly region. No correlation between distance to Chott of a borehole and TDS development exists (Kriaa, 2003). Oases adjacent to the Chott El Djerid such as Negga, Gueliada and Guidma do not show any signs of deterioration of TC water quality. A present day influence of the Chott's brine is not visible and its relevance as a source of salination is refuted. However, this may not hold true for the future when a regional scale gradient inversion will establish. The pertinence of this salination source with regard to planned aquifer exploitation will be discussed in Section 2.3.7.

In a second step, data on chemistry, temperature and isotopes available at the CRDA Kebili were complemented by sampling groundwater at 53 sites from deep wells in the TC and IC, surface wells, drains and Sebkhass in 2002. Subsequently,

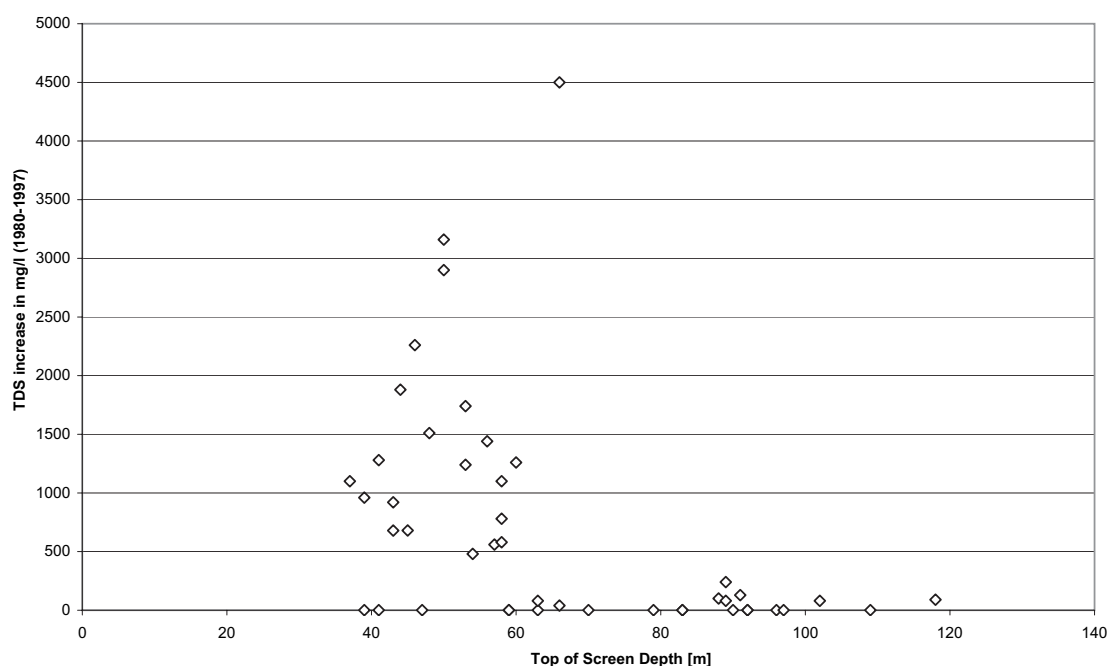


Figure 2.10: TC Salinity development between 1980 and 1997 in relation to the top of the screen at a particular borehole location (Kriaa, 2003).

chemistry, temperature, radioisotopes and environmental tracers (CFCs) were analyzed. All Sampling was coordinated with local representatives.

TC as well as IC water are of equal origin, having been recharged during the pluvial phases of the Pleistocene. This explains their similar ion ratios. However, TC samples deviate from the local meteoric water line (MWL in Figure 2.11). They are shifted below the MWL with their stable isotope composition following a characteristic evaporation line ($\delta^2\text{H} = 4.3\delta^{18}\text{O} - 25.9$, interpolated from all of the available TC samples). This shift along the evaporation line indicates mixing with newer water that was subject to evaporation prior to recharge. TC measurements close to the local MWL are geographically located in the PIK region whereas samples from the southern and eastern Nefzawa region cluster between the former and the unconfined TC values (see Figure 2.11). The strong mixing effect observed in the TC water samples from the south can be caused by local infiltration of drainage water from the oases aquifer. Alternatively, westward migration of water subject to evaporation before infiltration as well as evaporation of TC water along the general TC groundwater gradient can account for mixing. The recharge zone of this water is 30 – 50 km east of the study region, where the TC crops out. Mamou & Hlaimi (1999) present in their report stable isotope measurements of phreatic water samples taken in that region. They show a strong evaporative nature, being aligned along the characteristic evaporation line. Since the general groundwater flow direction is South-East to North-West towards the Chott, it is evident that the TC values of the southern and eastern Nefzawa are more depleted due to mixing with recent

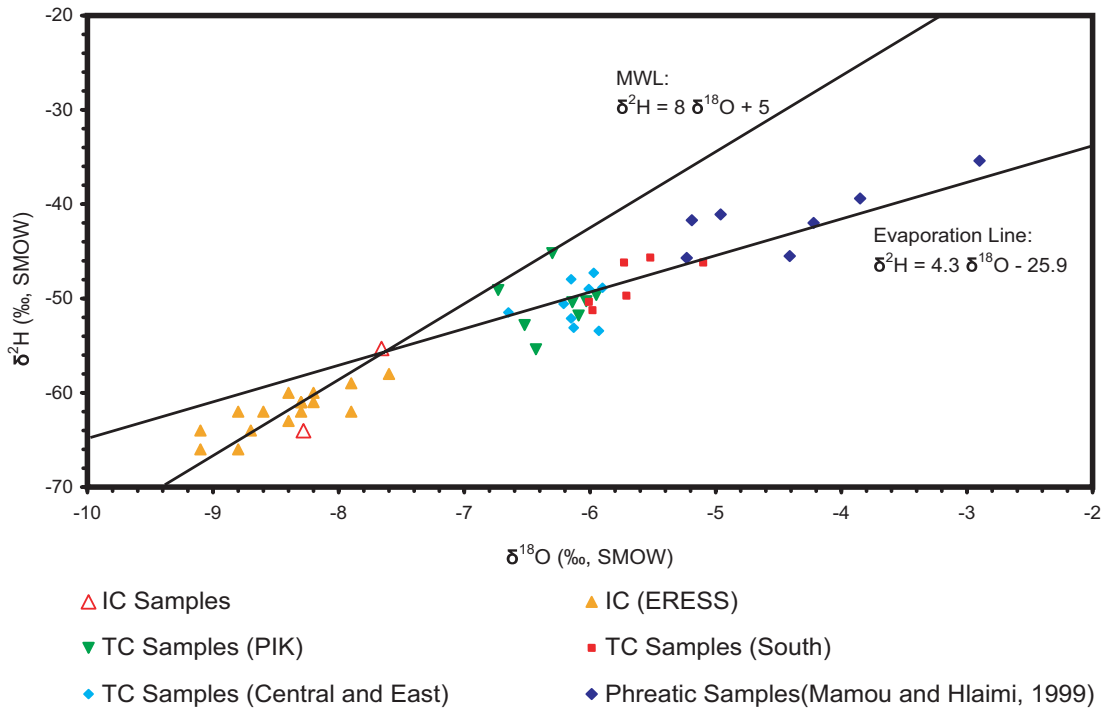


Figure 2.11: Relationship between δ^2H and $\delta^{18}O$ of waters from different origins.

water subject to strong evaporation. The percentage of TC water originating from recharge in the unconfined zone to fossil TC water is around 42% (42.3% for δ^2H and 41.7% for $\delta^{18}O$, mixing ratios calculated after Nair *et al.* (2001)). An influence of phreatic aquifer water cannot be excluded. However, it is highly improbable that such a high mixing ratio solely stems from the downward percolation of enriched water considering that the TC is mostly confined in the Nefzawa.

In contrast, the relative depletion in stable isotope values in the PIK region can either be caused by IC or even Turonian upwelling or direct recharge through preferential pathways in the fractured limestones and dolomites on the southern flank of the Djebel Tebaga mountains. An influence of the geothermal IC water in the PIK seems evident from the observed temperature anomaly of the TC groundwater. Average water temperature of the TC in the Nefzawa region is around 24 °C. The area of the PIK shows increased temperature values of around 27 °C. Mixing with water from the IC is a likely salination source in the PIK. It helps to explain the regionally increased background salinity as well as the depletion in radioisotopes. The relation between salination and isotopic composition is shown in Figure 2.12. Samples geographically located in the vicinity of the PIK all show the tendency towards depleted $\delta^{18}O$ and increased TDI values. Combined with the above findings, this confirms our basic understanding of the salination there. Samples located in the upper right corner of Figure 2.12 show high TDI as well as enrichment in $\delta^{18}O$ which signifies admixture of water exposed to evaporation prior to recharge. Measurements

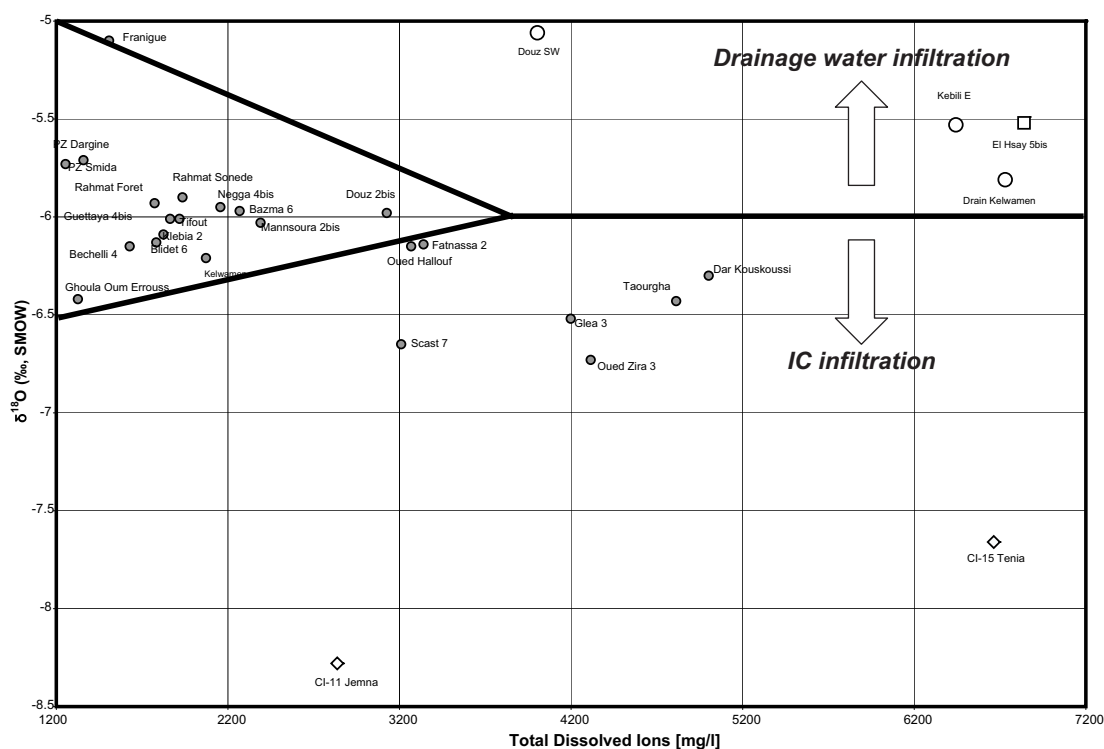


Figure 2.12: Relation between TDI and $\delta^{18}O$ showing TC waters (grey dots), IC waters (diamonds), and phreatic water samples (empty dots). The measurement of El Hsay 5b is located in the upper right corner.

from surface wells (Douz SW and Kebili E) and oases drains (Drain Kelwamen) are located here. Only the well of El Hsay 5b seems to be strongly affected by this process. El Hsay 5b is the well with the highest and fastest rising salinity in the region. There, salinity reached values of around 6.84 g/l TDS in 2001.

All over the Nefzawa, analysis of samples revealed high amounts of nitrates in the TC groundwater, ranging from 15 mg/l to 45 mg/l. Generally elevated values are to be found in the central region of the Nefzawa and near to the Chott El Djerid. At first, it seemed that this could be a proof for infiltration from agricultural surface waters. Such a salination, however, would have to be of more local character. No nitrate fingerprint should be visible west of the Smida/Kebili – line, where the TC still is artesian. Additionally, salinity patterns do not follow the nitrate distribution. The presence of high nitrate concentrations is a peculiarity of some desert groundwater and unrelated to man-induced pollution (Heaton, 1984; Edmunds & Gaye, 1997; Krusman, 1997). The nitrate seems to be persistent either under aerobic conditions or under anaerobic conditions where the amount of organic carbon is low. As there is no further proof for induced infiltration of nitrate from the surface, nitrate values will be considered as natural background concentrations.

The most plausible salination mechanisms therefore are

- salination of TC groundwater by mixing with agricultural drainage water in the southerly oases of Douz and El Hsay;
- salination by saline groundwater from the Turonian and IC in the region of the Kebili-Tozeur fault.

2.3.5 Groundwater Flow Model

In order to assess the future impact of pumping on the TC aquifer in the Nefzawa over the next fifty years, a quasi 3D finite-difference flow model was developed using Processing MODFLOW (Chiang & Kinzelbach, 2001). The development and calibration of the model are described in detail by Kriaa (2003). The study area covers an area of about 5500 km² and was horizontally discretized into square cells of 780 m side length. The north-eastern boundary of the model follows the TC basin boundary. The other limits are artificially chosen with third type boundary conditions that represent the hydraulic connection to the greater TC basin.

Vertically, the upper model layer corresponds to the phreatic aquifers which are laterally connected to the Chott aquifer. Only very limited information about those phreatic aquifers, i.e. their extent and formation, is available (Mamou & Hlaimi, 1999). Combining the oases aquifers, the Wadi aquifers as well as the Chott aquifer within one model layer, we assume that this aquifer extends over the whole study region in the mio–plio–quaternary sediments. Evapotranspiration occurs from this layer only. Recharge from precipitation at the southern flank of Djebel Tebaga is modeled by prescribed inflow. An estimated 10⁵m³/a gets recharged. This estimate corresponds to the one presented in Mamou & Hlaimi (1999). TC water, generally following the terrain gradient, flows towards the Chott where it gets removed by evaporation. On–farm drainage systems in the oases are represented by third type boundary conditions which allow to model exchange with the phreatic aquifer. The location and geometry of the drain network were obtained by the superposition of a Landsat image (Landsat–7–ETM, Feb. 08, 2001) with the model grid. For steady–state calculations, only the ancient oases have been accounted for, whereas the many new extensions of the irrigated perimeters from 1950 up to today are implemented in the transient model. Due to lacking knowledge of thickness and extent, the confining clays, marls and evaporites between the two aquifers have not been modeled explicitly. Instead, the TC and mio–plio–quaternary sediments are connected by a leakage term that was calibrated.

Accordingly, the lower model layer then corresponds to the TC aquifer. It incorporates the stratigraphic units of the upper and lower Senonian formations. Its geometry was interpolated on the model grid from borelog data. Springs are implemented as drains whose flow should be reproduced after model calibration. The connection to the Turonian is modeled by a third type boundary condition. Its representation should help to determine inflow via the Turonian to the TC in steady

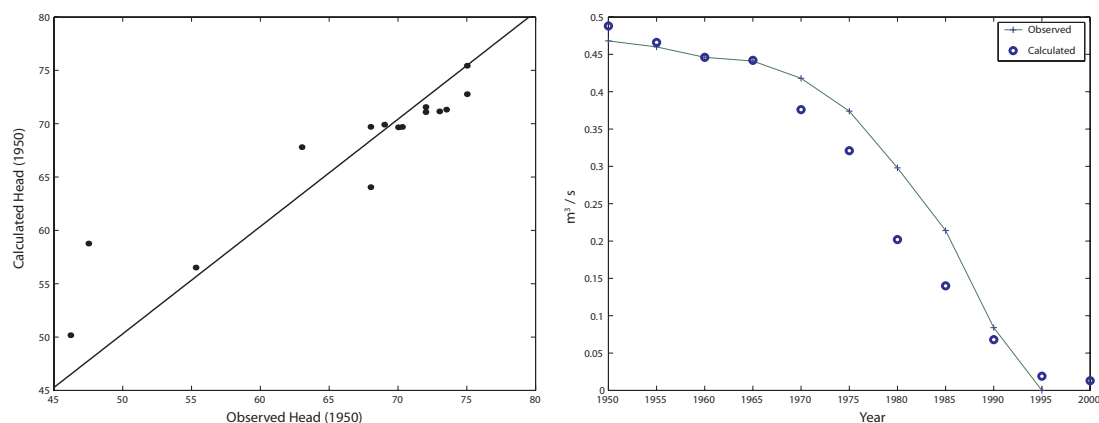


Figure 2.13: Left figure: Scatterplot of steady-state calibration. Right figure: Temporal reproduction of spring discharges (1950 – 2000)

and transient state. The prescribed heads that connect this regional model to the greater TC basin vary in time in relation with the historical regional decline of the TC piezometric levels. The latter is observed in observation wells that are located both inside and outside of the study area.

The period taken as reference for steady-state calibration of the model is 1950, in which the TC was considered in a state of equilibrium on a basin wide level (UNESCO, 1972; OSS, 2003). Steady-state calibration consisted of reproducing the general piezometric maps for the phreatic and TC aquifers as well as the discharge rates at Nefzawa springs as measured in 1950. The time period from 1951 to the year 2000 was taken as reference period for transient calibration. The reproduction of the drawdown trend as well as the temporal reproduction of the total measured spring discharge were taken as calibration criteria. Note that the availability of discharge data makes the calibration exercise a well-posed problem. The comparison of the available observed and calculated piezometric values of the TC aquifer in 1950 indicates a satisfactory model calibration with a correlation coefficient of $R^2 = 0.71$ and a root mean squared error $\sigma = 3.77$ m. The calculated drawdowns over the period 1951 – 2000 compared well to the observed ones and do not show any systematic deviation (Kriaa, 2003). Finally, we consider the temporal reproduction of the total measured spring discharge as acceptable (Figure 2.13).

The water budget (see Table 2.5) confirms the ongoing aquifer mining. As of the year 2000, strong changes in the hydrodynamic regime of the aquifer systems compared to the steady state situation are calculated. The loss of water by evaporation decreases from 3.0 to 1.2 m³/s. This includes water being removed by the drainage nodes inside the Chott El Djerid as well as by evapotranspiration from the phreatic aquifer. The inflow from the saline Turonian in 2000 (4.1 m³/s) is 12 times the value calculated in 1950 (0.3 m³/s). In the steady state, exchange through the semi-pervious clay layer intercalated between the TC and the phreatic aquifer was solely upward, i.e. from the TC towards the phreatic aquifer. Contrary to that, a

Oases aquifer	1950	2000
<i>Inflow (m³/s)</i>		
Reservoir depletion	–	1.29
Exchange with TC aquifer	3.15	0.45
Recharge	0.01	0.01
<i>Total</i>	3.16	1.75
<i>Outflow (m³/s)</i>		
Exchange with TC aquifer	0.00	0.51
Evaporation and Aioun springs	3.05	1.23
On-farm drains	0.11	0.01
<i>Total</i>	3.16	1.75
TC aquifer		
<i>Inflow (m³/s)</i>		
Reservoir depletion	–	0.66
Exchange with phreatic aquifer	0.00	0.51
Exchange with artificial limits	4.87	6.02
Exchange with Turonian aquifer	0.35	4.14
<i>Total</i>	5.22	11.33
<i>Outflow (m³/s)</i>		
Exchange with phreatic aquifer	3.15	0.45
Pumping	0.87	9.27
Exchange with artificial limits	0.72	1.60
Nefzawa springs	0.48	0.01
<i>Total</i>	5.22	11.33

Table 2.5: The water balance calculated in 1950 and 2000 according to the regional flow model.

reversed leakage from the TDS enriched phreatic aquifer to the TC amounting to 0.5 m³ /s is found in the year 2000. The comparison of the TC vs. phreatic aquifer piezometry in 2000 indicates that the hydraulic head of the former is still above the critical level of the Chott Djerid. A gradient inversion in a regional sense therefore has not yet been established. However, the strong drawdown caused by both, the artesian and pumped wells, slowly progressed westward towards the Chott over the last fifty years. The future implications of that will be discussed in Chapter 2.3.7.

2.3.6 Transport Model

Based on the satisfactorily calibrated flow model, a transport model was built. The goal was twofold: to cross-validate conceptualization by the comparison of the historical salinity development with the calculated one and to get an understanding of the future relevance of the three salination mechanisms discussed above. For this purpose, the layers of the flow model were further discretized vertically in order to avoid instantaneous vertical mixing. The phreatic aquifer was divided into 3, the TC

into 10 layers. Vertical and horizontal permeabilities, the geometry as well as the boundary conditions of the 13 layer model were correspondingly adopted to conform to the 2 layer flow model. To arrive at a more or less realistic initial salinity distribution, crude but nevertheless representative values were assigned to each of the water bodies, fluxes as well as boundary conditions. A uniform TC porosity value of 0.01 was chosen. Similarly, the porosity of the phreatic aquifer was uniformly set to 0.2. The initial salinity distribution of the TC was taken from a 1950 map with values ranging between 1.5 g/l and 3 g/l (UNESCO, 1972). In the phreatic aquifer, we distinguish between the Chott region and the oases and Wadi aquifers. In the latter, we adopted a uniform salinity of 8 g/l that corresponds to averaged observation values.

In the Chott, salinity decreases gradually from 175 g/l in the north-west to 10 g/l on its fringes according to actually measured concentration values (Gueddari, 1980). Information on water quality of the Turonian is only available in the PIK where the Turonian dolomites form part of the TC as well as in a borehole drilled in the south-eastern part of the Nefzawa region. There, a TDS of 7 g/l was measured. Lacking more detailed knowledge, the boundary condition representing the Turonian was assigned a uniform TDS of 7 g/l as fixed concentration. The same holds true for the TC boundary conditions with fixed concentrations ranging from 1.5 - 3 g/l. The imposed concentrations in the agricultural drains correspond to averaged observed TDS values which are regularly measured by the CRDA-Kebili. They range from 4 g/l in winter to 25 g/l in summer. On average, representative values are 16 g/l in Douz-El Hsay, 12 g/l in the PIK and Kebili and 8 g/l in the other drains. In the Sebkhass present in the vicinity of the oases, a TDS of 100 g/l is imposed. Based on these assumptions, a more consistent initial concentration was subsequently calculated by flushing the aquifer in the undisturbed state over several thousands of years to arrive at an approximation of the state in 1950.

Subsequently, the period 1951 - 2000 was simulated. Figure 2.14 shows the results obtained in seven selected oases. These oases were chosen to be representative for the corresponding region, i.e. the Chott-bordering area (Piezo Negga, El Fauoar 2), PIK (Fatnassa, Ziret Louhichi), the Kebili region (Ras el Ain 4) as well the southern part of the Nefzawa (Douz 2bis, El Hsay 5b).

In Figure 2.14, the calculated TDS values have been shifted vertically to make the first measured TDS value coincide with the calculated value. This procedure allows to mask the calibration deviation in the reconstitution of the initial concentrations. Generally, the transport model validates our understanding of the salination processes in the Nefzawa. Whereas so far, the Chott is of no relevance with regard to an increase in TDS (Piezo Negga), the fingerprints of upwelling from the confining deep layers in the PIK (Ras El Ain 4) as well as backflow from agricultural drainage water (Douz 2bis, El Hsay 5b) are visible. Yet, in the latter cases, calculated trends of TDS development are too low. This may be an indication of either underestimated fluxes in the model from the saline sources or an underestimation of effective porosity n_e or both. It may also be related to a conceptual issue of the model. For

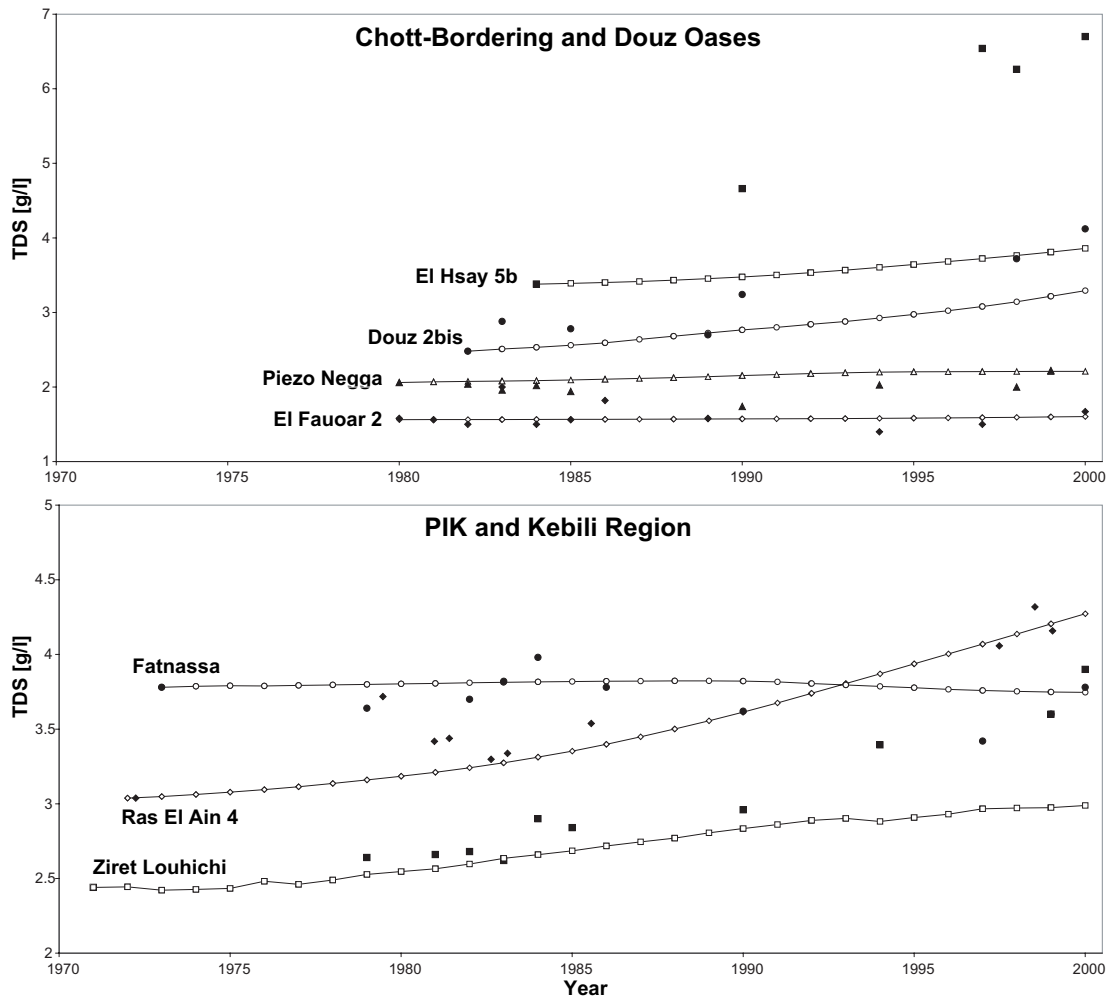


Figure 2.14: Comparison of calculated with observed TDS values for selected oases from the year 1970 to 2000. The filled dots are actual observations on TDS. Calculated TDS development is marked by the connected empty dots. The calculated values have been shifted vertically to make them coincide with first observed TDS values.

the region of Douz and El Hsay, analysis of the available piezometric data relating to the deep wells indicate that the observed piezometric levels in TC boreholes located in a sector of 3 km in diameter vary strongly. The hydraulic head difference can reach 10 m corresponding to a hydraulic gradient of 5×10^{-3} while on average, the regional hydraulic gradient is 7.5×10^{-4} . This is an indication for considerable spatial variability of the hydraulic conductivity. The drilling logs indicate a multi-layer structure of the TC aquifer that is composed of two chalk layers separated by a semi-pervious layer formed by marls and clayey limestones. The deeper wells tap the second chalk layer whereas the less deep wells tap the first one. This probably explains the existence of a vertical gradient of hydraulic head and concentration. Unfortunately, there is not sufficient data available about top and bottom of the screens in those boreholes to define a correlation between water salinity and the lithostratigraphic nature of the screened formation. Structural issues of the TC and the phreatic aquifer in the Douz region remain an area of future research.

Clearly, the assumption of regionally homogeneous porosity is not appropriate since the time-scales of the observed and modeled phenomena do not match in the Douz area. A local zone of a strongly decreased porosity could be introduced in the TC that would indicate a more clayey nature of the aquifer, the calculated TDS trend would increase naturally due to increased transport velocity. Such modifications would also account for any unresolved variations of the conductivities of the fractured limestones (Chiang & Kinzelbach, 2001). Nevertheless, the lacking knowledge of the spatial distribution of effective porosity does not justify a departure from our assumption of a homogeneous regional parameter value. With regard to that, one has to keep in mind that our modeling approach which covers an area of more than 5000 km² is regional. Despite shortcomings of local nature of the transport model, the threat to agricultural productivity due to increasing TDS in the pumped water can be assessed for the whole of the Nefzawa.

2.3.7 Future Development

Despite its imperfections, the contaminant transport model was used to predict the impact of the long-term application of existing and planned extraction projects on groundwater quality. Thus, the groundwater simulation model was extended to the year 2050 for various management alternatives: *Scenario 1*) maintaining present withdrawals ; *Scenario 2*) decreasing present groundwater extraction related to increased allocative and technical irrigation efficiency in Tunisia and *Scenario 3*) increasing groundwater pumping according to the planned extraction projects of Algeria, Libya and Tunisia (Table 2.6). In the three scenarios, the time-variation of the prescribed head along the artificial limits over the period 2000–2050 is consistent with the results of the groundwater simulation model developed for the whole SASS basin (OSS, 2003).

Flow model results show that the maintenance of the present pumping rates as of 2000 over the next 50 years (i.e. Scenario 1) provokes an average additional

Case Study: The Nefzawa Oases

Year	2000	2050		
		<i>Scenario 1</i>	<i>Scenario 2</i>	<i>Scenario 3</i>
Algeria	20.9	20.9	20.9	53.6
Tunisia	14.4	14.4	12.2	17.7
Libya	7.4	7.4	7.4	18.4
<i>Total</i>	42.7	42.7	40.5	89.7

Table 2.6: Country-wide pumping (in m^3/s) in the TC according to withdrawal scenarios investigated.

Fluxes	Scenario 1	Scenario 2	Scenario 3
Reservoir depletion	1.71	1.18	6.09
Phreatic aquifer	1.09	0.36	1.98
Artificial limits	1.86	2.45	-3.71
Turonian aquifer	6.32	4.81	7.58
On-farm drains	0.15	0.09	0.16
Pumping	-9.27	-7.62	-9.37
Evaporation and Aïoun Springs	-0.78	-0.92	-0.77

Table 2.7: Summary of the fluxes (in m^3/s) in 2050 according to scenarios (> 0 : inflow into TC; < 0 : outflow from TC).

drawdown of 20 m in the Nefzawa region. In the second scenario, it was assumed that irrigation water efficiency in the Djerid and Nefzawa oases could be increased by 15% by means of capital investment to modernize deficient irrigation networks and technology. This could then, of course, imply a corresponding reduction of 15% in the total pumped quantity. In this case, the average additional drawdown in the Nefzawa would amount to approximately 9 m. Scenario 3 finally, explores regional effects by a cumulative increase of more than 100% in pumping over the whole TC basin. Model results in this case yield an average additional drawdown of 34 m.

The results from the scenario analysis backs the conjecture that all three pumping strategies cause a major quality deterioration of the waters of the TC all over the Nefzawa (see Figure 2.15). The already affected PIK (Ziret Louhichi, Ras el Ain 4) and Douz (Douz 2bis, El Hsay 5b) region show an even more pronounced TDS development than the Chott-bordering oases (Piezo Negga, El Fauoar 2). According to Scenario 3, TC groundwater pumped in the southern Nefzawa will become unusable for irrigation purposes with the TDS load close or even above 6 g/l towards 2050. In fact, it is in the southern part of the study region where according to governmental planning abstractions should be increased most. Scenarios 1 and 2 do not show any significant difference in their negative influence on water quality. The reduction in pumping by 15% lowers the influx from the Turonian as well as the phreatic aquifer (see Table 2.7). However, salinity still rises although at a lower

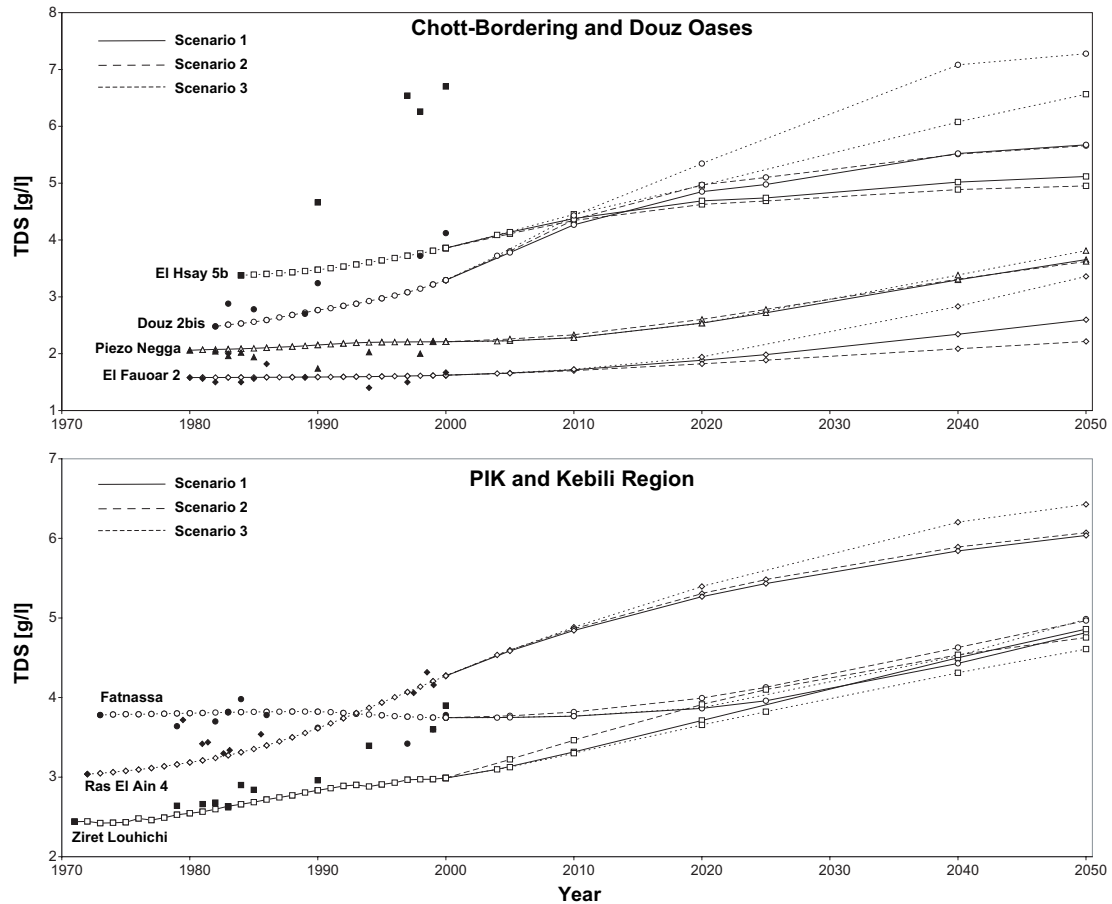


Figure 2.15: TDS development from 2000 – 2050 according to the scenarios. The filled dots are actual observations on TDS. Calculated TDS development is marked by the connected empty dots. The calculated values have been shifted vertically to make them coincide with first observed TDS values. The TDS rise in the Chott bordering area is not induced by brine. Rather, it depicts the general TDS rise in the TC caused by upwelling of Turonian/IC water and backflow of agricultural drainage water.

rate. Therefore, this measure is not sufficient to stabilize salinity at present levels.

2.4 Conclusion

The simulation results show, that neither present nor planned pumping schemes for the Nefzawa region are sustainable. All scenarios investigated show a strong decline in the general piezometric levels. However, the main concern is due to quality issues. All over the study area, a pronounced regional TDS increase will be observed. As in the case of the Douz region, the locally pumped TC water would have to be diluted with fresher water in order to be still suitable for irrigation purposes. The northern part of the Nefzawa and the PIK region are mainly affected by Turonian

upwelling which is promoted by the lowering of the TC piezometric heads. Since the overall pumping on the whole basin is responsible for this to occur, local measures of reduced pumping are only of limited effect there.

In the region of Douz, drainage water backflow is the main cause for salination. With regard to this, a simple back of the envelope calculation is instructive. The TDS of the pumped TC water derives from the mixture of phreatic aquifer, TC and Turonian water. By using calculated average fluxes and concentrations of the individual contributions, it is easy to show that a 50% reduction of drainage water backflow would cause a TDS reduction in the pumped water of 21%. A backflow reduced by 75% would lead to a TDS reduction of 32% and result in an average concentration of 3.5 g/l. Evidently, the replacement of the traditional furrow irrigation by PVC tubes, a switch to precise irrigation practices as well as removal of drainage water from the area are effective measures to stabilize TDS values.

Transport model results revealed problems in the south-eastern part of the model. Sensitivity analysis showed the importance of the effective porosity parameter on results. Model results could certainly be improved by better knowledge of the distribution of this parameter.

Control measures to limit TC contamination would include the following. First, planned extraction projects in the south of Nefzawa have to be abandoned. Second, pumping will have to be significantly reduced within the Nefzawa region and the extension of the irrigated perimeters halted so as to minimize the contamination risk from the sources of salinity discussed above. Continuation of the present pumping regime cannot be sustained over the next 50 years. The rise in salinity of TC water would necessitate a relocation of the TC pumping to more distant places and its subsequent conveyance to the fertile oases soils. Although the private farmers agricultural production is more efficient with regard to their input vs. output relationship, their borehole drilling and pumping activity is not monitored and the uncontrolled growth of their perimeters is not supportable under the prevailing conditions in the Nefzawa. Legal regulation could help to avoid a further increase of groundwater utilization by private farmers not subject to governmental planning. Third and finally, increasing irrigation efficiency as well as the implementation of effective drainage measures should go hand in hand with a strategy of moderation.

Chapter 3

Regional–Scale Simulation Optimization Approach

3.1 Introduction

The problems described in Chapter 2 related to a particular oasis and its irrigated agriculture are widespread in the arid environment (Hillel, 1994). They have become more severe with increasing public and private investments in irrigated agriculture and are directly threatening these projects (Pérennès, 1993). Figure 3.1 shows the piezometric heads in the IC aquifer in 1950 and 2050 as calculated by a finite difference aquifer model. The red areas in the right graphic of Figure 3.1 indicate regions where drawdown has reached an economic scarcity depth from which it is no longer economically feasible to pump water for agricultural use. Libyan Water Authorities, for example, consider a drawdown of more than 200 meters to cause forbiddingly high lift costs (oral communication with O. Salem and L. Madi, GWA Libya, 2001). As a consequence, pumping will be halted until a substantial recovery of the head is observed or, in case of no recovery due to a regional lowering of piezometric pressure, completely stopped. Furthermore, the absent salination threat in the Nefzawa by brine from the Chott Djerid does not preclude this danger in other oases locations that are situated around the salt lakes in Algeria and Tunisia. Similar conclusions hold true for the north–eastern costal areas in Libya where the possibility of sea water intrusion exists.

Options to alleviate these problems exist. Since water, unlike soil, is a mobile resource, it is conceivable that pumping could be redistributed upon the existing infrastructure so as not to violate such drawdown and gradient inversion constraints. In doing so, a planner would consequently seek a pumping configuration that promises the greatest overall benefit with regard to capital invested.

To evaluate such strategies that ensure the highest benefit, both, inputs and outputs would have to be valued. As we have seen in the case of the Nefzawa Oases, productivity even within a single oasis is greatly variable and has to be estimated with proxy data that, for a basin of more than 10^6 km², is not readily available (see Section 2.2 in Chapter 2). Furthermore, considerable uncertainty exists as to how to aggregate benefits on a basin–wide level. The problems related to this aggregation are extensively discussed by Haimés (1977). A more modest approach is taken here. We calculate the costs of public irrigation water provision as proposed by the decision–makers, i.e. the *Status Quo* allocation scenario and investigate whether these can be minimized by intelligent distribution of pumping over a certain time horizon under compliance to resource and environmental constraints. The social planner therefore seeks to minimize the present value of the future cost stream

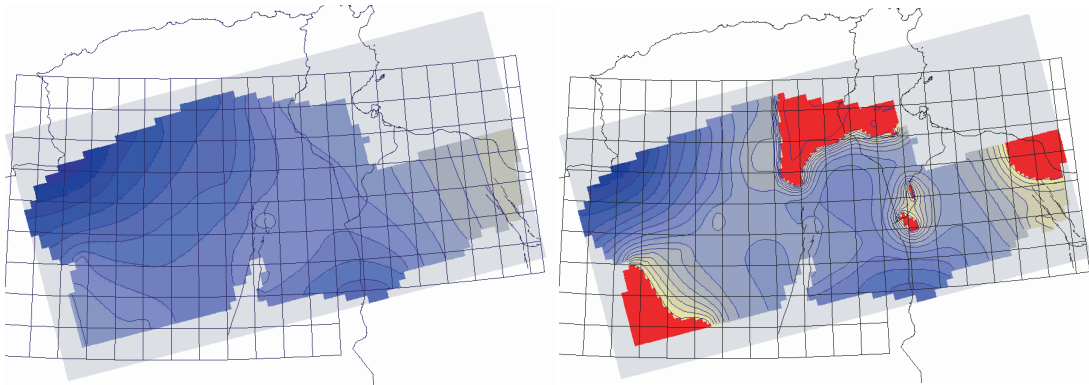


Figure 3.1: Piezometry of the IC aquifer at different years. Left: Undisturbed heads in the year 1950 (initial model condition). Right: Heads calculated in 2050 with a tripled basin-wide demand over the next 50 years (Abegglen *et al.*, 2001b).

$$\int_0^{T_{end}} \exp^{-\delta t} (\hat{g}(\cdot)) dt \quad (3.1)$$

over the planning horizon (compare Equation 1.2 in Chapter 1). Due to the scale of the resource and the fact that more than 50% of the public sector investment in agriculture is related to water provision in Northern Africa (Pérennès, 1993), capital gains due to such optimal resource management, if any, will be considerable. In Tunisia for example, the cost of irrigation development for the public schemes varies between \$US 6'000 and 7'000 \$US/ha depending on the size of the scheme (in year 2'000 \$US). The annual operation and maintenance costs are about 130 \$US/ha (FAO, 2004b). Clearly, freed capital assets resulting from an optimal management enhance social welfare. Intrinsically related to that, it would increase national income defined as the amount of consumption that can occur without the depletion of one's wealth, including natural resources. Such will be our motivation in the following simulation–optimization approach. For that purpose, a finite difference model of the NWSAS is developed and consecutively coupled with an optimization algorithm to identify cost minimizing allocation patterns in time and space.

3.2 NWSAS Finite–Difference Aquifer Model

A finite difference groundwater model was realized in PMWIN using MODFLOW (Chiang & Kinzelbach, 2001; Harbaugh & McDonald, 1996). It provides the feedback necessary to evaluate strategies. The detailed description of the model development and its calibration can be found in Abegglen *et al.* (2001b), Abegglen *et al.* (2001a) and Beck (2002). The initial cell discretization was chosen to be 25 km x 25 km. For later use in the simulation–optimization calculations, a coarser model with cell size 50 km x 50 km which was built upon the detailed one, was utilized. The aquifer layers were modeled to be partially convertible between confined and unconfined,

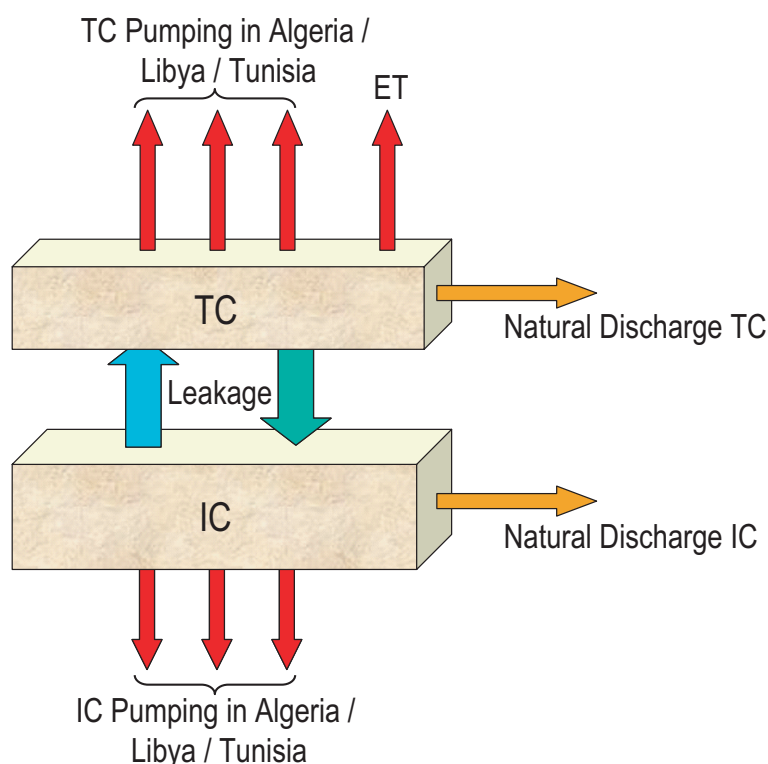


Figure 3.2: Conceptual model of the NWSAS used in the implementation of the finite-difference model. The TC and IC aquifers are connected by a leakage term without the explicit modeling of the Cenomanian aquiclude.

transmissivity being constant throughout simulation. The incorporation of layer geometry allowed representing the change in storage in case of aquifer conversion from confined to phreatic due to pumping. Aquifer geometry was derived from geological cross sections published in UNESCO (1972) and Pallas & Salem (2000). Generally, hydrogeological data on the Libyan part of the NWSAS was difficult to obtain. It was assumed that the topography corresponds to the top of the TC. The topography was determined by the establishment of a digital terrain model based on GTopo30-Images (USGS, 2001).

A leakage term depending on rock properties and thickness of the separating Cenomanian establishes hydraulic contact between the IC and TC. Drain cells were used to represent the Algerian-Tunisian Chotts, the Foggaras of the Adrar region in western Algeria and the Libyan spring Ain Tawargha because they adequately reproduce the physical nature of the sinks dewatering the system while at the same time they become inactive once the piezometric heads fall below the drain level. Due to the lacking knowledge about present day recharge quantity and its location (Edmunds *et al.*, 1997) as well as the fact that already present day withdrawal greatly exceeds recharge estimates, it was decided not to incorporate present day recharge. This causes our calculations to be conservative.

Regional–Scale Simulation Optimization Approach

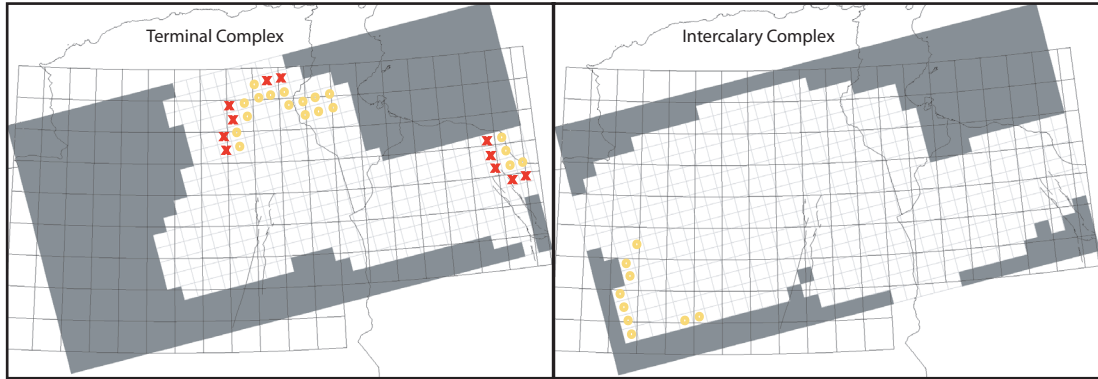


Figure 3.3: Left: Finite difference (FD) grid of the TC aquifer. Right: FD grid of IC aquifer. Grey cells are inactive. The national borders of Algeria, Tunisia and Libya are shown. Cell size is 2500 km^2 . The yellow circles indicate drain cells, the red cross are head gradient restricted cells.

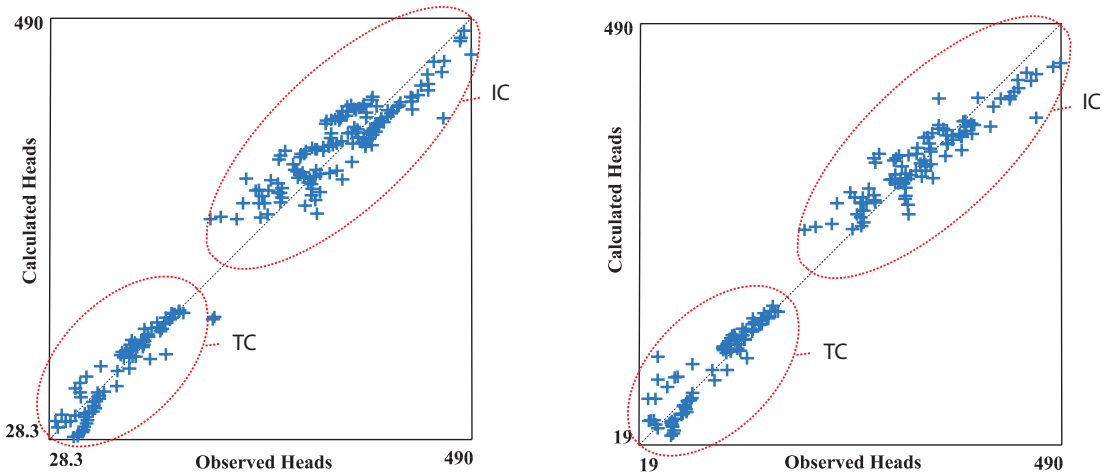


Figure 3.4: Left: Comparison of calculated vs. observed heads in 1950 after calibration of the steady-state model, $\sigma = 22.7 \text{ m}$. Right: Ditto for transient model showing head comparison in 1970, $\sigma = 21.9 \text{ m}$.

Leakage and transmissivity zones were determined according to geological aquifer properties. A total of 9 parameters (transmissivity, leakage and drain conductance) were calibrated for the steady-state model using data from 1950 (Sahara and Sahel Observatory, 2000). For the calibration of the transient flow model parameters (storage coefficient and specific yield), data from 1950 to 1970 were available. The comparison of observed vs. calculated heads as well as drain yields of springs were used as quality measures. Figure 3.4 shows calibration results. Generally, a satisfactory calibration with no systematic errors resulted with a standard deviation of about 22m over a head range of approx. 470 m.

Well documented spring yields exist for the western, central as well as eastern

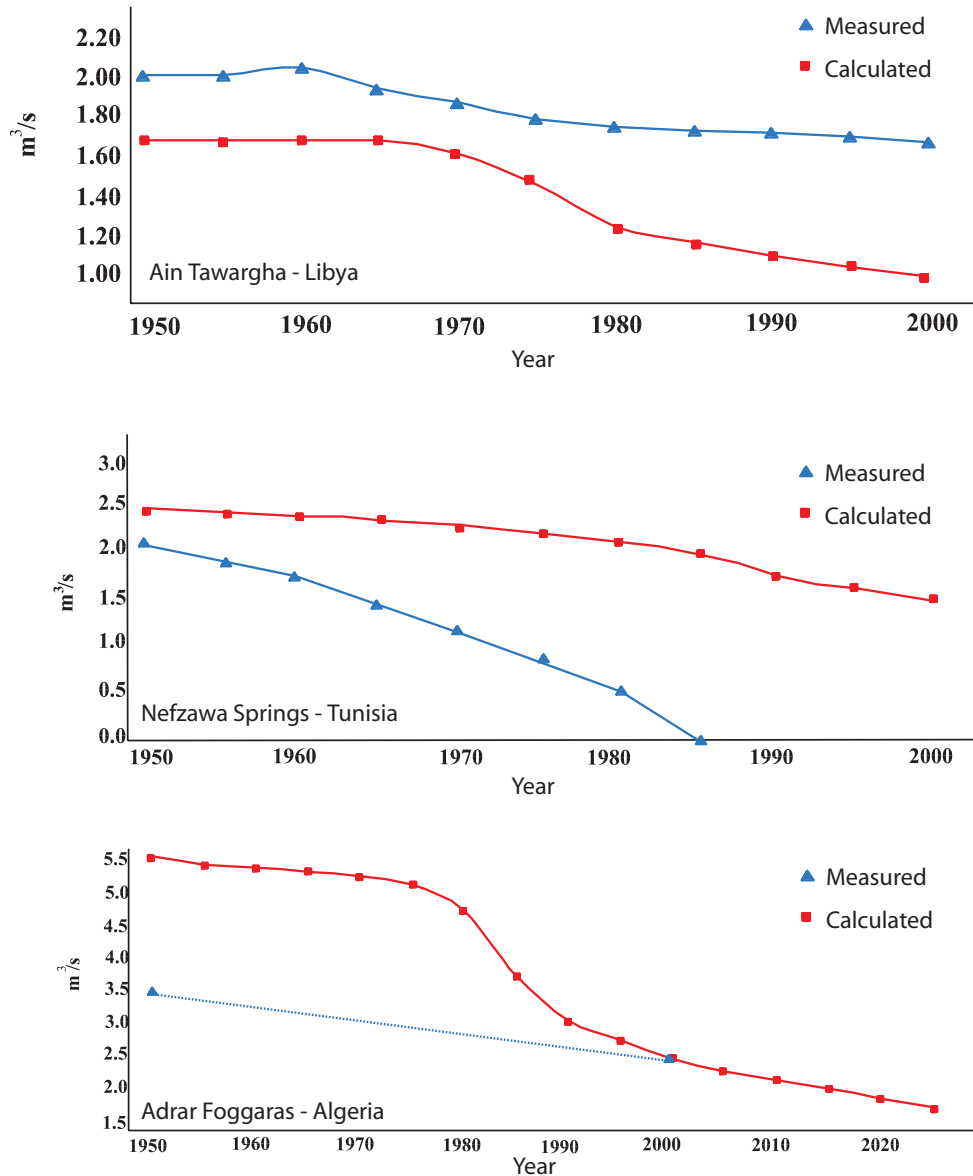


Figure 3.5: Reproduction of spring yield by the NWSAS model.

basin of the NWSAS. The reproduction of those by the model is shown in Figure 3.5. Apart from the Nefzawa springs reproduction, the declining yields are reproduced. The Nefzawa springs however ran dry in the mid-eighties whereas model yield decline is generally too slow (see also Section 2.3). This might be related to the fact that the Nefzawa springs were found on so-called spring mounds. These mounds are generally 10 m to 30 m higher than surrounding topography. The model resolution is not adequate to resolve this topographic variation which determines the time when a spring runs dry given a declining piezometry. Another reason might be the storage coefficient which was assumed to spatially constant.

3.3 Optimization Formulation and Methodology

A decision has to be taken on how to meet future water demand over a certain time horizon T_{end} . Obviously, many ways exist in doing so, the sole constraint being the demand at a certain time and location. The object of the problem is to determine the allocation distribution of TC/IC groundwater over time and space which minimizes the discounted costs of meeting a set of final demands and constraints.

Algeria, Tunisia and Libya have existing infrastructure and expansion plans leading to the growth of demand $Q(t)$. It is conceivable that the predetermined demand can be redistributed upon the present and planned system so as to minimize costs. In order to get a preliminary estimation of such possible benefits, a linearly constrained optimization formulation is utilized to solve the simulation–optimization task. The only costs that occur in this model are the groundwater lift costs, i.e. energy costs. Infrastructural costs are not accounted for in this approach as distributed infrastructure is assumed constant in time.

In mathematical terms, we seek to minimize

$$f = \sum_{t=1}^{T_{end}} \left(\sum_{i,j} ((1 + \delta_i)^{-t} c_{i,j}^t h_{i,j}^t(q_{i,j}(t)) \Delta t) \right) \quad (3.2)$$

subject to

$$\begin{aligned} \mathbf{h}_{i,j}^t &\geq \mathbf{h}_{i,j}^{lb} \\ \nabla \mathbf{h}^t|_{i,j} &\geq 0 \\ \sum_{i,j} q_{i,j}(t) &= Q(t) \\ q_{i,j}(t) &\leq q_{i,j}^{max}(t) \end{aligned} \quad (3.3)$$

where $h_{i,j}^t(q_{i,j}(t))$ is the head in stress period t at location j in country i and $Q(t)$ is the basin–wide future demand. Note that Equation 3.2 is the discrete–time formulation of Equation 3.1. Quite arbitrarily, yet in accordance with the planning horizon of the three countries, T_{end} has been set to 50 years. $(1 + \delta_i)^{-t} c_{i,j}^t$ is the time–value of the associated pumping cost with δ_i being the discount rate. Δt is the length of stress period t . $h_{i,j}^t$ is the head at location i, j at t and $h_{i,j}^{lb}$ the drawdown constraint at that particular place. $\nabla \mathbf{h}^t|_{i,j} \geq 0$ are gradient constraints where applicable (see Figure 3.3 for the location of these constraints). The gradient constraint criteria can be thought of as being head constraint criteria in the finite difference cells that are neighboring cells of potential sources of salination.

Because soils suitable for irrigation are limited in extension at particular locations, pumping restrictions $q_{i,j}^{max}(t)$ on individual cells are added (Sahara and Sahel Observatory, 2002, and oral communication with P. Pallas, 2002). The candidate

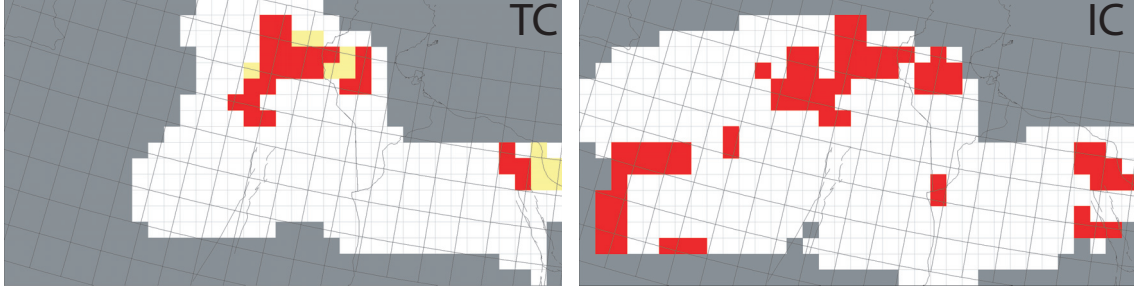


Figure 3.6: Candidate well locations in both aquifers, the TC and IC upon which the total basin-wide demand is distributed as proposed by the simulation-optimization model. Each FD cell has an upper yield limit so as to prevent pumping to be concentrated within a single region, leaving others 'dry'.

stress locations i, j were chosen to lie within present and future agricultural development areas or in close proximity to those (see Figure 3.6). Like this, 104 such locations were identified in 10 stress periods of 5 year durations thus yielding a total of 1040 decision variables. For the purpose of this investigation, it was assumed that $Q(t)$ grows linearly with t over the next T_{end} years (cf. scenario CI8 in Sahara and Sahel Observatory (2002)). Traditional gradient-based optimization methods are capable of efficiently solving such a problem.

The discontinuity of the derivatives in the drain flux and switching from confined to unconfined conditions with respect to aquifer head introduce non-linearity. Sequential linear programming was used to express head as a function of stress in the vicinity of the current solution point (Ahlfeld & Riefler, 2003). Like this, the head response $h_{i,j}^\tau$ at location i, j and time τ with $0 < \tau < T_{end}$ to a change in stress $|\mathbf{q}^{n+1}(\tau) - \mathbf{q}^n(\tau)|$ can be approximated by

$$h_{i,j}^\tau(\mathbf{q}^{n+1}(\tau)) = h_{i,j}^\tau(\mathbf{q}^n(\tau)) + \sum_{t=1}^{\tau} \sum_{k,l} \frac{\partial h_{i,j}^\tau(\mathbf{q}^n(\tau))}{\partial q_{k,l}(t)} (q_{k,l}^{n+1}(t) - q_{k,l}^n(t)) \quad (3.4)$$

where $h_{i,j}^\tau(\mathbf{q}^{n+1})$ is the head in the neighborhood of the optimal stress \mathbf{q}^n obtained by solving the n^{th} linear program and \mathbf{q}^{n+1} is the perturbed stress. The above head approximation can be plugged into Equations 3.2 and 3.3 which makes the problem linear in its objective and the conditions are purely stated in terms of stresses $\mathbf{q}(t)$. Hence, equation 3.2 becomes

$$f = \alpha + \sum_{\tau=1}^{T_{end}} \sum_{i,j} \frac{c_{i,j}}{(1 + \delta_i)^\tau} \left[\sum_{t=1}^{\tau} \sum_{k,l} \frac{\partial h_{i,j}^\tau(\mathbf{q}^n(\tau))}{\partial q_{k,l}(t)} (q_{k,l}^{n+1}(t) - q_{k,l}^n(t)) \Delta t \right] \quad (3.5)$$

with $\alpha = \sum_{\tau=1}^{T_{end}} \sum_{i,j} h_{i,j}^\tau(\mathbf{q}^n)$. The term in the squared bracket is the summed history of influence of each well on itself and the others up to a certain stress period

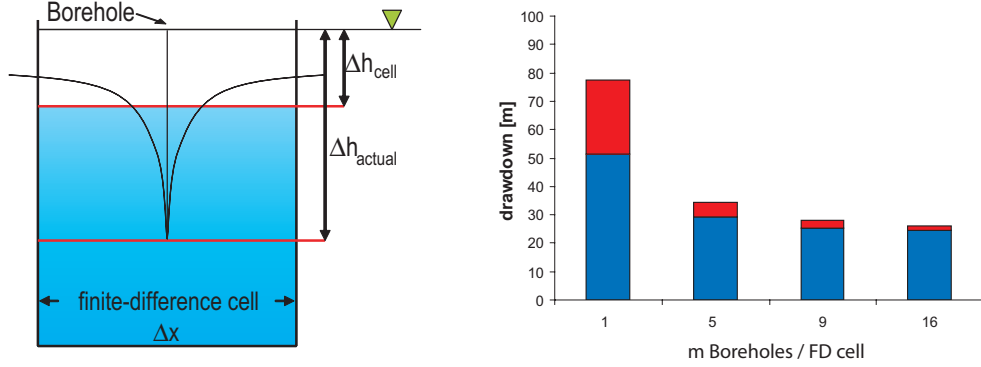


Figure 3.7: Left: Correcting the calculated drawdown in a finite difference cell. Right: Sample head correction as a function of the number of boreholes $m_{i,j}$ which, in total, pump $q_{i,j}(t)$ from a finite difference cell with $\Delta x = 5\text{km}$.

τ and the double summation of the squared bracket yields the cumulated effect over the optimization horizon T_{end} for each well.

The drawdown calculated by the finite difference model in such a regional model is an averaged value over the cell and does not correspond to the actual drawdown that is observed around a well (see Figure 3.7). Therefore, the $\frac{\partial h_{i,j}^\tau}{\partial q_{k,l}}|_{i=k,j=l}$ were corrected by a term $d_{i,j}$ derived from the Thiem-formula where

$$d_{i,j}(q_{i,j}) = 0.3665 \frac{q_{i,j}(t)}{m_{i,j} T_{i,j}} \log \left(\frac{\Delta x}{4.81 r_{BH}} \right) \quad (3.6)$$

with m being the number of wells that operate in a FD cell i, j assuming uniform pumping values within that particular cell, $T_{i,j}$ is the transmissivity, Δx the cell size and r_{BH} the radius of the pumping well. Equation 3.6 assumes that: a) flow is within a squared FD cell and can be described by a steady state equation with no source term except for the well discharge; b) the aquifer is isotropic and homogeneous within the FD cell; c) flow is laminar and d) head loss in the well is negligible (Prickett & Lonquist, 1971).

The solution of this optimization problem was obtained by a modified version of the MODOFC code (Ahlfeld & Riefler, 2003; Ahlfeld & Mulligan, 2000). The adapted code is available from the author upon request.

3.4 Sensitivity Analysis

Due to the non-linearity of the problem, the choice of perturbation values is critical. Therefore, sensitivity analysis for different perturbations Ψ was carried out. We found that choosing Ψ in the order of magnitude of the decision variables produces stable solutions. Figure 3.8 shows the normalized number of active wells ω inside a finite difference cell of the optimal solution as a function of Ψ (normalization with respect to the year 2000). ω has been calculated by equating the ratio of the

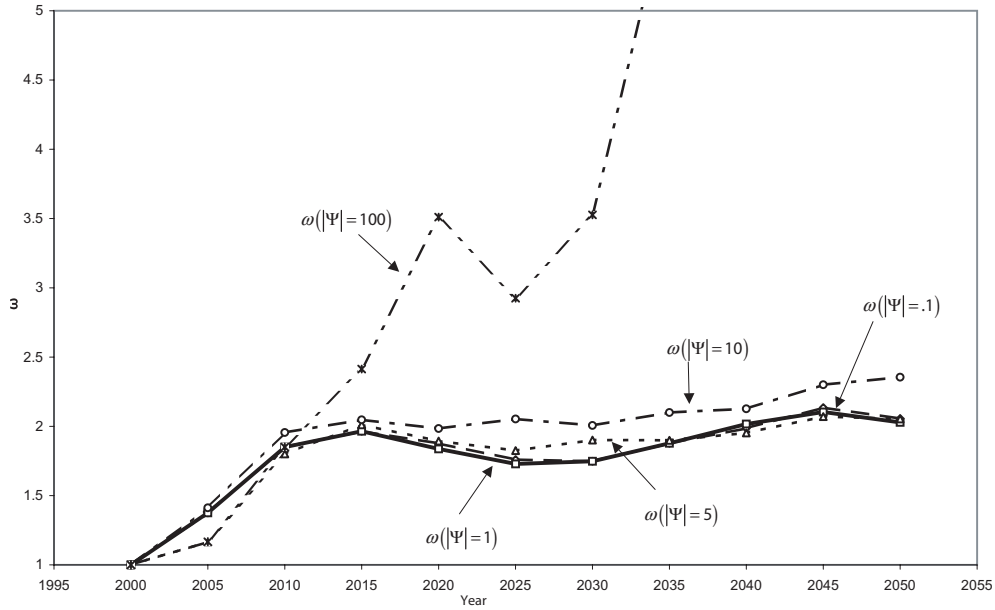


Figure 3.8: Sensitivity of the optimal solution to the choice of the perturbation value Ψ . ω as a function of Ψ is the averaged normalized well density at time t (averaged of all active FD cells and normalized with regard to the year 2000).

maximal regional yield per borehole and the pumped quantity determined by the optimal solution. Information on well yields has been provided by P. Pallas (oral communication with P. Pallas, 2002). Choosing $\Psi = 1$ bounds from below the set of solutions and therefore provides the least cost implementation.

The magnitude of the individual FD cell pumping restriction influences the optimization results. The less is allowed to be pumped at one FD cell, the more the optimal solution spreads over the candidate locations. Figure 3.9 shows the sensitivity of optimal solutions to different restrictions. The individual FD cell time-dependent pumping restrictions $q_{i,j}^{max}(t)$ were chosen to be proportional to the growth of the overall water demand $Q(t)$ multiplied by a scaling factor s with $s \in 1, 2, 3$. Hence, $q_{i,j}^{max}(t) = q_{i,j}^{max}(0) + s \cdot \Delta Q(t)$ where $q_{i,j}^{max}(0)$ is the actual pumped quantity within a FD cell in the year 2000.

The number of pumping FD cells at time t decreases with a relaxation of the constraints (upper curves in Figure 3.9). In this case, the more is allowed to be pumped in one FD cell, the less pumping has to be spread to the candidate FD cell locations. However, since the same overall demand has to be met, average borehole density in the active FD cells increases (curve ω^{UB} in Figure 3.9). The present model does not allow to decide which of the restrictions is most cost efficient since well installation and conveying costs are not accounted for. Therefore, we present optimization results depending on the choice of such restriction.

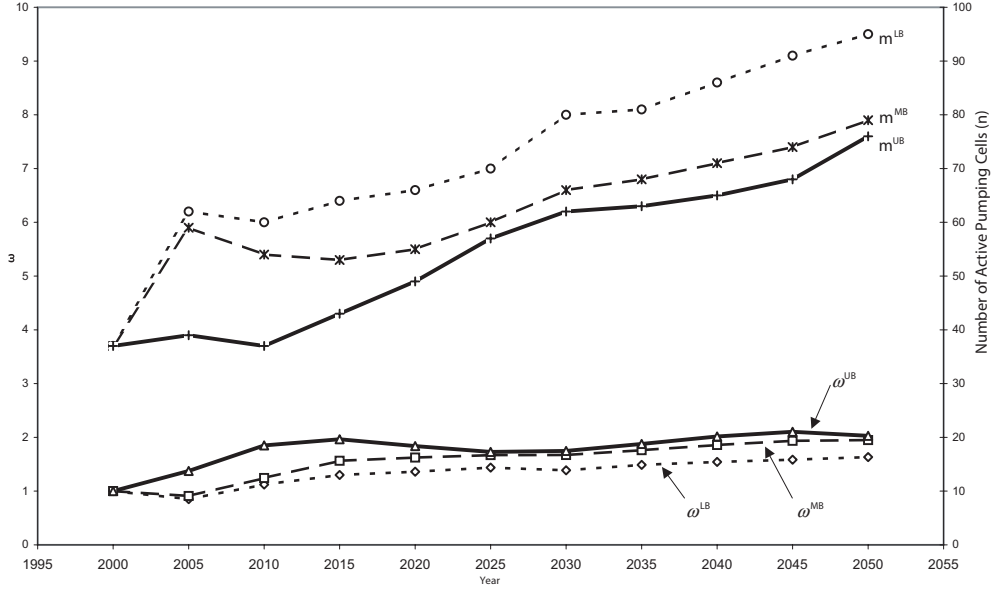


Figure 3.9: Sensitivity of the optimal solution to a variation in $q_{i,j}^{max}(t)$. Lower bound (LB): $s = 1$; middle bound (MB): $s = 2$ and upper bound (UB): $s = 3$. Number of active pumping cells m and average well density per pumping cell ω is given at time t is shown.

3.5 Results

After the 50 years period, the number of active pumping cells has approximately doubled (see upper curves in Figure 3.9). The curves indicate an early spreading of the pumping which is necessary so as not to drop below the economic scarcity depth of 200m during the course of simulation. The basin–wide demand can be covered over the next 50 years by the chosen pumping cells without violating any of the criteria in Equation 3.3.

Inevitably, the prices of groundwater provision will rise over the next 50 years because the countries are running down the resource. The special case of the NWSAS, with the easily accessible TC and the deeper IC resource suggests that the latter acts as a backstop to the former. As prices of TC abstraction rise and cheaper drilling technology are gradually available, the previously uneconomic IC stock becomes economically recoverable. This development has already been going on for some time as can be seen in Figure 3.11. The concavity of $q_{TC}^s(t)$ and convexity of $q_{IC}^s(t)$ in Figure 3.10 shows the continuing shift of the relative importance of the two aquifers in relation to each other with regard to future exploitation.

Capital recovery costs between the allocation as proposed by the countries, i.e. the *Status Quo* strategy) and the optimal solution can be compared. We calculate an average price for water which would have to be charged in order to exactly balance the sum of costs at the end of the payout period with a discount rate of $\delta = 3\%$. Under the assumption of similar basin–wide energy costs, these capital recovery costs can be lowered by 15% in the optimal solution compared to the *Status Quo*

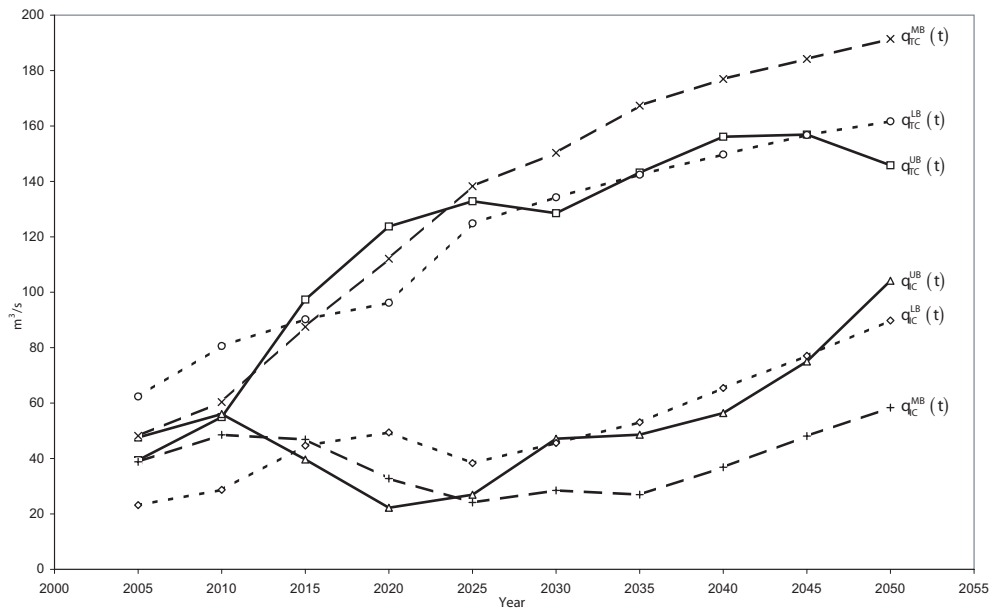


Figure 3.10: Distribution of the total pumping over the TC and IC aquifers. Sensitivity relative to $q_{i,j}^{max}(t)$ is shown.

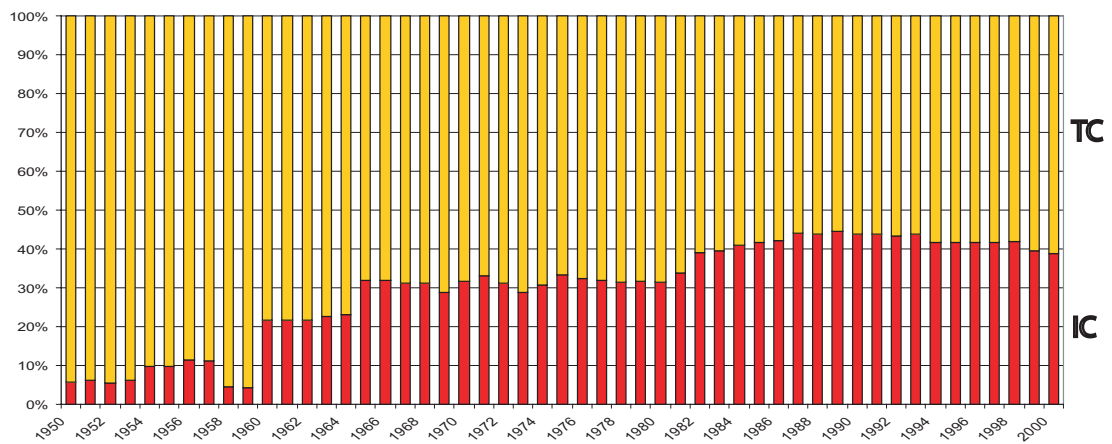


Figure 3.11: TC and IC percentage share of the total annual volume abstracted by Algeria, Tunisia and Libya. Data shown from 1950 to 2000 (Sahara and Sahel Observatory, 2002).

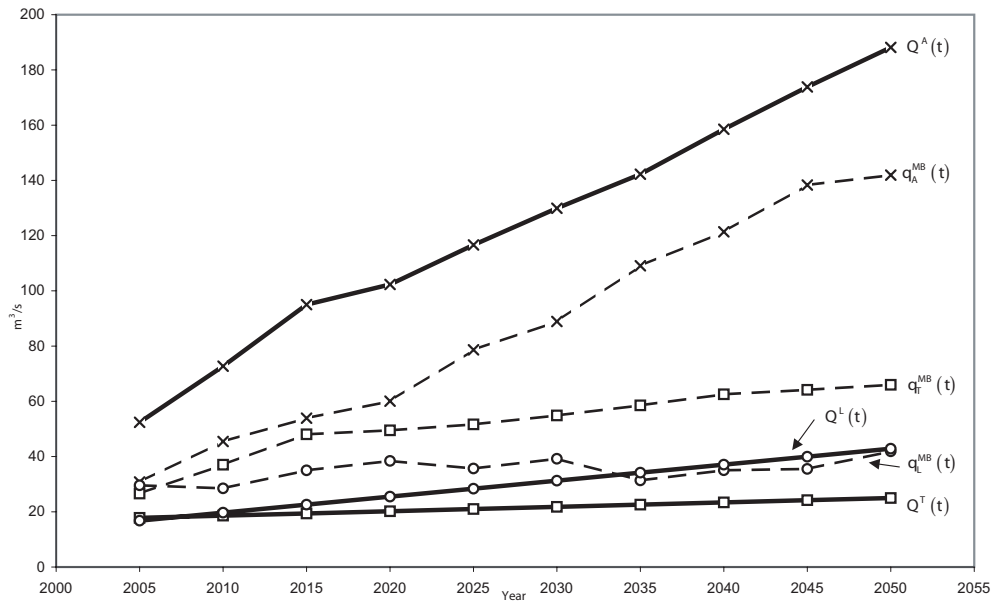


Figure 3.12: Planned country demand (bold lines) in comparison with the optimal solution for $q_{i,j}^{MB}(t)$ (dashed lines).

strategy. This benefit is on the order of magnitude of studies carried out by Noel *et al.* (1980), Feinerman & Knapp (1983) and Worthington *et al.* (1985) on other basins.

The distributive effect of the optimal solution is portrayed in Figure 3.12. The Figure shows that while Tunisia and Libya could pump more water compared to their planned allocation, Algeria would have to reduce future pumping activity by an average of 30%. This is due to the fact that the majority of the Algerian TC candidate well locations are restricted in their yield due to the gradient constraints. Additionally, the Algerian IC on average is 1000 m below surface. The heads at the Algerian pumping locations in the central part of the basin fall below the economic scarcity depth of 200 m after an average of 8 years. There, supply can no longer be secured through these candidate pumping locations.

Such findings show, that benefits from a redistribution of pumping over the system exist. However, it has to be kept in mind that these benefits are likely to be substantially reduced by the fact that transaction costs (e.g. conveyance costs), which result from the implementation of such scheme, result. Furthermore, a tri-national politics would have to be worked out so as to compensate Algeria for the foregone net benefit due to its reduced pumping. It is questionable whether such a solution will ever be implemented since it leaves no room for negotiation. Finally, the optimization did neither include installation nor conveyance costs. Under the consideration of these additional costs, the allocation characteristics of such optimal allocation scheme might substantially be altered. These problems inherent to our model formulation shall be addressed in the Chapter 4.

Chapter 4

Multi-Objective Groundwater Management Model

4.1 Introduction

The regional-scale simulation optimization approach presented in Chapter 3 was based on the assumption that an overall water demand can be spread over existing and planned pumping infrastructure so as to minimize associated provision costs. Its solution is determined entirely by the geometry and constraints of the problem, i.e. the aquifer properties, the head distributions and the development of the overall demand as well as the choice of given candidate pumping locations from which to pump from and the associated quantity restrictions placed upon them.

The optimization formulation, however, seems to be overly restrictive with regard to available options. In Libya, for example, the decision to pump groundwater to the coast from distant places in the southern desert was taken 20 years ago. As a result, one of the biggest water related engineering projects, the so-called *Great Man Made River*, was constructed. At full capacity, Libya plans to pump 5×10^6 m³/day from the desert to the coast to supply the population living there with drinking and irrigation water (Schliephake, 1995). The water will be transported over a total distance of more than 4000 km, including 2 aqueducts of approx. 1000 km length. The total project costs are estimated to be as high as 25 billion US\$ (year 1990 US\$). Figure 4.1 shows a main conveyor pipe as utilized in the *Great Man Made River*-Project with a diameter of 4 m. On first sight, the project, to which the Libyan government preferably refers to the *eighth wonder of the world*, seems megalomaniac. Yet, its defendants emphasize that such is a statement of the untutored eye. In fact - so their argument - the *Great Man Made River* is visionary, because future patterns of distant pumping and subsequent transportation of water to well defined demand centers inevitably will result due to increasing demand, local resource characteristics and constraints.

Options of groundwater management are restricted by the fact that soils suitable for agriculture in the Saharan desert and on its fringes are limited in extension. Furthermore, a majority of them is already under cultivation. Figure 4.2 shows agricultural soils in the Algerian central basin as identified by remote sensing in combination with ground truth validation (BRL, 1999). Agricultural production is therefore primarily constrained by soil productivity and not by lacking water availability. With appropriate capital investment, the latter can be secured. If local pumping and quality constraints can no longer be met, relocation of wells will have to happen. Unlike the previously suggested simulation-optimization approach, strategies of resource utilization therefore involve the choice of locating pumping and its relocation. As such, this allocation dynamics becomes part of realistic future



Figure 4.1: Conveyance pipe segment of the Great Man Made River-Project as displayed in Tripoli. The concrete pipes are pre-stressed steel wire enforced. The artwork inside the pipe segment depicts the successful struggle of the Libyan people against foreign aggressors while enjoying the benefits that result from the greening of the desert.

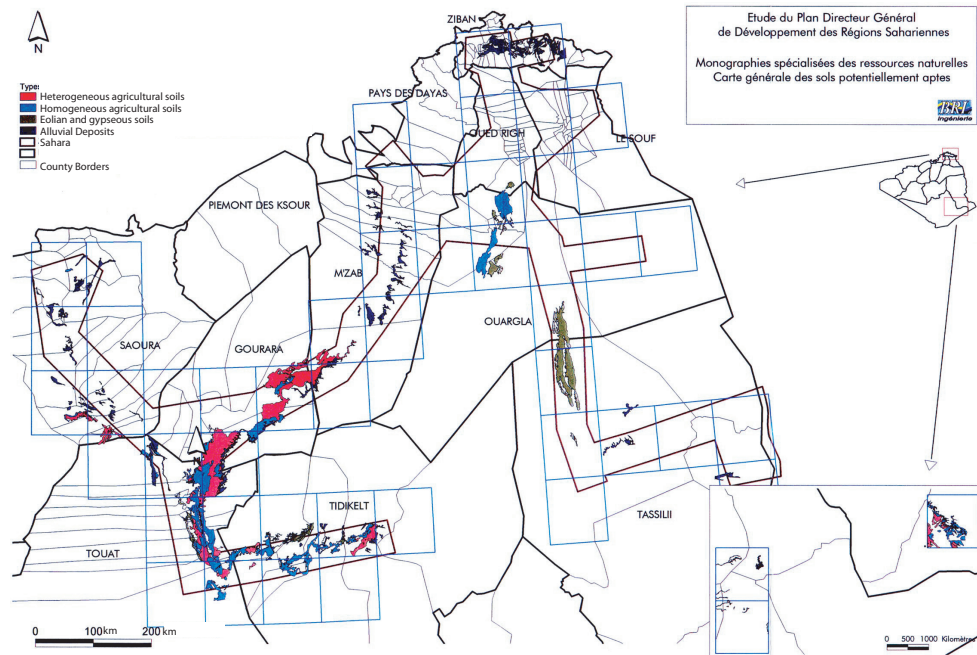


Figure 4.2: The limited extension of soils suitable for agriculture (colored red and blue) in the Algerian Chott region is shown. Map taken from BRL (1999).

groundwater resource utilization strategies.

A finite set of wells, as determined by the planners, can serve the agricultural demand centers with groundwater. Generally, any set of built wells with enough capacity connected through an appropriate conveyance network is sufficient for such purpose (see Figure 4.3). According to the planners preferences and resource as well as capital constraints, they might opt to concentrate a few boreholes locally. Similarly, environmental and capital constraints allowing, it might be preferable for them to spread the demanded quantity regionally over a large number of boreholes. Each one of the decision-makers faces the following set of questions,

- How many pumping facilities should be located?
- Where should such facilities be located?
- How should local water pumping be distributed over such facilities in time?

so as to minimize the associated costs, each one of the national planners having his own set of preferences. In the case of the transboundary NWSAS, there exists no benevolent dictator as a sole decision maker. The transboundary NWSAS implies multiple objectives from the start. The placement of wells in this system has a strategic component – namely the drawdown inflicted by one user upon the others. A particularly interesting configuration for planner *A* might be – circumstances permitting – to place his wells on the border to country *B* to effectively

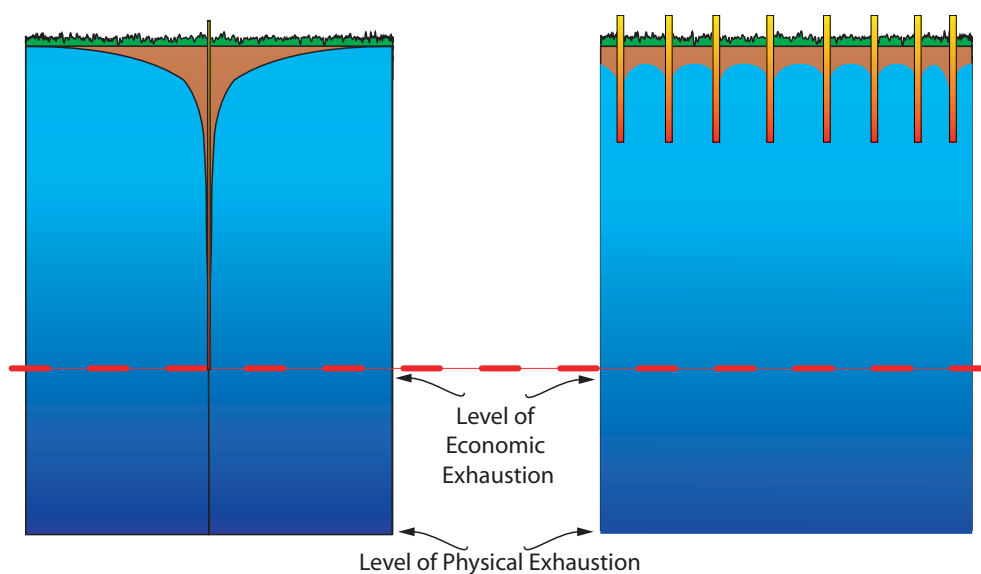


Figure 4.3: Management options in groundwater systems. The effects of different well configurations are shown. Left: A specified demand is pumped from one borehole, resulting in minimal infrastructural costs but leading to excessive drawdown. Right: The pumped quantity is spread over a large number of boreholes minimizing the drawdown while causing high installation costs.

divide the stock effects felt by his own by a factor of 2. Clearly, B would not be supportive of such a strategy. A national planner therefore also considers what the choice of his own allocation strategy implies upon the choices of the strategies of the other planners. Each spatial configuration is therefore a trade-off between the individual objectives of the planners involved. Any agreement on a basin-wide coordination of allocation depends on whether the outcome of such planning is an improvement over the *Status Quo* allocation, i.e. the payoff for each one of the planners if such agreement were to fail (Binmore, 1994). Instead of a single optimal allocation solution, a decision-supporting model for the allocation of a transboundary resource should therefore identify a set of compromise solutions, for which none of the trade-offs contained can be said to be better than the others in the absence of preference information. Such set is called a set of *Pareto-optimal* solutions upon which international negotiations can be based (see also Chapter 1).

4.2 Determinants of Spatial Allocation Patterns

Intuitively, optimal spatial patterns of groundwater utilization are governed by clumping or *centripetal* and dispersive or *centrifugal* forces (see Krugman (1996) for a discussion of such forces in a different context). Transportation costs limit the range from which water can be conveyed to a demand location since net costs augment with increasing transportation distance. However, the nature of aquifer re-

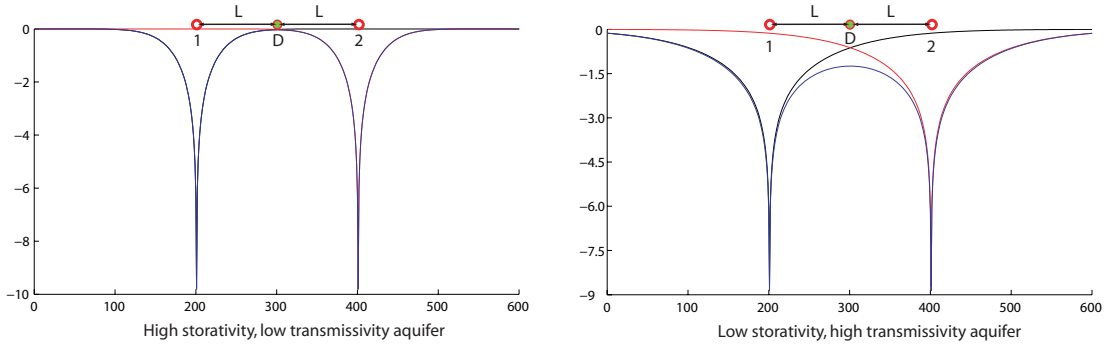


Figure 4.4: Two sample aquifers with drawdown caused by 2 players. The two users pump at a distance L from a demand center D .

response with logarithmic drawdown cones occurring at the pumping locations leads to increasing lift costs in time. Drawdown constraints imposed by a limited filter depth, local gradient constraints as well as an economic scarcity depth beyond which lift costs become forbiddingly high, all promote dispersion. That is, the relocation of pumping in the course of time to more distant places which, so far, are less affected by exploitation. We expect this dynamic pattern to be governed by aquifer properties and the ratio of transportation versus lift costs.

With the aid of a simple model, it is easy to show that this intuition is actually true. Let us assume a uniform confined aquifer structure with infinite extent and 2 users pumping water from 2 boreholes. The arrangement is shown in Figure 4.4. Both users pump water at a distance L from a demand center D to which it is conveyed.

For any pumping schedule $q_i(n)$ at location i with constant periodicity Δt , the drawdown at distance r and time $T_{end} = m\Delta t$ can be written as

$$h_i(m\Delta t, r) = w(\Delta t, r)q_i(m) + \sum_{n=1}^{m-1} \beta((m-n)\Delta t, r) q_i(n) \quad (4.1)$$

with

$$\beta((m-n), r) = w((m-n+1)\Delta t, r) - w((m-n)\Delta t, r) \quad (4.2)$$

and

$$w(t, r) = \frac{1}{4\pi T} \int_{a(r)}^{\infty} \frac{e^{-z}}{z} dz \quad (4.3)$$

T is the transmissivity, S the confined storage coefficient and $a(r) = \frac{r^2 S}{4Tt}$. Equation 4.3 is the well function (Bear, 1979).

If we assume similar and constant pumping rates $q_i(m) = q \forall m$ of both users and by using Equation 4.1, the drawdown at either of the two boreholes i and j at time $t = T_{end}$ can be calculated by

$$h_{i,j}(T_{end}, \vec{L}) = q \cdot (w(T_{end}, r) + w(T_{end}, 2(L - r))) \quad (4.4)$$

$\vec{L} = (r, 2(L - r))$ denotes the vector of distances. The right hand side term in Equation 4.4 is the drawdown component at location i caused by the pumping at i whereas the second term refers to the influence from the pumping that occurs at a distance $2(L - r)$ with r being the borehole radius. Here we make use of the fact that arithmetic summation of independent well functions can be used to calculate the drawdown through time at any point in the aquifer with multiple wells. This holds true because of linearity of the underlying transient flow equation (cf. Equation 1.3 in Section 1.2 of Chapter 1). For simplicity, let us denote the conveyance distance as $\lambda = 2(L - r)$.

A social planner is seeking a distance λ so that the summed stream of the present provision costs from time $t = 0$ to $t = T_{end}$, i.e.

$$g(\cdot) = 2 \sum_{n=1}^{T_{end}/\Delta t} \frac{1}{(1 + \delta)^{n-1}} \left(c_L h_{i,j}(n\Delta t, \vec{L}) q \Delta t + c_T \frac{\lambda}{2} q^3 \Delta t \right) \quad (4.5)$$

with $h_{i,j}(n\Delta t, \vec{L})$ given by Equation 4.4, gets minimized (for a derivation of the cost function $g(\cdot)$, see Section 4.5.3). In Equation 4.5, n denotes the n^{th} time period of pumping assuming constant schedule time intervals Δt . For the sake of simplicity, we do not account for initial infrastructural installation costs since their inclusion does not change the main conclusion. c_L is the cost of energy that determines the lift cost and incorporates pump efficiency η . Finally, c_T is a conveyance cost term. Since we have chosen $\Delta t = T_{end}$, the discount factor δ drops out of Equation 4.5.

The minimum is found by setting $\frac{\partial g}{\partial \lambda} = 0$. Doing so leads to

$$\frac{e^{-\frac{S\lambda^2}{4T\Delta t}}}{\lambda} = -\pi\kappa Tq \quad (4.6)$$

with $\kappa = c_T/c_L$ being the ratio between conveyance and pumping costs. The resulting expression involves λ in an essentially non-algebraic way. The solution for the optimal distance λ^* can be obtained by a computer algebra program such as *Mathematica*. Thus,

$$\lambda^* = \sqrt{\frac{2T\Delta t}{S} W\left(\frac{S}{2\pi^2 T^3 q^2 \Delta t \kappa^2}\right)} \quad (4.7)$$

with $W(\cdot)$ being the Lambert W -Function. Assuming transmissivity and storage coefficient values as well as a constant pumping rate, λ^* can be plotted as a function of the cost ratio κ . Figure 4.5 shows the results for 3 different aquifer properties. Generally, with increasing κ the transport costs start to dominate the lift costs, the optimal distance \vec{L} shrinks and vice versa. The limits are given by $\lim_{\kappa \rightarrow \infty} \lambda^*(\kappa) = 0$ and $\lim_{\kappa \rightarrow 0} \lambda^*(\kappa) = \infty$. Optimality requires a trade-off between conveying distance and drawdown due to the dual nature of the cost objective. This confirms that

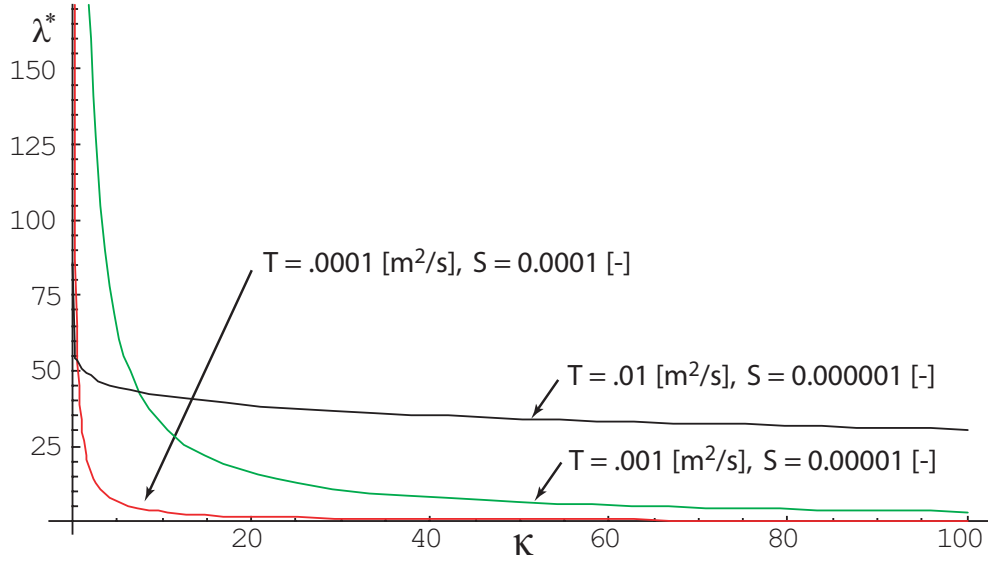


Figure 4.5: Optimal distance [m] between boreholes for different transmissivity (T) and storage coefficient (S) values as a function of the cost ratio κ for a given time t .

our basic intuition was not misleading. In the case of dominating transport costs, there is then relatively little interregional water transfer whereas in the opposite case, water transfer is favorable. In Figure 4.5, solutions for high storativity, low transmissivity (red graph) as well as low storativity, high transmissivity aquifers (black graph) and for an intermediate solution are shown.

Comparing Figure 4.4 and Figure 4.5, it is easily visible that, for a given cost ratio κ , the optimal distance λ^* shrinks with decreasing $w(\Delta t, \lambda)$ which is the additional drawdown imposed by one user on the other. If we treat the aquifer as a bathtub, i.e. we assume infinite transmissivity, the cost-optimal placement of boreholes vanishes since from Equation 4.7 follows: $\lim_{T \rightarrow \infty} \lambda^* = 0$. Thus, the additional drawdown (i.e. externality) imposed on one user by another determines an optimal spatial configuration and refutes the simplistic notion that *closer is always better*. Having said so, it is obvious that poor location decisions for resource allocation lead to increased costs and reduced economic efficiency. The optimization of the quantifiable cost objective in groundwater management should therefore incorporate location decisions as well as be based on realistic groundwater models, that reproduce the spatially and temporally variable heads.

A straightforward extension of the above formulation would be the spatial optimization of n boreholes that operate in order to supply a demand center. Similarly to Equation 4.4, the drawdown at location i would then become

$$h_i(t, \vec{L}) = q \cdot \left(w(t, r) + \sum_{j=1}^{n-1} w(t, \bar{L}_{i,j}) \right) \quad (4.8)$$

Multi-Objective Groundwater Management Model

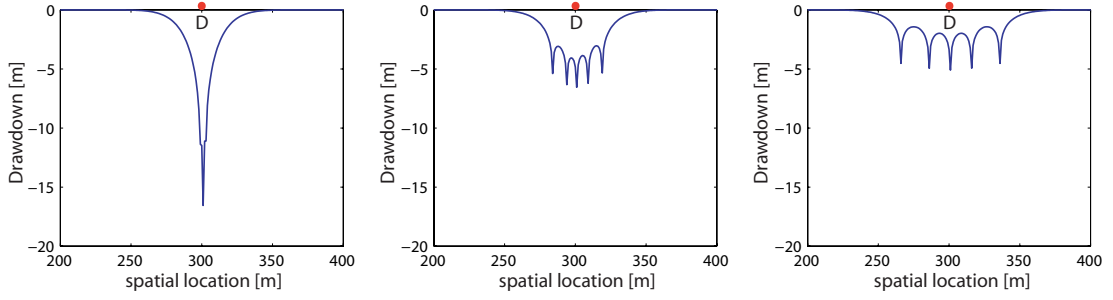


Figure 4.6: Sample incremental drawdown caused at time t by 5 boreholes placed so as to minimize provision costs. Left: $\kappa = 1$ (all boreholes collapse in one), Center: $\kappa = 0.1$, Right: $\kappa = 0.01$. Optimization carried out with the `fmincon`-Matlab function (MathworksInc., 2003a).

with $\bar{L}_{i,j}$ being the distance between the wells i and j . The size of the distance vector \mathbf{L} in this case is given by the number of boreholes n . The cumulative effect of well interference is larger for wells towards the center of the borehole cluster than for boreholes on the fringe of the pumping cluster as can be seen in Figure 4.6.

With $\Delta t = T_{end}$, the objective function in this case gets

$$g(\cdot) = \sum_{i=1}^n \left(c_L h_i(T_{end}, \vec{L}) q T_{end} + c_T \lambda_i q^3 T_{end} \right) \quad (4.9)$$

Note that the elements of the vector \mathbf{L} , i.e. the distances between boreholes, can be expressed as linear combinations of transportation distances vectors $\vec{\lambda}$. Hence, $\bar{L}_{i,j} = f_{i,j}(\vec{\lambda}) = \left| \sum_m \alpha_m \vec{\lambda}_m \right|$.

Again, by calculating $\partial g(\cdot) / \partial \vec{\lambda} = 0$, optimality requires that

$$\frac{\partial}{\partial \lambda_i} \left(\sum_{j=1}^{n-1} w(t, f_{i,j}(\vec{\lambda})) \right) = -\kappa q^2 \quad (4.10)$$

which means that the overall effect on each well from the remaining $n - 1$ wells must be equal for all wells (remember that pumping is the same at each well). This however is only true if there exists an infinite number of wells that pump from the aquifer. Only in this case, every well would get the same contribution of cumulated well interference. Hence, under the above assumptions, optimal uniform spatial allocation strategies with equidistant boreholes will not exist like in the case of the bathtub aquifer. Rather, we expect patterns to emerge which are determined by the aquifer nature and the cost structure of the problem. Figure 4.6 shows optimal borehole placement for 5 boreholes and different cost ratios κ as obtained by a numerical solution of the optimization problem given by Equation 4.10.

In the case of multiple boreholes operating, dispersive forces prevail if the overall costs can be reduced by increasing the spacing between the wells. This, however,

is only true as long as the contribution of a reduction of well interference is greater than the additional costs that arise due to greater conveyance length.

Wrong conclusions are likely drawn from incomplete simulation–optimization approaches that do not take into account the full provision costs and account for actual aquifer properties (for such approaches see for example Gisser & Sanchez (1980); Noel *et al.* (1980); Lee *et al.* (1981); Feinerman & Knapp (1983); Nieswiadomy (1985); Worthington *et al.* (1985); Brill & Burness (1994)). The problem formulation in these cases was constrained by the optimization method at hand and often, overly simplistic assumption about the nature of the modeling system had to be taken. Most of these methods use a deterministic point–to–point procedure for approaching an optimal solution and are not capable of handling complex, non–linear, mixed discrete–continuous constrained problems. The development of recent stochastic optimization techniques has helped to overcome such deficiencies and has allowed the approximation of optimal solutions of realistic physical and economic models. Such a model will be introduced in the following.

4.3 Model Formulation

The simulation–optimization model presented here belongs to the class of location–allocation problems (Daskin, 1995). It has the following characteristics:

- The model is multi–objective with the three nations Algeria, Libya and Tunisia each one interested in identifying cost minimal solution.
- It associates present water provision costs with a groundwater allocation pattern by the coupling of the finite difference NWSAS model as presented in Section 3.2 of Chapter 3 with a nonlinear cost module. Facility installation costs of boreholes and pipelines as well as pumping and conveying costs are taken into account.
- It involves both, discrete (i.e. well location and the discrete time-varying control policy) and continuous decision variables (i.e. well yield) subject to conditions which any feasible solution must satisfy.
- Optimization is carried out without any prior preference information given. The resulting set of solutions are equally important and are the basis for negotiation.

The optimization goal is to *minimize* the vector valued objective function $\mathbf{g}(\mathbf{q}, \cdot)$ with

$$\mathbf{g}(\mathbf{q}, \cdot) = \left(\sum_{j=1}^m g_{A,j}(\mathbf{q}, \cdot), \sum_{j=1}^n g_{T,j}(\mathbf{q}, \cdot), \sum_{j=1}^l g_{L,j}(\mathbf{q}, \cdot) \right) \quad (4.11)$$

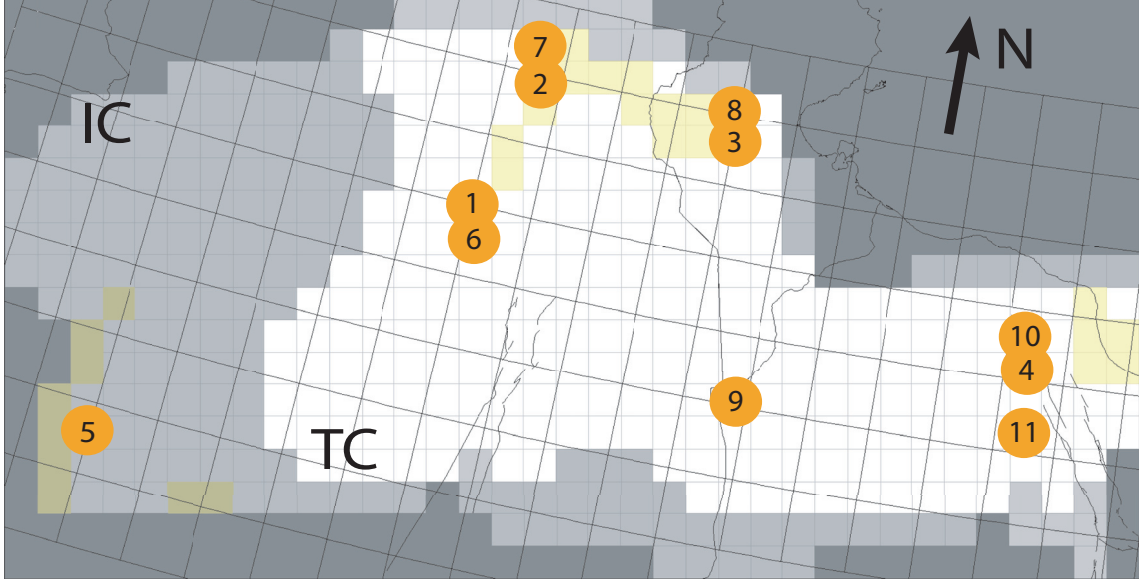


Figure 4.7: Demand centers in the model domain. Numbers refer to location and aquifers which are utilized there. 5: Adrar / Gourara / Turat / In Salah (IC); 1&6: Ghardaia / Zelfana / Ouargla (TC and IC); 2&7: M'Rhaier / El Oued (TC and IC); 3&8: Nefzawa, Djerid (TC and IC); 9: Ghadames (IC); 4&10: Libya Coast (TC and IC); 11: Libya Sud (IC).

subject to

$$\begin{aligned}
 \mathbf{h}_{i,j}(t) &\geq \mathbf{h}_{i,j}^{lb} \\
 \nabla \mathbf{h}(t)|_{i,j} &\geq 0 \\
 \sum_{i,j \in k} q_{i,j}^k(t) &= Q^k(t) \quad \forall k
 \end{aligned} \tag{4.12}$$

where \mathbf{q} is the decision vector of pumping depending on the location j and time t in country i . $g_{A,j}$ denotes the summed present costs for Algeria at its j th pumping location and $g_{T,j}$ resp. $g_{L,j}$ similarly for Tunisia and Libya. $\mathbf{g}(\mathbf{q}, \cdot)$ is the vector of the summed present costs stream from $t = 0$ to $t = T_{end}$. Equations 4.12 are head, gradient and pumping constraints and define the set Θ of feasible decision vectors \mathbf{q} . The $Q^k(t)$ is the water quantity demanded at a certain time by the k th demand center. The location of the demand centers within the NWSAS is shown in Figure 4.7. Each of these areas of agricultural production has a irrigation water demand $Q^k(t)$ that can be covered with any feasible well location and pumping distribution configuration.

The optimization task is to find a set Θ^* of Pareto-optimal location-allocation patterns $\mathbf{q}^* \in \Theta$ in the sense that an improvement in one component of $\mathbf{g}(\mathbf{q}^*, \cdot)$ can be achieved only at the expense of another. In mathematical terms, we seek to find

$$\Theta^* := \{\mathbf{q}^* \in \Theta \mid \nexists \hat{\mathbf{q}} \in \Theta : g(\hat{\mathbf{q}}, \cdot) \prec g(\mathbf{q}^*, \cdot)\} \quad (4.13)$$

with Θ^* being the set of trade-offs upon which future discussions on the common utilization of the TC / IC groundwater resources can be carried out.

4.4 Optimization Method

Traditional approaches of solving such problems relied on the aggregation of the objectives into a single, parameterized goal function. The optimizer would then systematically vary the parameters to achieve a set of solutions that approximate the Pareto-optimal set (Zitzler, 1999). These approaches however are sensitive to the shape of the Pareto-optimal front and generally do not exploit synergies between solutions that could help to reduce computational time of the search (Deb, 2001). This is a major drawback in cases where the search space is conceivably complex as in our approach.

A simple example of a location-allocation problem shall illustrate this and is shown in Figures 4.8 and 4.9. The problem for a social planner is to locate three boreholes that serve corresponding demand centers D_1 , D_2 and D_3 within the aquifer domain so that the associated single-objective, i.e. the summed present cost over a time horizon of 50 years, gets minimized. This cost is given by $\sum_{i=1}^3 g_i(q_i, \cdot)$ with each cost component $g_i(q_i, \cdot)$ being defined by Equation 4.17 depending on the pumping configurations. It is assumed that all three wells pump the same constant quantity $q_i(t) = q = 0.06 \text{ m}^3/\text{s}$ from time $t = 0$ to T_{end} . A squared, confined aquifer with edge length of 100 km and fixed potentials as western and eastern boundary condition (0 masl) is the underlying aquifer system. The aquifer is confined with transmissivity $T = 10^{-3} \text{ m}^2/\text{s}$ and a storage coefficient $S = 10^{-6}$. Drawdown constraints do not exist and the relocation of boreholes is not allowed during the course of simulation time.

The conveyance costs have been chosen to dominate the lift costs, i.e. $\tilde{c} = 1000$. Remember that \tilde{c} is the ratio between conveyance and lift costs. The optimal solution of such location-allocation problem would be to place the three operating wells at the corresponding demand center so that conveying costs would completely vanish. Depending on the 'quality' of the initial guess, the non-linear programming algorithm `fmincon` (MathworksInc., 2003a) fails to converge and gets trapped in a local minimum as shown in Figure 4.8. In contrast, the solution of this problem is readily obtained by using a stochastic optimization method, i.e. a genetic optimization algorithm (see Figure 4.9).

In the simulation-optimization groundwater literature, there exist several examples of the application of such optimization techniques that are inspired by evolutionary principles to nonlinear discrete-continuous problems. Dougherty & Marryott (1991) present a simulated annealing algorithm to solve groundwater management models formulated as combinatorial optimization problems. McKinney & Lin (1994)

Multi-Objective Groundwater Management Model

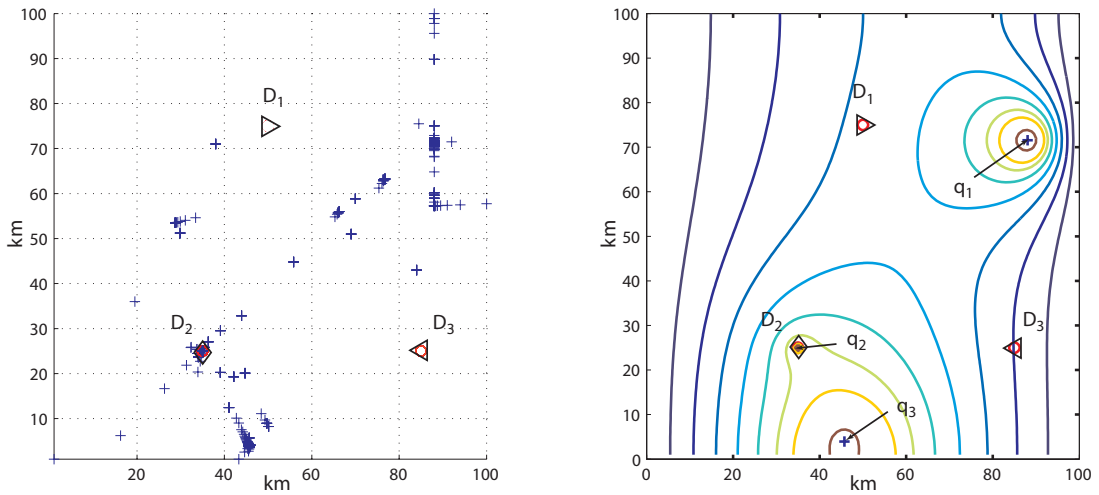


Figure 4.8: The failure of the minimization of a simple location-allocation model by utilizing a constrained non-linear programming algorithm. Left: Sampled locations during optimization search. Right: Final solution of well placement with corresponding piezometric head after 50 years. The triangles resp. diamond indicate the locations of the three demand centers D_1 – D_3 . The crosses in the right figure mark the well position q_i as proposed by the optimization.

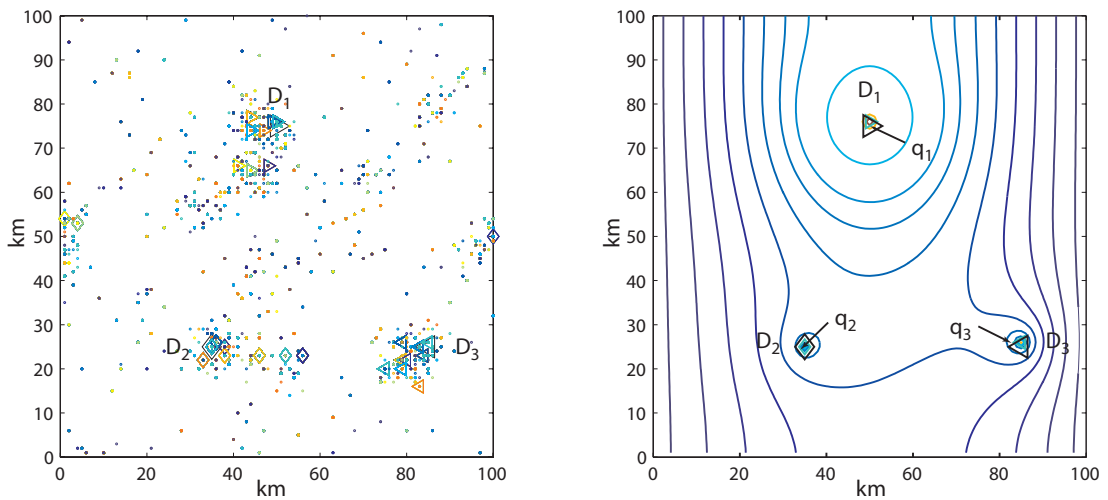


Figure 4.9: Optimal solution obtained by stochastic optimization using the multi-objective evolutionary algorithm SPEA2 (Zitzler et al., 2002). After 243 generations, the objective vector of the best individual can no longer be improved. Left: Sampled locations during search. Right: Overall best solution of well placement with piezometry after 50 years is shown.

use a genetic algorithm approach to solving groundwater management problems with discrete decision variables. The authors demonstrate the methodology for a variety of hypothetical examples and compare the genetic algorithm solution with a linear or nonlinear programming solution. Rogers & Dowla (1994) combine artificial neural networks with a genetic algorithm to design remediation strategies for a hypothetical aquifer. In all of the above studies, the genetic algorithm solution compares favorably with the solution found using the gradient-based methods.

Wang & Ahlfeld (1994) present a groundwater management model that identifies optimal well locations and well rates by defining the spatial coordinates of wells as decision variables to be determined along with the pumping rates. Their method uses a composite objective that minimizes pumping and also constrains the wells to be within a predefined sub-domain of the model. Using a hypothetical aquifer system, they study the problem of groundwater remediation design with the goal of identifying the minimum pumping remediation strategy. For their examples, the 'moving well' model outperformed the 'fixed well' model both in terms of total pumping and number of wells needed. Finally, Wang & Zheng (1997) developed the *Modular Groundwater Optimizer* which is an evolutionary algorithm that can be readily coupled with the MODFLOW code (Harbaugh & McDonald, 1996) for the study of optimal site remediation. Problems of maximum contaminant removal for given costs or minimal costs for given contaminant removal can be tackled (Zheng & Bennett, 2002). None of the above studies however uses these recent optimization techniques in a context of multiple, conflicting objectives. The paper by Erickson *et al.* (2001) is a notable exception to that where the authors investigate pump-and-treat strategies to remove the most contaminant at the least cost within a small well catchment.

Here, we utilize the recent elitist multi-objective evolutionary algorithm SPEA2 to approximate the Pareto-set. In comparison to similar other evolutionary techniques, this algorithm has shown good performance in problems with large and complex search spaces (Zitzler *et al.*, 2002). The coupling of the simulation part with SPEA2 is facilitated by the availability of a platform and programming language independent interface (Bleuler *et al.*, 2003). This implementation allows the problem-independent *Selector* SPEA2 to interact with the problem-specific *Variator* with minimal overhead. The former contains the selection procedure, while the latter encapsulates the representation of solutions, the generation of new solutions, and the calculation of objective function values.

The general algorithmic structure developed to solve the problem given by Equation 4.11 and 4.12 is shown in Figure 4.10. A detailed description of module C, i.e. the *Selector*, is given in Zitzler *et al.* (2002) and (Zitzler, 2001). All of the coding has been carried out in MATLAB and is available from the author upon request. The FD flow calculation is based on a finite difference implementation in the MATLAB-environment using a conjugate gradient algorithm for its solution.

Optimization can be carried out over an arbitrarily chosen time horizon T . Furthermore, the modularity of the program allows adding code quickly. All of the

underlying data such as economic data and aquifer characteristics are spatial and readily available in matrices. As, for example, more detailed information on price structures or aquifer parameters gets available, changes can be incorporated in a supposable simple manner. As such, trade-offs of optimal allocation from any conceivable future demand pattern can be investigated.

4.5 Model Components

4.5.1 General Algorithmic Structure

The genetic algorithm models the evolution of a population of 'creatures' through successive generations using three probabilistic operators: reproduction, crossover, and mutation. The reproduction process serves to retain those strategies with high fitness (i.e. favorable cost objective), the cross over operator seeks to improve the design by combining the high-fitness strategies, and the mutation operator protects against convergence to a local minimum by adding random noise. The effect of these operators is that designs with high fitness will persist as the management strategies evolve from one generation to the next.

SPEA2, i.e. the *Selector*, works on a population of ε individuals. Their characteristics are stored in an archive and subject to change according to the individuals quality or 'fitness' as calculated by the *Selector*. The initial individuals are randomly determined. To reduce memory requirements, only data necessary during the course of optimization is stored, i.e. pumping values $q_{i,j}(t)$, pumping locations, related conveyance network information and associated current pumping costs. Each archive member gets assigned a unique identification number. In order to reduce the computational overhead, only this number together with the objective vector $\mathbf{g}(\cdot)$ is passed on between the archive and the *Selector*. The *Variator* creates new offspring individuals out of the set of individuals ξ that were chosen for mating by the *Selector*. The objective vector will be subsequently calculated for the offspring. Based on that, the *Selector* then determines whether offspring individuals will be stored in the archive or discarded. This process is repeated until a termination criteria is met (see Figure 4.10).

4.5.2 Network Clustering

For each individual, a random well configuration is determined and based upon that, a conveyance network topology identified. Such networks are modeled as directed networks which are composed of a finite set of nodes \mathcal{N} and a set of directed arcs \mathcal{A} (Daskin, 1995). For each node $n_{i,j}$ in \mathcal{N} , there exists a divergence $q_{i,j}(t)$. If $q_{i,j}(t) < 0$, $n_{i,j}$ is a demand node. If $q_{i,j}(t) > 0$, it is a pumping node. Otherwise, it is a conservative node such is the case for nodes that simply convey water. The associated arc and node costs are discussed in the next Section 4.5.3.

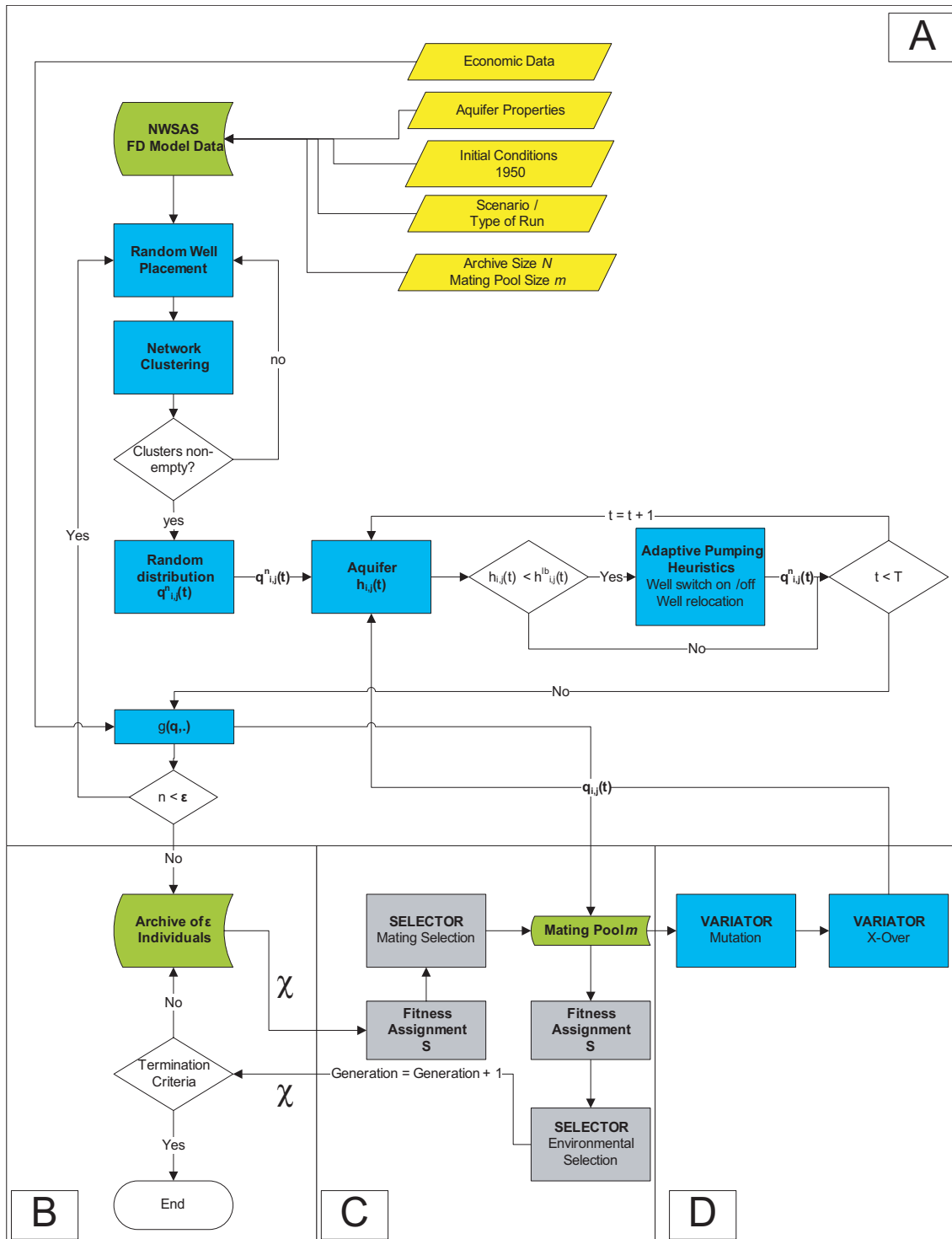


Figure 4.10: Top level model structure Variator (Modules A, B and D) and Selector (Module C) as discussed in Section 4.5. Module A: Creation of population, calculation of aquifer state and objective; Module B: Archive of individuals storage, maintenance and book keeping; Module D: Random mutation of pumping and crossing over of conveyance networks.

Multi-Objective Groundwater Management Model

Each network realization consists of a random spatial localization of n pumping nodes distributed over the whole basin (where n itself is a random number), and k nodes $d_{i,j}^k$ that have a determined demand $Q_k(t) > 0$ for each period t . In order to cover this quantity $Q_k(t)$ demanded at $d_{i,j}^k$ in period t , the nodes have to be grouped into clusters. With this, each demand node gets its water from a set of wells which are member of a cluster and provide the supply over the simulation time. An algorithm for the determination of such a network contains the following steps which are subsequently described:

1. Cluster membership identification, $\mathcal{N} \rightarrow \mathcal{N}^k$.
2. Creation of network topology \mathcal{A}^k for each k ;
3. Determination of $q_{i,j}^k(t)$ for each i, j and k .

Cluster membership information is obtained by a double pass k-means clustering method. K-means clustering can best be described as a partitioning method. That is, k-means clustering partitions the set of pumping nodes into k mutually exclusive clusters. Each cluster in the partition is defined by its member objects and by its centroid. The centroid $c_{i,j}^k$ for each cluster is the point to which the sum of distances from all objects (including the demand center – centroid distance) in that cluster is minimized. The `kmeans`-Matlab function implementation has been used for the cluster identification (MathworksInc., 2003b) which solved the minimization problem by numerical methods. Like in other problems of numerical minimization, the choice of the initial partition can greatly affect the final clusters that result. To improve optimization performance of the `kmeans`-function, the demand locations were chosen as initial guesses for the primary cluster centroids.

For each data point, the following first pass procedure determines the primary cluster membership k , defines node connections and randomly distributes pumping upon the wells.

Algorithm 1: kmeans determination of node–cluster membership and network topology together with random distribution of pumping (time subscripts are dropped). ‘ \rightsquigarrow ’ signifies node connections.

Data: $n_{i,j}$, $d_{i,j}$

Result: $n_{i,j}^k$, $q_{i,j}^k$, $c_{i,j}^k$, \mathcal{A}^k

begin

Partitioning of the dataset into k clusters and the data points are randomly assigned to the clusters;

Determine centroids $c_{i,j}^k$;

Iteration counter $v = 1$.

while for any pair $\{n_{i,j}^{k_v}(v), n_{i,j}^{k_{v+1}}(v+1)\}$ there exists $k_v \neq k_{v+1}$ **do**

 Calculate the distance from the well $n_{i,j}$ to each of the clusters centroid;

if If the well $n_{i,j}^k$ is closest to its own cluster k **then**

$k_{v+1} = k_v$ for $n_{i,j}^k$

else if

 Well is not closest to its own cluster, move it to the closest cluster

 and determine k_{v+1} for $n_{i,j}^k$;

 update centroid $c_{i,j}^k \forall k$

$v = v + 1$

$n_{i,j}^k \rightsquigarrow c_{i,j}^k$ and $c_{i,j}^k \rightsquigarrow d_{i,j}^k \Rightarrow \mathcal{A}^k$, set of network arches

Determine $q_{i,j}^k$ by $q_{i,j}^k = w_{i,j}^k Q_k$ with $w_{i,j}^k$ being random numbers and

$\sum_{i,j} w_{i,j}^k = 1$.

end

Based on this, a directed network is identified that, for all k , routes the flow from each $n_{i,j}^k$ to the $c_{i,j}^k$ and from there to $d_{i,j}^k$. The above procedure is portrayed in Figure 4.12 (Plate A). It is clear, that such a network does not resemble much a real conveyance network since many of the borehole – centroid connections appear redundant. The same holds true for a simple double pass clustering which is shown in Plate B in Figure 4.12. Whatever closeness of a borehole to its corresponding demand or conveying node, water will be routed via the primary centroid through the whole network. Thus, a more sophisticated, two pass subtractive clustering method was developed that determines primary ($n_{i,j}^k$) as well as secondary level cluster membership $n_{i,j}^{k,l}$ of the wells and the corresponding centroids $c_{i,j}^k$ and $c_{i,j}^{k,l}$.

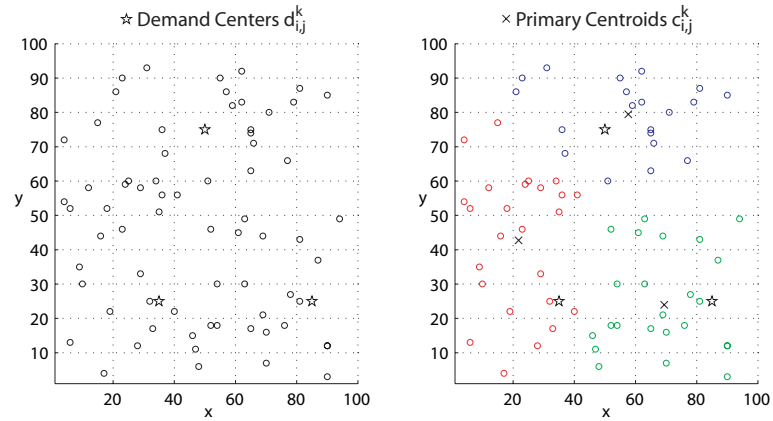


Figure 4.11: Identification of primary clusters with corresponding centroids $c_{i,j}^k$, out of a set of randomly placed wells by the kmeans-algorithm. Color coded cluster membership is shown.

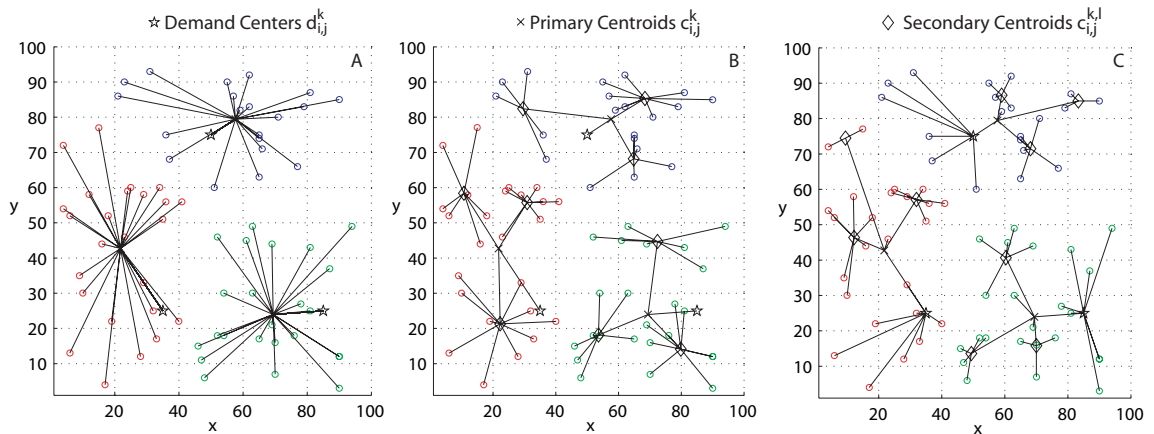


Figure 4.12: Sample network topology. The wells are shown as circles. A: Primary clustering algorithm; B: Simple double pass clustering; C: Two pass subtractive clustering method, wells are conveying the water towards primary and secondary level centroids as well as to the demand center directly.

Algorithm 2: Algorithmic structure of the proposed double pass subtractive clustering method (time subscripts are dropped).

Data: Input: $n_{i,j}$, $d_{i,j}$

Result: Output: $n_{i,j}^{k,l}$, $q_{i,j}^{k,l}$, $c_{i,j}^k$, $c_{i,j}^{k,l}$

begin

Partitioning of the dataset into k clusters and the data points are randomly assigned to the clusters;

Determine centroids $c_{i,j}^k$;

Iteration counter $v = 1$.

while for any pair $\{n_{i,j}^{k_v}(v), n_{i,j}^{k_{v+1}}(v+1)\} \exists k_v \neq k_{v+1}$ **do**

└ Determine k -membership by Algorithm 4.1 $\Rightarrow \mathcal{N}^k$.

for $k = 1 : K$ **do**

└ Determine for each $n_{i,j}^k \in \mathcal{N}^k$ the secondary level membership $n_{i,j}^{k,l}$;

└ $\tilde{n}_{i,j}^k = \overline{n_{i,j}^k, d_{i,j}^k} \leq \overline{n_{i,j}^k, c_{i,j}^k}$;

└ Remove $\tilde{n}_{i,j}^k$ from set \mathcal{N}^k ;

└ Determine l -membership by Algorithm 4.5.2 $\Rightarrow \mathcal{N}^{k,l}$;

└ **for** $l = 1 : L$ **do**

└ $\hat{n}_{i,j}^{k,l} = \overline{n_{i,j}^{k,l}, c_k} \leq \overline{n_{i,j}^{k,l}, c_{i,j}^{k,l}}$;

└ Remove $\hat{n}_{i,j}^{k,l}$ from set $\mathcal{N}^{k,l}$;

$n_{i,j}^{k,l} \rightsquigarrow c_{i,j}^{k,l}$, $c_{i,j}^{k,l} \rightsquigarrow c_{i,j}^k$, $\hat{n}_{i,j}^k \rightsquigarrow c_{i,j}^k$, $\tilde{n}_{i,j}^k \rightsquigarrow d_{i,j}^k$, $c_{i,j}^k \rightsquigarrow d_{i,j}^k \Rightarrow \mathcal{A}^k$

└ Determine $q_{i,j}^{k,l}$ by $q_{i,j}^{k,l} = w_{i,j}^{k,l} Q_k$ with $\sum_{i,j,l} w_{i,j}^{k,l} = 1$

end

The $\tilde{n}_{i,j}^k$ that lie closer to $d_{i,j}^k$ than to $c_{i,j}^k$ get directly connected to the $d_{i,j}^k$ and are removed from the set $n_{i,j}^k$ that is utilized for the second level clustering. After having run the latter, the remainder $n_{i,j}^k$ closer to the primary level centroid $c_{i,j}^k$ than their corresponding secondary level centroid $c_{i,j}^{k,l}$ get connected to $c_{i,j}^k$. The remainder $i_{k,m}$ connect then to $c_{k,m}$. The result of such a clustering is shown in Figure 4.12 (Plate C).

The resulting conveyance network cluster k supplying a specific demand center therefore is entirely defined by $\mathcal{N} = \{n_{i,j}^{k,l}, c_{i,j}^k, c_{i,j}^{k,l}, d_{i,j}^k\}$ and the connectors \mathcal{A} between those. A sample random configuration of such networks tapping water from the TC and IC aquifer in the study area is shown in Figure 4.13.

For each individual ε , the whole network structure and its information on prices and conveyance quantity can be conveniently stored in a sparse connectivity matrix (see Figure 4.14).

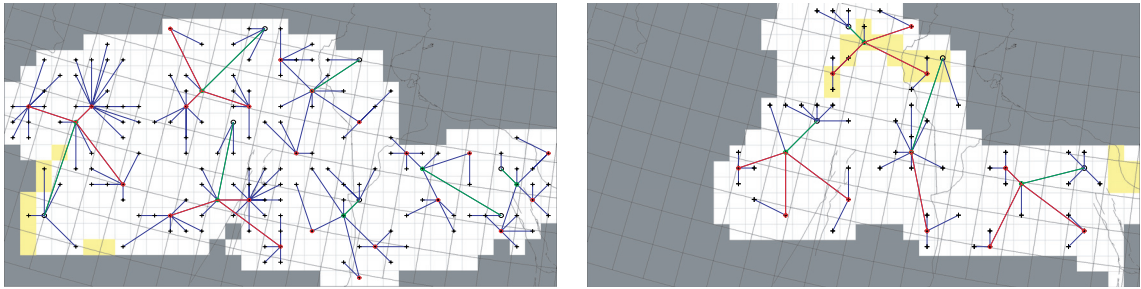


Figure 4.13: Sample network configuration in the IC and TC aquifer as determined by the two pass subtractive clustering method. The black circles represent the demand centers (compare with Figure 4.7). $d_{i,j}^k \rightsquigarrow c_{i,j}^{k,l}$: main conveyors (green); $c_{i,j}^k \rightsquigarrow c_{i,j}^{k,l}$: secondary conveyors (red); $c_{i,j}^{k,l} \rightsquigarrow n_{i,j}^{k,l}$: tertiary level conveyors (blue).

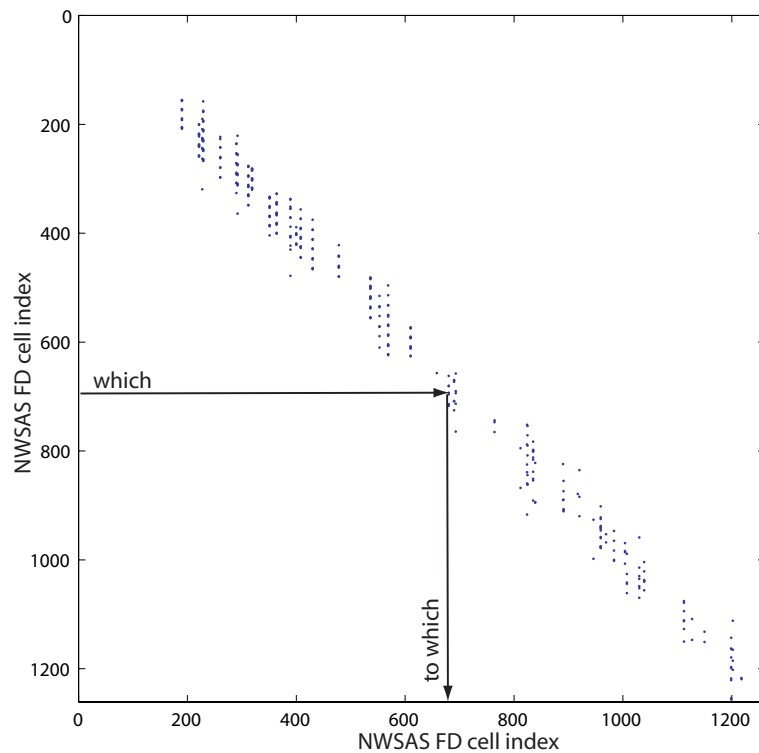


Figure 4.14: Sample connectivity matrix for network information. In the NWSAS FD model, there are 1256 active FD cells. Each blue dot indicates a from-to connection with the sparse matrix row and column indices corresponding to the FD-cell aquifer model indices.

	$\min(\zeta_1)$	$\max(\zeta_1)$	$\min(\zeta_2)$	$\max(\zeta_2)$	$\min(\zeta_3)$	$\max(\zeta_3)$
q_{tot} (m ³)	1.57E+07	1.57E+07	1.57E+07	1.57E+07	1.57E+07	1.57E+07
\bar{d} (m)	8.91E+00	6.74E+01	2.58E+01	6.74E+01	9.10E+00	6.74E+01
A_k (m ²)	6.50E+06	9.69E+08	6.50E+06	7.88E+08	6.50E+06	1.44E+09
l_k (m)	1.22E+05	3.34E+07	1.22E+05	1.21E+06	1.22E+05	2.49E+07
ζ_i (-)	5.76E-02	1.19E+02	2.79E+01	1.29E+03	6.49E+01	3.28E+03

Table 4.1: Sample data of cluster and aquifer characteristics according to the identification by the dimensionless numbers ζ_i .

Characterization of Allocation Patterns

Dimensionless analysis can be used to easily characterize spatial network configurations and the state of the aquifer at a certain time t . Equations 4.14 to 4.16 define a set of such possible numbers.

$$\zeta_1 = \frac{l^k}{\bar{d}} \quad (4.14)$$

$$\zeta_2 = \frac{A^k \bar{d}}{q_{tot}^k t} \quad (4.15)$$

$$\zeta_3 = \frac{\zeta_1}{\zeta_2} = \frac{l^k q_{tot}^k t}{A^k \bar{d}^2} \quad (4.16)$$

where l^k is the sum of all $\frac{n(n-1)}{2}$ distances between the n^k boreholes that are members of a pumping cluster k and pumping at a certain time t , A^k is the area inside the convex hull defined by the active boreholes within a cluster, \bar{d} is the average drawdown in the pumping cells of the cluster compared to steady-state, q_{tot}^k is the volume of water pumped from t_0 to t . ζ_1 relates the network length with an average observed (or computed) drawdown over the cluster. The area spanned by the convex hull divided by an averaged measure of the spread of the drawdown cone defines ζ_2 . It is straight forward to define a third dimensionless number ζ_3 that contains information of both, ζ_1 and ζ_2 .

Figure 4.15 shows the same hypothetical squared confined aquifer with 50 randomly chosen pumping patterns of a conveyance network. Obviously, many of the spatial configurations shown have few things in common apart from the underlying aquifer characteristics and the same overall pumped quantity q_{tot}^k . The average borehole to borehole distances within the clusters vary from a minimal 5.82 km to a maximal 57.53 km with a standard deviation of $\sigma = 10.11$ km (see Table 4.1). Similarly, the average drawdown at the pumping locations varies between 7.9 m in the case of a lot of active boreholes and 67.4 m in the case of few pumping wells with $\sigma = 10.33$ m.

Figure 4.16 shows the corresponding configurations for minimal and maximal values of ζ_1 , ζ_2 and ζ_3 . Generally, a low ζ_i means few boreholes begin spatially

Multi-Objective Groundwater Management Model

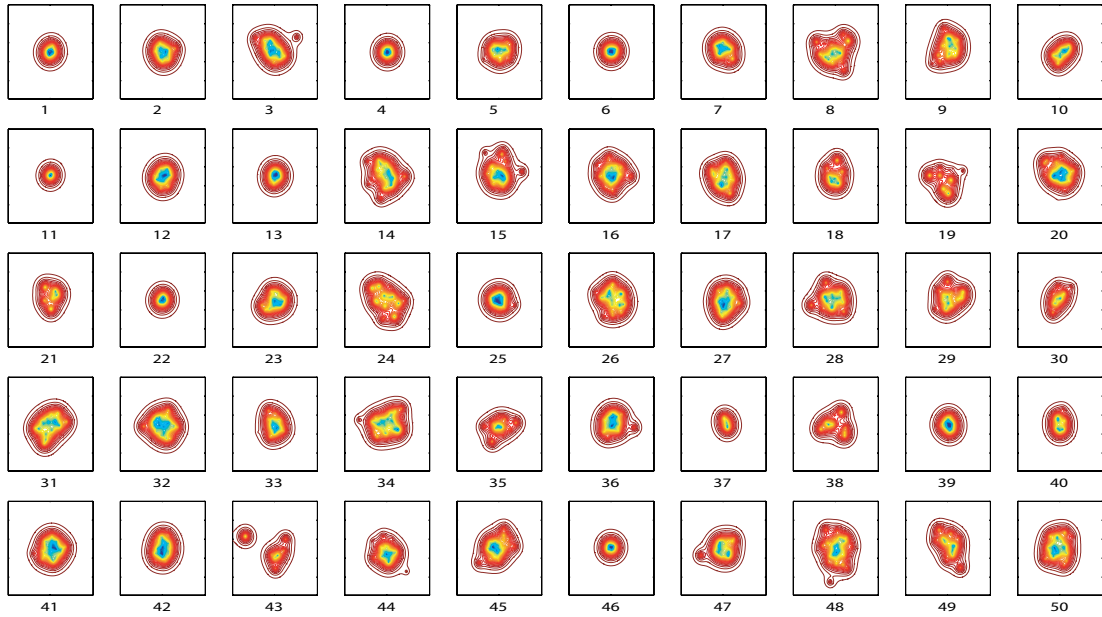


Figure 4.15: 50 random borehole cluster configurations on a rectangular confined aquifer with 100 km easting and northing. For each realization, the random number of wells pumping the same quantity q_{tot} are arbitrarily spread over the aquifer domain. The figures show the drawdown curves after one year of pumping.

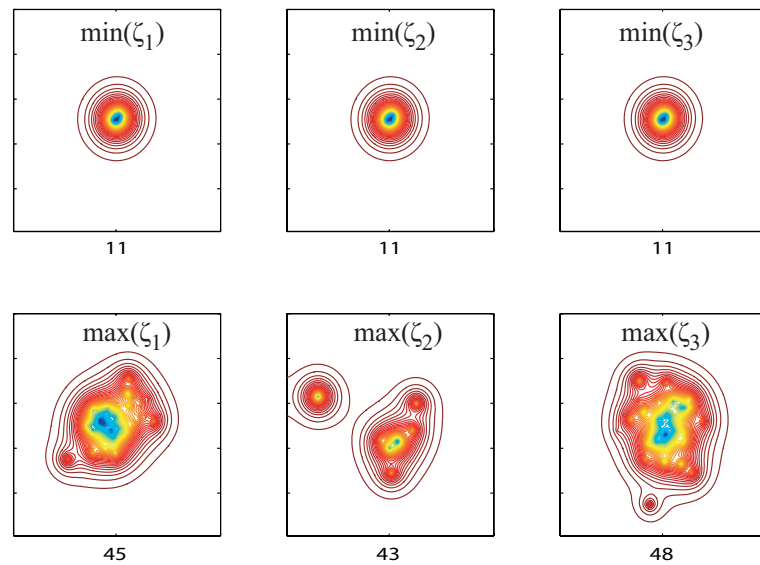


Figure 4.16: Minimal and maximal cluster configurations of ζ_1 , ζ_2 and ζ_3 out of the previously displayed set of 50 random realizations. The numbers correspond to the realization number (see Figure 4.16).

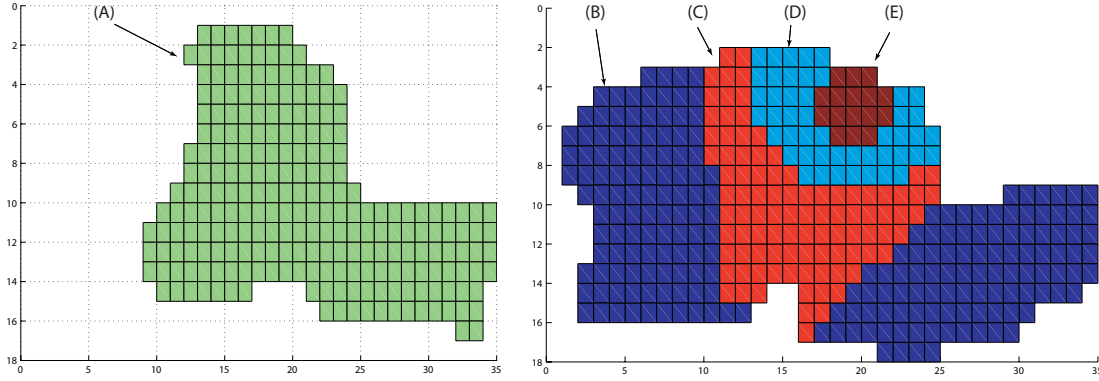


Figure 4.17: Spatial distribution of per-drilling-meter costs C_{IP} . A: 500 \$/m; B: 890 \$/m; C: 1000 \$/m; D: 1200 \$/m; E: 2100 \$/m (rule of thumb values from Southern Tunisia, year 2000 values). The costs are highest in the central part of the IC basin, where the top of the IC is more than 1 km below earth surface.

concentrated and causing a local drawdown cone of considerable depth. Similarly, a big ζ_i indicates spread out cluster formation with low pumping intensity at the wells, causing the piezometry to fall more homogeneously over the extent of the cluster. Since ζ_3 contains information from both, ζ_1 and ζ_2 , we shall use ζ_3 as a descriptive for the analysis of 2D allocation patterns.

The development of ζ_3 over time in the case of our squared, confined sample aquifer with constant pumping rates would be governed by $\zeta_3 \propto (t/\ln t)^2$ since A_k and l_k both are constant and $\bar{d} \propto \ln t$ whereas the total pumped quantity grows linearly in time.

4.5.3 Cost Calculation

Each node $\nu_{i,j} \in \mathcal{N}$ has associated costs. Arc costs can be related to nodes by adding them to the sink nodes at the end of each corresponding arc. Costs occur from groundwater pumping and its conveyance and include both, fixed costs and running costs. Fixed costs occur at a certain time $t = \tau$ where the related infrastructure is realized, be it either borehole or conveyance infrastructure. Running costs occur at each point in time and are proportional to the cost of energy at t .

In general, dropping the location subscripts i and j , present costs at node ν can be described as

$$g_\nu(\cdot) = C_{IP} + C_{IC} \cdot \lambda + \sum_{t=t_0}^{T_{end}} \frac{1}{(1 + \delta)^{(t-t_0)}} \cdot (c_L q(t) \Delta h(t) \Delta t + c_T \lambda q^3(t) \Delta t) \quad (4.17)$$

where C_{IP} are the total present installation costs of borehole infrastructure, taken to be proportional to filter depth. The filter depth for each FD cell is assumed to correspond to the top of the aquifer at that cell. C_{IC} is the associated present

Multi-Objective Groundwater Management Model

per-conveyor-meter installation costs of the conveyance system, λ is the distance over which water is conveyed, δ is the discount rate, $\Delta h(t)$ being the head difference between the level to which the water has to be raised in order to be conveyed and the actual groundwater level $h(t)$. c_L and c_T are constants which account for pumping plant efficiency η and hydraulic losses in the pipe and incorporate the cost of energy (Glover *et al.*, 1992). More specifically, $c_L \propto g\rho\eta$ with g being the gravitational constant and ρ the average density of water. $c_T \propto \frac{\rho}{d^5}$ with d being the pipe diameter and $C_{IC} \propto d^2$. Hence both, C_{IC} and c_T depend on the pipe diameter. For all practical purposes and due to lack of more specific information, it is assumed that an optimal pipe diameter has been determined by the equation of the marginal running costs with the installation costs over the planning horizon.

Depending on location, technology of infrastructure and the market prices of energy, the cost coefficients C_{IP} , C_{IC} , c_L and c_T can vary spatially and temporarily. For this study, spatially varying per-drilling-meter tube installation costs C_{IP} have been implemented. They account for the fact that it is more costly to tap the deeper IC aquifer. Figure 4.17 shows the spatial distribution of the per-drilling-meter costs and their corresponding values. These are rule of thumb values that have been taken from drilling experiences in Southern Tunisia (discussion with Y. Ben Salah and F. Horriche, DGRE, 2002). Boreholes and conveyors located in remote desert areas such as the Grand Erg Oriental, Grand Erg Occidental or the Hamada el Hamra in Libya are costlier to realize than infrastructure nearby already existing one or easily accessible areas. No rule of thumb values could be obtained from North African water experts for an estimation of per-meter-conveyance system costs C_{IC} . However, it is well known that a great part of the Saharan desert is difficult to access. In order to penalize solutions in the outback, the values of C_{IC} have been arbitrarily chosen to be one magnitude of order higher in the inaccessible areas (see Figure 4.18). Furthermore, it is supposed that the conveying system is uniformly built with regard to material and operational properties and that energy prices do not change over the simulated time horizon T_{end} . The latter implies that no technical progress is assumed to take place.

Lacking better knowledge, the pump cost related term c_L has been arbitrarily chosen to equal 1 \$/(kg/(m²s^{2\delta = 3\% has been chosen.}

The above holds true for conveyors that connect a pumping node with a conveying node. The costs between conveying nodes $c_{i,j}^{k,l}$ and $c_{i,j}^k$ can be determined in a similar fashion. The sink nodes have the following costs associated with them

$$g_\nu(\cdot) = \lambda \cdot \left(C_{IC} + c_T \cdot \sum_{t=t_0}^{T_{end}} \frac{1}{(1 + \delta)^{t-t_0}} \sum_i q_i(t)^3 \Delta t \right) \quad (4.18)$$

where the rightmost summation is accounting for the summed flux that is conveyed to the corresponding sink node.

This method of cost calculation implies that we are actually not calculating real

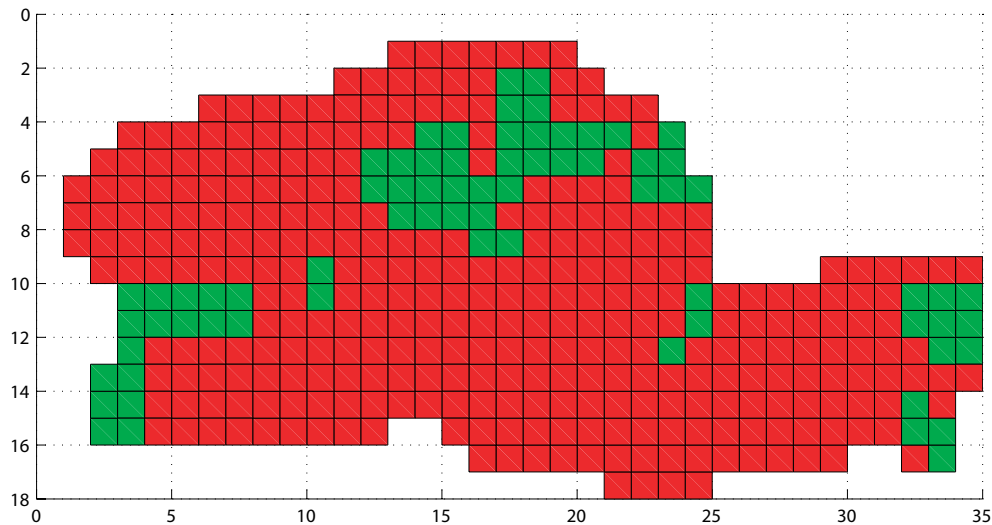


Figure 4.18: Green areas mark the settled areas throughout the basin. The vast desert stretches are colored red. Per-conveyor-meter installation costs C_{IC} are assumed to be 50 \$/m in the former and 500 \$/m in the latter (year 2000 values).

costs in commensurable units that can be used in any comparative study outside the scope of this thesis. Rather, due to the few available price and cost data, the calculated costs are to be solely used as the values of the objective functional that allows comparison between the discussed allocation strategies. These costs therefore represent a magnitude, which the decision maker, according to his value judgment, wishes to minimize.

4.5.4 Variation - Mutation

After the process of mating selection, the *Selector* passes candidate individuals for variation to the *Variator*. There, the mutation operator arbitrarily alters one or more components of a selected individual so as to increase the structural variability of the population. The role of mutation is that of restoring lost or unexplored genetic material in the population to prevent the premature convergence of the algorithm to suboptimal solutions and it ensures that the probability of reaching any point in the search space is never zero (Deb, 2001).

Mutation, as implemented here, adds random disturbance to the distribution of pumping within a certain cluster k at a certain time t . Within one cluster, wells are randomly chosen for mutation if $p < p_{mu}$, where $p \in [0, 1]$ is a random number assigned to each $n_{i,j} \in k$ and p_{mu} is the mutation threshold. For all the optimization runs, $p_{mu} = 0.05$ was utilized. The pumping rate at a particular well needs to be counterbalanced by a corresponding change in the remaining locations chosen for mutation so as not to violate the demand constraint. Therefore, if the list of well locations to experience pumping rate muta-

tion contains less than two entries, no mutation takes place (see Algorithm 4.3).

Algorithm 3: Mutation algorithm.

Data: Input $q_{i,j}^k(t)$

Result: Output $q_{i,j}^k(t)$

begin

for $k = 1 : K$ **do**

 within k , identify set of well locations l that experience mutation;

 within k , identify set of active well locations n ;

if $\text{length}(l)$ greater 1 **then**

$\sigma_k = \sigma(q_n^k(t))$;

 Out of set l , randomly choose one location l_m ;

$q_{mut}^k = N(0, \sigma_k)$;

$q_{l_m}^k = q_{l_m}^k + q_{mut}^k$;

$\tilde{l} = l - l_m$;

$q_{\tilde{l}} = q_{\tilde{l}} - q_{mut}^k / (n - 1)$;

else if

 no mutation takes place.

end

4.5.5 Variation - Crossing Over

The crossover operator is a method for sharing information between individuals; it combines the features of two parent individuals to form two offspring with the possibility that good individuals may generate better ones. The type of the problem suggests the implementation of a simple crossover algorithm which has been proposed by Wright (1991). Equation 4.19 shows the cluster representation of two parent individuals in the mating pool. After crossing over, the offspring's attributes are changed correspondingly. In other words, randomly chosen networks supplying individual demand centers were swapped between the parent individuals. In the example, the clusters 3,5 and 10 are swapped. Figure 4.19 shows the parent and offspring individuals for the TC aquifer.

$$\begin{aligned} \mathcal{K}_{P1} &= \{k_{P1}^1, k_{P1}^2, \dots, k_{P1}^{11}\} \\ \mathcal{K}_{P2} &= \{k_{P2}^1, k_{P2}^2, \dots, k_{P2}^{11}\} \end{aligned} \tag{4.19}$$

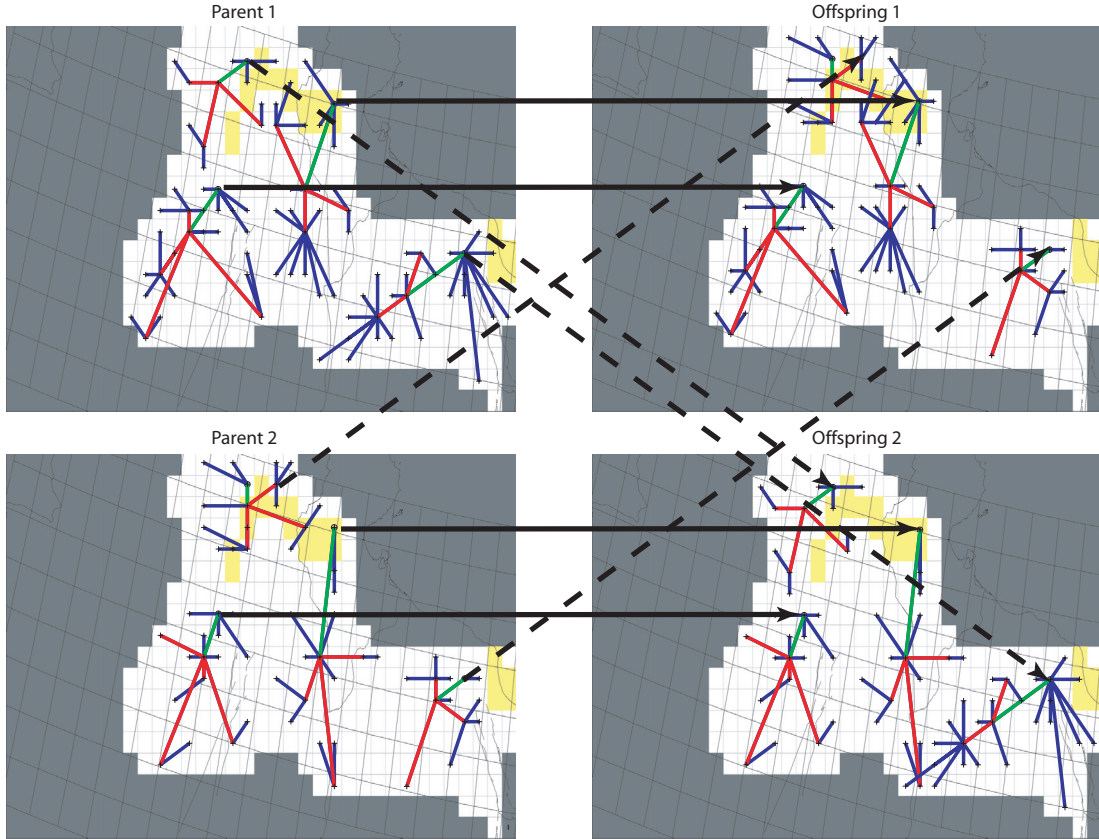


Figure 4.19: Visualization of crossing over of TC clusters in two individuals. The horizontal arrows point to network clusters that are identical in parent and offspring. The dashed diagonal lines mark clusters that are swapped.

$$\begin{aligned}
 \mathcal{K}_{C1} &= \{k_{P1}^1, k_{P1}^2, k_{P2}^3, k_{P1}^4, k_{P2}^5, k_{P1}^6, k_{P1}^7, k_{P1}^8, k_{P1}^9, k_{P2}^{10}, k_{P1}^{11}\} \\
 \mathcal{K}_{C2} &= \{k_{P2}^1, k_{P2}^2, k_{P1}^3, k_{P2}^4, k_{P1}^5, k_{P2}^6, k_{P2}^7, k_{P2}^8, k_{P2}^9, k_{P1}^{10}, k_{P2}^{11}\}
 \end{aligned} \tag{4.20}$$

For any k , $k \in \mathcal{K}$, two conveyance clusters are swapped if $p^k \geq p_{xo}$ where p^k is a random number between 0 and 1 assigned to cluster k and p_{xo} a crossing over probability. For all optimization runs, $p_{xo} = 0.5$ was chosen.

4.5.6 Adaptive Pumping Heuristics

In a real world setting, the strategies discussed above would require precommitment of the decision makers and complete knowledge or foresight with regard to properties of the resource as well as the future demand structure. It is hardly imaginable that such a situation will ever exist. Rather, an infrastructural change in existing well

configurations at a certain point in time may be necessary due to various reasons. On the one hand, it may be related to drawdown, quality or capacity constraints violation as well as to installation failure at a certain location. One possible way to deal with constraint violation are methods based on penalty functions. Approaches incorporating these penalties suffer from two problems. First, the optimal set of solutions Θ^* depends on the magnitude of the penalty R . Users normally have to try different values of R to find a value which steers the search towards the feasible region. Second, the inclusion of a penalty term may critically distort the objective function (Deb, 2001). On the other hand, it may be related to the development of new irrigation perimeters that itself is driven by changing demand. Patterns of allocation are therefore not static but rather dynamic.

In order to represent such dynamics, we propose an adaptive pumping heuristics that relocates pumping at a particular location $n_{i,j}$ once a head or gradient constraint is no longer fulfilled there. The heuristics relocates wells in the direction of the steepest ascent, $\nabla h(t)$. If the direction of steepest ascent is ambiguous, the decision with regard to direction is randomly taken. The displacement distance is assumed to be proportional to $|\nabla h(t)|$. In Figure 4.20, a sample run over 50 years of pumping in a sample confined aquifer is visible. If at a certain location and point in time, drawdown constraints are violated, relocation occurs. The development of ζ_3 over time shows peaks which indicate configuration changes in the number of operating well locations from one time step to the next. With the spread of the spatial extent of the drawdown cone A_{dd} over time, ζ_3 increases correspondingly.

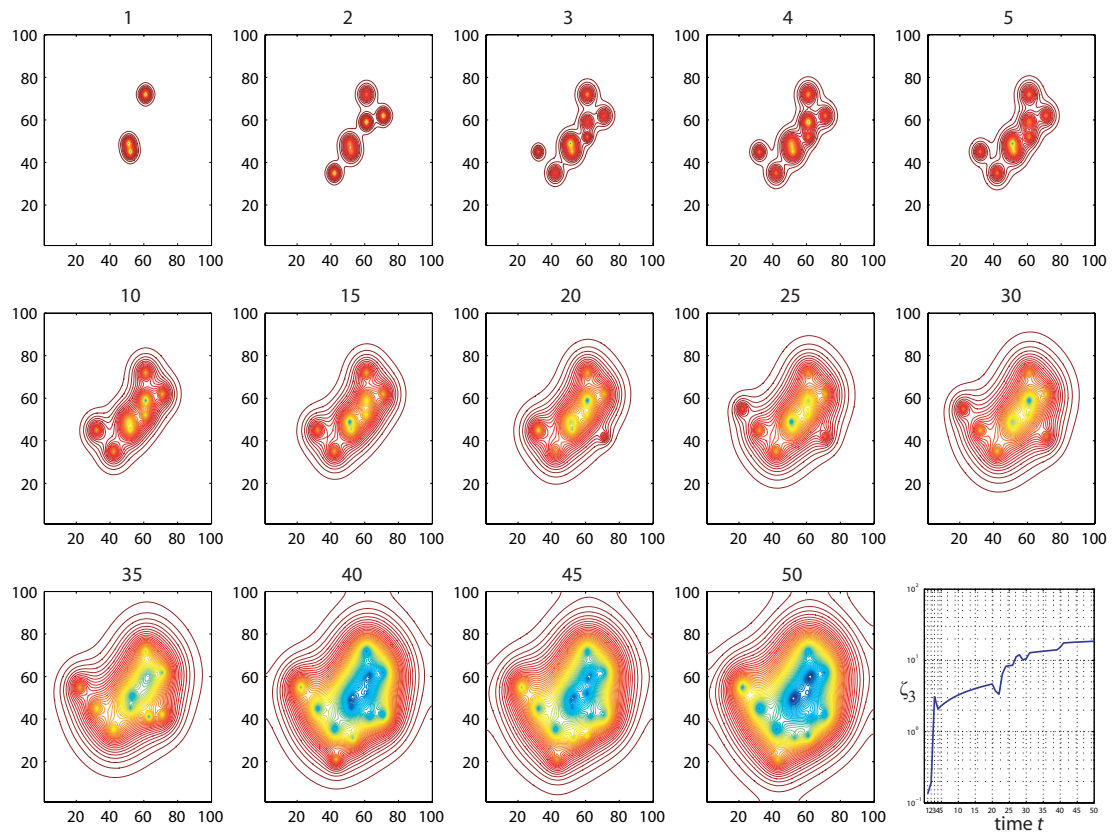


Figure 4.20: Adaptive pumping heuristics. The figures show drawdown contour lines that emerge from a random initial well placement and the relocation of pumping forced by drawdown constraint violation. Lower right Figure shows the development of ζ_3 (note the log-plot).

Chapter 5

Optimization Results

5.1 Sample Optimization Run

We demonstrate how the optimization tool presented above can be utilized as a descriptive and prescriptive tool. Descriptive because it helps to explain the emergence of likely allocation strategies within a certain socio-political environment. Prescriptive in the sense of a normative tool which can identify *Pareto*-optimal location-allocation designs that, compared to a *Status Quo*, are beneficiary for a the rational decision-maker if adopted. A synthetic simulation-optimization example is utilized for demonstration purposes before the discussion of the NWSAS optimization results.

The groundwater system in the synthetic example consists of a one layer aquifer that has homogeneous properties. The model layer is partially convertible between confined and unconfined, the transmissivity being constant throughout simulation. It has a thickness of 400 m and a transmissivity value of $10^{-3}\text{m}^2/\text{s}$. The confined storage coefficient is $S = 10^{-3}$ and the specific yield equals $S_y = 0.25$. The domain extends over 100 km x 100 km with a FD cell discretization of 1km. An economic scarcity depth of 200 m is valid for each of the three demand centers. Clustering and conveying methods as well as the behavioral heuristics apply as introduced in Section 4.5 of Chapter 4. A discount factor of 3% is chosen. Optimization is carried out over 50 years.

Three agricultural centers exist in close proximity. They demand a similar, constant water quantity of $Q = 60\text{l}/\text{s}$ throughout simulation (left plate in Figure 5.1 for the location of the demand centers in the aquifer domain). It is assumed that each demand center belongs to a country within which the decision-makers can distribute pumping. The setup is such, that the push and pull forces related to a pumping strategy of a country interact with the ones of the other countries (see also Chapter 4, Section 4.2). No transboundary cooperation exists in the *Status Quo* case where each national decision-maker pursues his interests in an egoistic way. Contrary to that, borders are not present in a second setup, termed *imaginary future*. In this case, the decision-makers strategic opportunities are not restricted by territoriality, everything else being similar. The latter would then represent the case where the parties involved have agreed on transboundary aquifer management.

Figure 5.1 shows the geometry of the problem as well as the well locations that have been sampled during optimization for both configurations. For both optimization runs, an archive size of $\varepsilon = 60$ and a mating set size of $\xi = 4$ has been chosen.

No substantial change in the objective function is observed after approximately 800 generations. Figure 5.2 shows the development of the mean present costs over

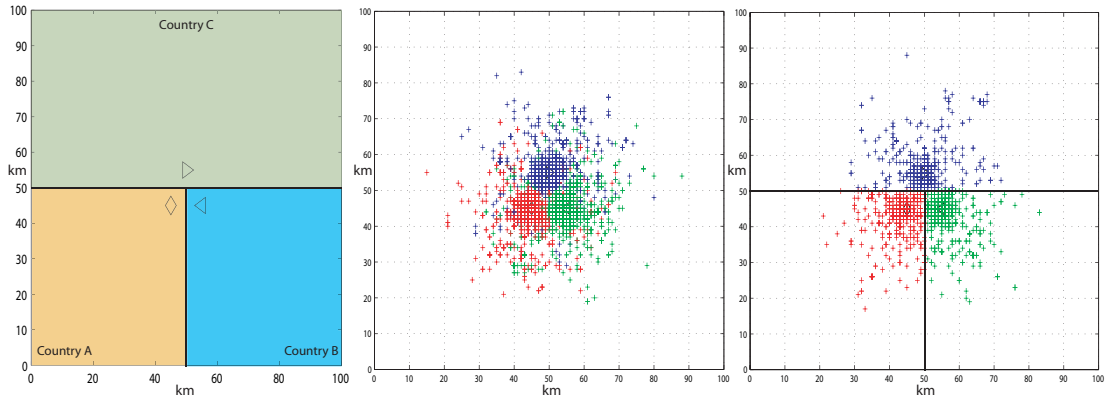


Figure 5.1: Left: Demand centers with corresponding color coded country territories. Center: Spatial sampling during optimization without territorial restriction. Right: Country borders restricting the set of location options of spatial sampling.

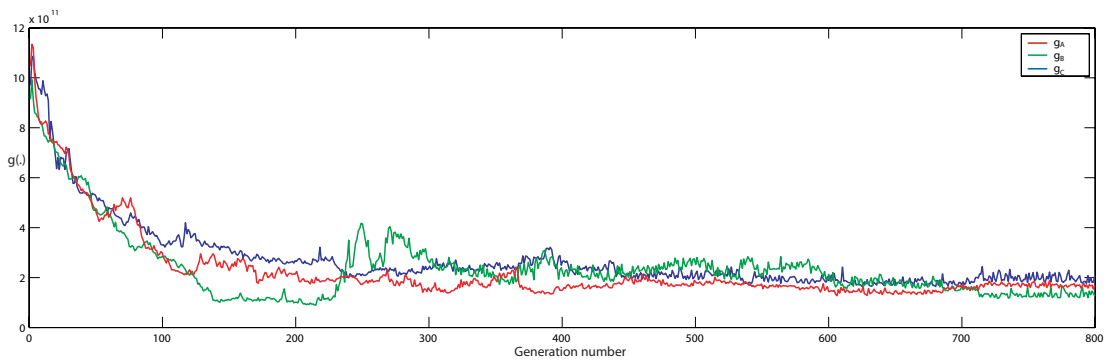


Figure 5.2: For each demand center, the development of the generational mean objective value of the non-dominated individuals is shown for the Status Quo case.

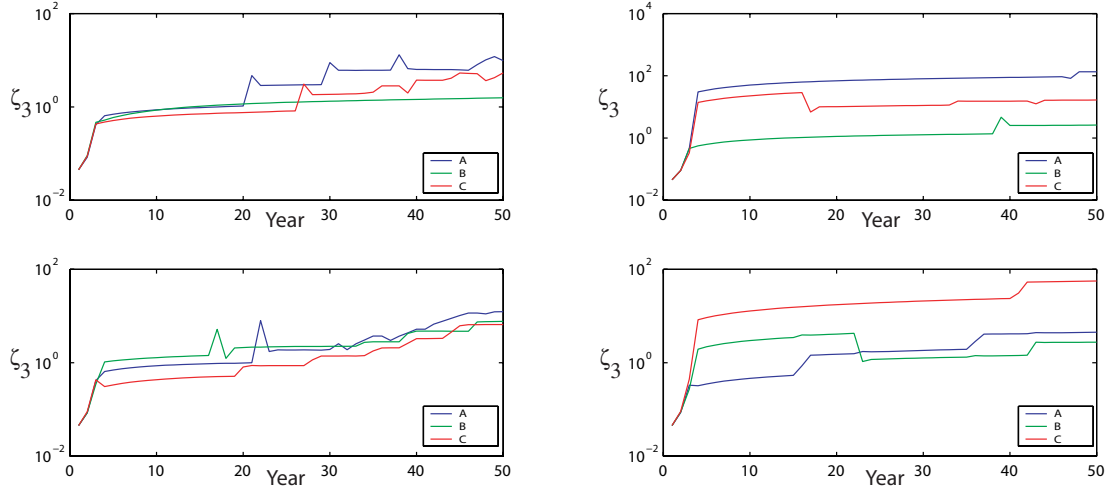


Figure 5.3: The figures show the development of ζ_3 for each of the three demand centers. 4 randomly picked individuals from the archive prior to optimization are shown. No territorial restrictions apply.

each generation for the optimization run. The noise observed is induced by the *Variator*, i.e. the mutation and crossing over of the individuals characteristics. For both cases, the set of non-dominated individuals as determined by optimization is portrayed in Figure 5.6. The restriction of well placement by borders leads to optimal solutions that have overall higher mean present costs compared to the unrestricted case (see Table 5.1).

Independent of territoriality, an interesting result emerges from the comparison of ζ_3 as defined by the random initial spatial well locations on the one side and the pump schedules with the locations and schedules defined by the optimal solutions on the other. Figure 5.3 displays the development of ζ_3 for 4 arbitrarily chosen individuals from the archive ε prior to optimization. Due to the randomness of the first generation individuals, no structure is visible.

Compared to that, allocation patterns that emerged after optimization show structure (see Figure 5.4). They are characterized by an early increase in the number of wells operating over which pumping is distributed. With the drawdown constraint being the limiting factor, pumping soon thereafter starts to oscillate between the wells built by then. If the regional drawdown has progressed so that the desired head recovery at the built wells is no longer observed, further wells get active. This extension in infrastructure adds more options for the spatio-temporal redistribution of the pumping in subsequent periods. The oscillation is also visible in Figure 5.7 where the active wells in stress period t are superimposed on the development of the piezometry.

It is well known that in the real world setting, cooperation is difficult to establish due to claims of territorial integrity and often mutual distrust against the competing resource extractors (Puri *et al.*, 2000). Furthermore, in the case of strategic

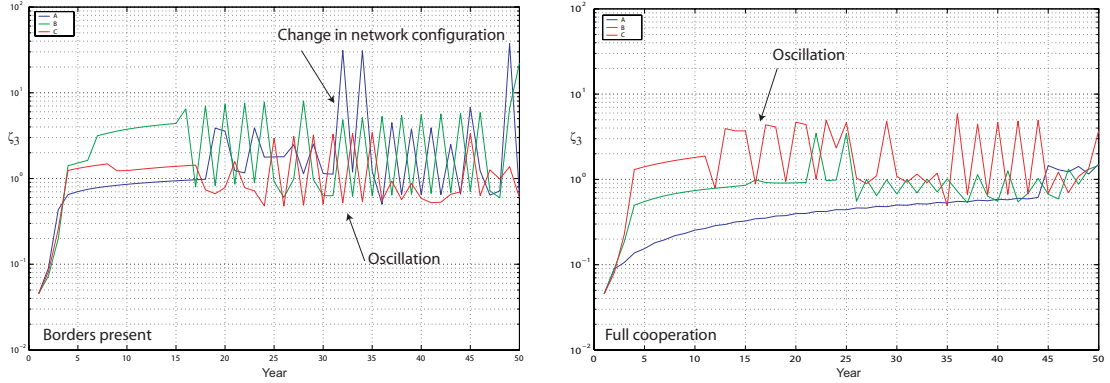


Figure 5.4: ζ_3 of the overall cheapest solution for both cases. Optimization proposes an early network extension upon which pumping is oscillating until the progression of regional drawdown necessitates a further spread of pumping activity to more distant places.

interactions between actors utilizing a common-property, altruist behavior does not necessarily pay (Baland & Platteau, 1996). In fact, it is straight forward to show that, based on the non-cooperative case, there is little incentive for the rational decision-makers in the above example to depart from egoist, non-cooperative allocation strategies. For each country i , let us define an externality parameter χ_i which can be thought of as ratio of the overall share of external drawdown effects in the $i \neq \hat{i}$ countries over \hat{i} 's own destorage. Hence,

$$\chi_i = \sum_t \frac{\sum_{i \neq \hat{i}, j} \Delta h_{i,j}(t)}{\sum_j \Delta h_{i,j}(t)} \quad (5.1)$$

with $\Delta h_{i,j}(t)$ being the drawdown observed at time t at location i, j . Figure 5.5 shows χ_i of the set of Pareto-optimal solutions in relation to the normalized value of the associated present costs. Clearly, strategic well placement is encouraged as the decision-makers want to minimize their cost objective. For each, it pays to be egoist and decide upon an allocation pattern for which the numerator of Equation 5.1, i.e. the magnitude of drawdown imposed on the others, is large and the present costs correspondingly minimal. Based on the individual preferences, altruism is not favored as an outcome of rational choice. Rather, each one of the resource utilisers has a natural inclination to harm the others which, quite obviously, is a bad precondition for entering into negotiations about imaginary transboundary allocation strategies.

Model results also show that overall benefits can result from transboundary resource management. The cooperative case indicates overall benefits for each decision-maker since on average, the calculated present costs are lower. A combination of the two Pareto-fronts consists of 77% of transboundary solutions. In other words, for 77% of the cooperative strategies, each decision-maker can be made strictly better off. Under the assumption, that no decision-maker will settle for higher present costs than his *Status Quo* level, it is individually rational for them

Form	μ_A	μ_B	μ_C	σ_A	σ_B	σ_C
<i>Borders</i>	6.13E+10	7.15E+10	4.64E+10	1.83E+10	4.75E+10	1.63E+10
<i>Cooperation</i>	3.75E+10	6.56E+10	2.78E+10	9.23E+09	2.33E+10	2.48E+10

Table 5.1: First and second moment characterising the Pareto-front for both configurations. In average, the summed present costs of the cooperative solution are 38% smaller than in the case of territorial restrictions.

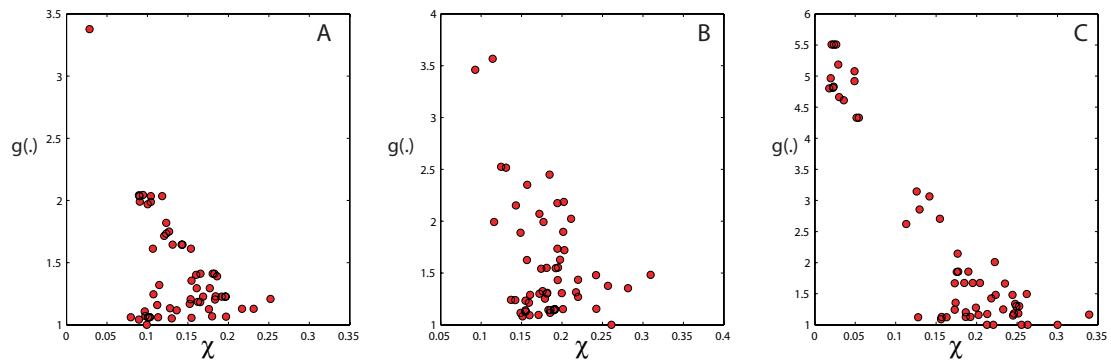


Figure 5.5: For each decision-maker, his goal is to minimize his present costs. Preference is therefore given to allocation patterns with small g_i (normalized present costs shown on ordinate). However, cost minimal strategies are characterized by an increased external drawdown effect χ (abscissa). Egoistic strategies (lower left corner of diagrams) are likely to emerge.

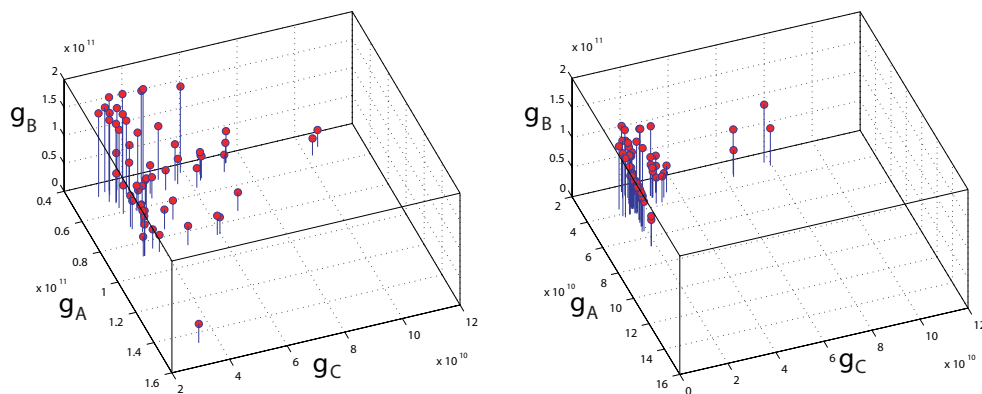


Figure 5.6: Convex Pareto surface with $\varepsilon = 60$ after 261 generations. Left: The restriction of national borders leads to increased overall costs. Right: No territorial restriction with regard to well placement.

Optimization Results

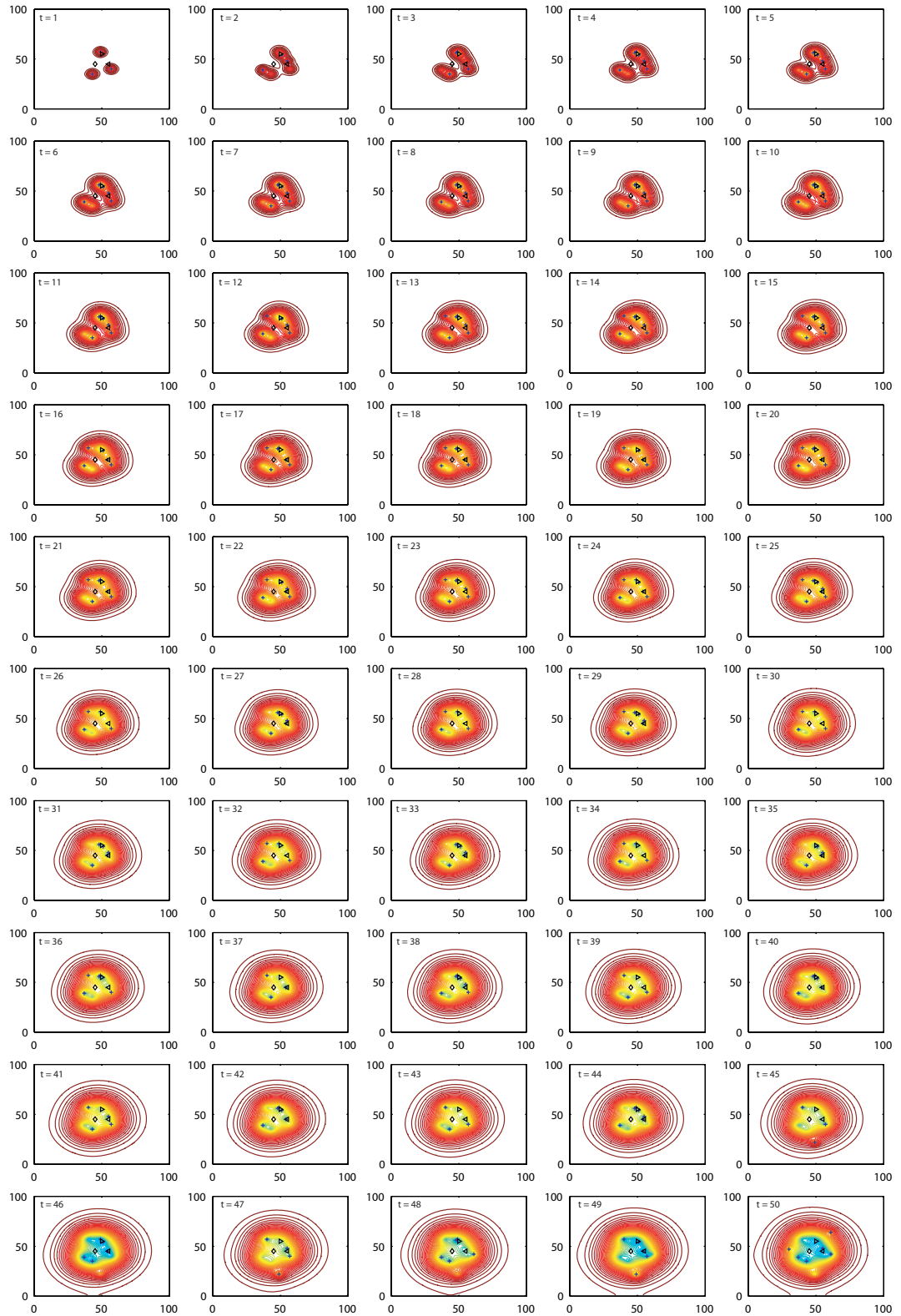


Figure 5.7: Head development and well placement of the overall cheapest allocation solution for the cooperative case. Crosses indicate active boreholes at a certain time t .

to cooperate. It is therefore conceivable that – under the assumption of costless negotiations – transboundary strategies will emerge. Yet, under real-world conditions, associated transaction costs might turn out to be forbiddingly high and thus prevent such cooperation.

5.2 NWSAS Allocation Optimization

5.2.1 Description of Strategies

Here, we investigate whether a motivation for transboundary management of the NWSAS exists on quantitative grounds. As in the case of the linear simulation-optimization approach presented in Section 3.3 of Chapter 3, the basic question to be answered is, whether gains from alternative utilization patterns, given a specific demand, exist and, if so, what do these imply in terms of policy recommendations for the allocation of NWSAS groundwater. For this purpose, two alternative strategies are presented which are ranked against a *Status Quo* allocation. For each decision-maker, the *Status Quo* is simply his security level because he can guarantee at most this much simply by never agreeing to any transboundary strategy at all (Neumann & Morgenstern, 1966). All calculations are carried out over the time horizon of 50 years, i.e. from the year 2000 to 2050.

The *Status Quo* allocation is one where decision-makers follow their declarations of intent about the distribution and magnitude of future pumping within national territories over the next fifty years. Starting from the year 2000, regional demand development over the next 50 years is given in Table 5.2 for each agricultural center. The rising demand of pumped groundwater determines the aquifers response. Draw-down constraints guide locations of future pumping as proposed by the relocation-distribution heuristics (see Section 4.5.6, Chapter 4). During simulation, each FD pumping cell has a predetermined pumping quantity $q_{i,j}(t)$. No infrastructural costs occur at $t = t_0$ since pumping and conveyance infrastructure already exist. Any later change in the system configuration is accounted for as defined by Equation ???. Note that the *Status Quo*-strategy as presented in Chapter 3 is not directly comparable to the one presented here since the latter involves a nonlinear cost formulation as well as the option for the relocation of wells.

In the first alternative strategy, subsequently called *Perpetuation*-strategy, transboundary management is established. Based on the existing infrastructure, *Pareto*-optimal location-distribution patterns of pumping are sought. For that purpose, optimization is carried out upon an archive of individuals with random distributions of $q_{i,j}^k(t)$ so that for each demand center k , the overall demand $Q^k(t)$ is covered at time t . Boreholes are allowed to be moved all over the basin irrespective of national borders. Existing infrastructure causes no additional costs at $t = t_0$. Only if the random initial pumping quantity assigned to a FD cell exceeds the maximum yield of the already built wells, additional borehole construction costs proportional to the number of new wells and C_{IP} occur.

Optimization Results

Demand Center	Year										
	2000	2005	2010	2015	2020	2025	2030	2035	2040	2045	2050
1 & 6	19	24	30	38	41	46	51	56	62	68	73
2 & 7	19	24	30	38	41	46	51	56	62	68	73
3 & 8	13	17	19	20	20	20	21	21	21	21	22
4 & 10	9	11	14	17	19	21	23	25	28	30	33
9	4	5	7	9	9	10	12	13	14	15	17
5	10	12	15	19	21	23	26	28	31	34	37
11	4	5	7	9	9	10	12	13	14	15	17
Sum	79	97	122	148	160	177	195	211	233	250	271

Table 5.2: Development of the regional demand [m^3/s] in the corresponding agricultural centers (Sahara and Sahel Observatory, 2002). The demand center numbers correspond to the ones in Figure 4.7 as shown in Section 4.3, Chapter 4.

Contrary to that, in the second *Imaginary Future*-strategy, pumping and infrastructure of the initial population of individuals are randomly distributed, not taking into account existing constructions. Although initially more expensive, it might turn out that the optimization with such additional degree of freedom is able to identify interesting allocation patterns that, in the long run, cause overall lower present costs.

Sensitivity analysis showed convergence of the objective function and Pareto-front population diversity to be crucially dependent on the archive and mating pool size. A good trade-off between computational demand and optimization quality has been achieved with the following values: archive size: $\varepsilon = 300$; mating pool size: $\xi = 4$.

5.2.2 Optimization results

Comparative Analysis

Figure 5.8 shows the development of the mean present costs over each generation during optimization. The following termination criterion was chosen

$$S^N - S^{N-1} \leq 1000 \quad (5.2)$$

where the left-hand side difference denotes the n -moving average between the last two entries of the sequence $S = \{s_u\}_{u=1}^{N-n+1}$ with

$$s_u = \frac{1}{n} \sum_{v=1}^{u+n-1} \bar{g}_v(\cdot) \quad (5.3)$$

where $\bar{g}_v = \frac{1}{\varepsilon} \sum_{u=1}^{\varepsilon} g_u$ is the mean of the overall sum of present costs of the v th generation. $n = 31$ has been arbitrarily chosen. Thus, optimization terminated after 2777 generations for the *Perpetuation*-strategy and after 2711 generations for the *Imaginary Future*-strategy run, respectively.

The optimization result proposes a pumping schedule based on locations and aquifers. Pareto-optimal solutions of both optimized strategies are characterized by lower mean terminal present values of the objective compared to the *Status Quo* (see

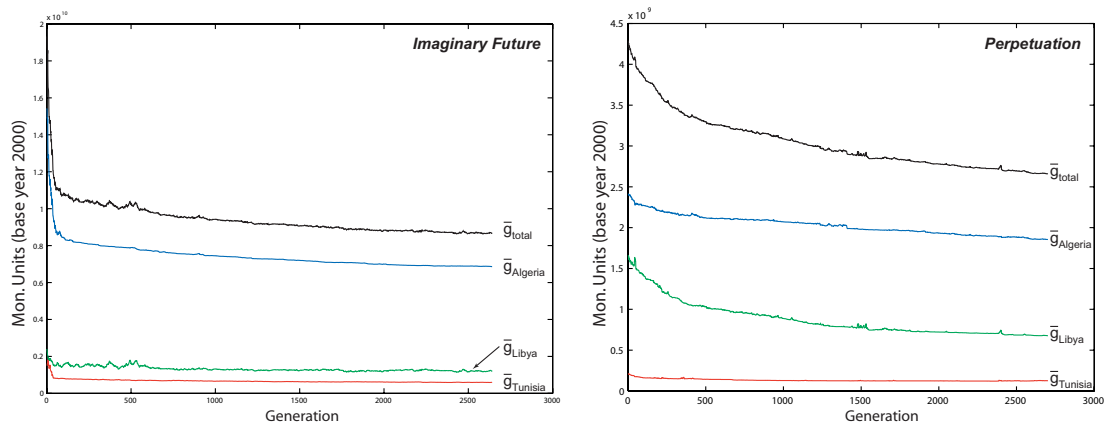


Figure 5.8: Development of the generational mean present costs \bar{g}_i during optimization (differently scaled ordinates). Population diversity is bigger in the *Imaginary Future*-strategy compared to the *Perpetuation*-strategy due to the additional degrees of freedom for the initial borehole placement. For the former, the mean objective values decline markedly in the initial phase of optimization due to expensive solutions being segregated from the archive.

Figure 5.9). For each country, the development of the mean cumulative costs for the *Perpetuation*-strategies is generally lower compared to the *Status Quo*. Contrary to that, the mean cumulative costs of the *Imaginary Future*-strategies are initially higher due to the complete initial renewal of pumping and conveying infrastructure. Over the long run, they are in the same order of magnitude as in the case of the *Status Quo*. The transition times, i.e. the time from whereon the mean total present costs of the *Imaginary Future*-strategies are lower than the corresponding costs of the *Status Quo*-strategy are the following: Algeria ~ 3 years; Tunisia ~ 6 years, Libya ~ 18 years. Since the input values of fixed and running costs are not well known so far, these are tentative values which are likely to change once better input data on prices is available.

For none of the countries however, it seems to be worth to use *Imaginary Future*-strategies since for each, the overall mean costs exceed the ones proposed by the *Perpetuation*-strategy as shown in Table 5.3.

In average, total present costs of *Perpetuation*-strategies are $78 \pm 2\%$ lower (77% for Algeria, 90% for Tunisia and 85% for Libya) than for the *Status Quo*-strategy. The mean current prices of 1 m^3 of water relative to the *Status Quo*-strategy are shown in the Tables 5.4 to 5.6 for the corresponding years. In general, the current costs for the *Perpetuation*-strategies are lowest. The renewal of infrastructure in the *Imaginary Future*-strategies causes greatly increased initial costs for Algeria and Libya. Contrary to that, Tunisia could profit by adapting either *Perpetuation*-or *Imaginary Future*-strategies from the beginning.

To put it in other words, significant capital gains can be achieved while following the *Perpetuation* strategy (see Table 5.4). On average in the case of the *Status Quo*

Optimization Results

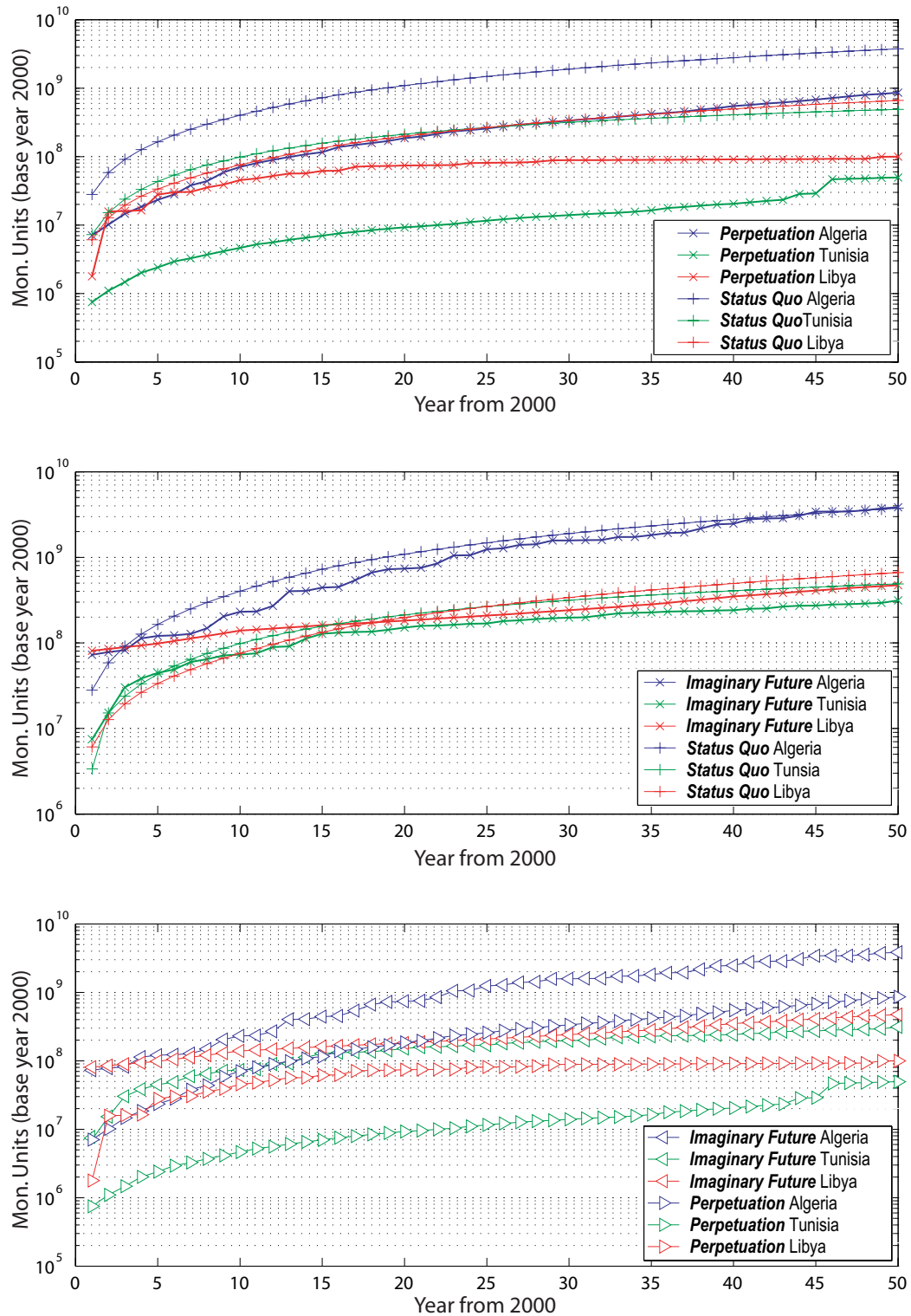


Figure 5.9: Development of cumulative present costs for each country according to strategies chosen (mean over last generation). On the average, the Perpetuation-strategies compare favorable to both, the Status Quo- and Imaginary Future-strategies.

	<i>Status Quo</i>	<i>Imaginary Future</i>	<i>Perpetuation</i>
μ_{g_A}	3.744E+09	3.850E+09	8.595E+08
σ_{g_A}	-	8.513E+06	3.922E+07
μ_{g_T}	4.896E+08	3.135E+08	4.948E+07
σ_{g_T}	-	4.267E+06	3.143E+07
μ_{g_L}	6.632E+08	4.728E+08	9.986E+07
σ_{g_L}	-	1.589E+08	8.624E+06

Table 5.3: Mean and standard deviation of total present costs (mon. units as of year 2000) of the archive population of the last generation. The Perpetuation–strategy is favorable for all countries.

Year	<i>Status Quo</i>			<i>Perpetuation</i>		
	2000	2050	Ratio	2000	2050	Ratio
<i>Algeria</i>	3.1E-02	2.8E+00	35.0	2.1E-02	6.5E-01	8.0
<i>Tunisia</i>	5.7E-02	1.8E+00	31.3	5.8E-03	1.8E-01	3.2
<i>Libya</i>	6.5E-02	1.9E+00	28.8	1.9E-02	2.8E-01	4.3
<i>Average</i>	7.3E-02	2.5E+00	34.4	1.7E-02	5.2E-01	7.1

Table 5.4: Unit groundwater prices (mon. units / m^3) in the years 2000 and 2050 as well as their ratios. All countries experience a significantly lower price–rise ratio when they follow the Perpetuation strategy.

strategy, the costs in the year 2050 for providing one unit of pumped groundwater would be more than 30 times higher than in the year 2000. Contrary to that, the provision costs in the case of the optimized *Perpetuation* strategy would only rise by a factor of 7. Quite obviously, this finding should provide a strong incentive to embark on such strategy.

No absolute costs are provided due to the following two reasons. First, input prices are not well known and absolute costs clearly depend on them. Second, neither depreciation nor failure of infrastructure have been taken into account which are likely to increase absolute costs. The relative cost comparison remains, however, valid.

Benefits can be achieved mainly from intelligent scheduling upon the existing pumping and conveying system. For the set of optimized *Perpetuation*–strategies,

Algeria	Year										
	2000	2005	2010	2015	2020	2025	2030	2035	2040	2045	2050
SQ	100%	100%	100%	100%	100%	100%	100%	100%	100%	100%	100%
PER	25%	13%	22%	11%	22%	16%	16%	22%	38%	35%	36%
IF	260%	20%	51%	52%	20%	225%	4%	98%	54%	372%	112%

Table 5.5: Current provision costs per meter cube of water for Algeria in selected years relative to the SQ–strategy. Mean values are given for the PER– and IF–strategies. SQ: Status Quo–strategy; PER: Perpetuation–strategies; IF: Imaginary Future–strategies.

Optimization Results

Tunisia	Year										
	2000	2005	2010	2015	2020	2025	2030	2035	2040	2045	2050
SQ	100%	100%	100%	100%	100%	100%	100%	100%	100%	100%	100%
PER	10%	4%	4%	4%	4%	5%	4%	8%	7%	6%	8%
IF	213%	62%	15%	135%	81%	15%	31%	38%	18%	18%	252%

Table 5.6: Current provision costs per meter cube of water for Tunisia in selected years relative to the Status Quo–strategy. Mean values are given for the PER– and IF–strategies. SQ: Status Quo–strategy; PER: Perpetuation–strategies; IF: Imaginary Future–strategies.

Libya	Year										
	2000	2005	2010	2015	2020	2025	2030	2035	2040	2045	2050
SQ	100%	100%	100%	100%	100%	100%	100%	100%	100%	100%	100%
PER	29%	162%	69%	38%	9%	7%	2%	1%	2%	1%	3%
IF	1326%	70%	102%	38%	34%	41%	48%	52%	97%	68%	72%

Table 5.7: Current provision costs per meter cube of water for Libya in selected years relative to the Status Quo–strategy. Mean values are given for the PER– and IF–strategies. SQ: Status Quo–strategy; PER: Perpetuation–strategies; IF: Imaginary Future–strategies.

Figure 5.10 shows a cross-generational density plot of the pumping locations. In the TC aquifer, solutions are similar in character in as far as they all feature the same pumping location set. Even with gradient restrictions in place, no spatial relocation of pumping is proposed. Two reasons are responsible. First, at the pumping FD cell, the TC gets unconfined. The drainage of the effective porosity causes less deep drawdown cones. Second, once a gradient constraint of the TC is hit, pumping can be increased in the IC until recovery is observed. This again confirms the basic understanding of the IC as backstop in an economic sense. Contrary to that, relocation of IC wells is observed in the strategies of the final population. IC boreholes in the central basin region around the Chott get gradually switched off. Reddish to yellow and green FD cells appear in the IC in Figure 5.10. This is just an indication of the diversity of the non-dominated, optimized *Perpetuation*–strategies.

The left graphic in Figure 5.11 shows the oscillatory nature of an optimal pumping schedule in the TC and IC aquifers for the overall best individual out of the set of *Pareto*–optimal *Perpetuation*–strategies in the last generation. As in the synthetic example of the preceding Section 5.1, oscillation is additionally observed within the pumping networks that provide the water for a specific demand center (see right graphic in Figure 5.11). Although the fossil groundwater stocks of the NWSAS are being run down, the technique of adaptive pumping and the presence of the backstop IC aquifer add management options that help to secure future supply over the next 50 years.

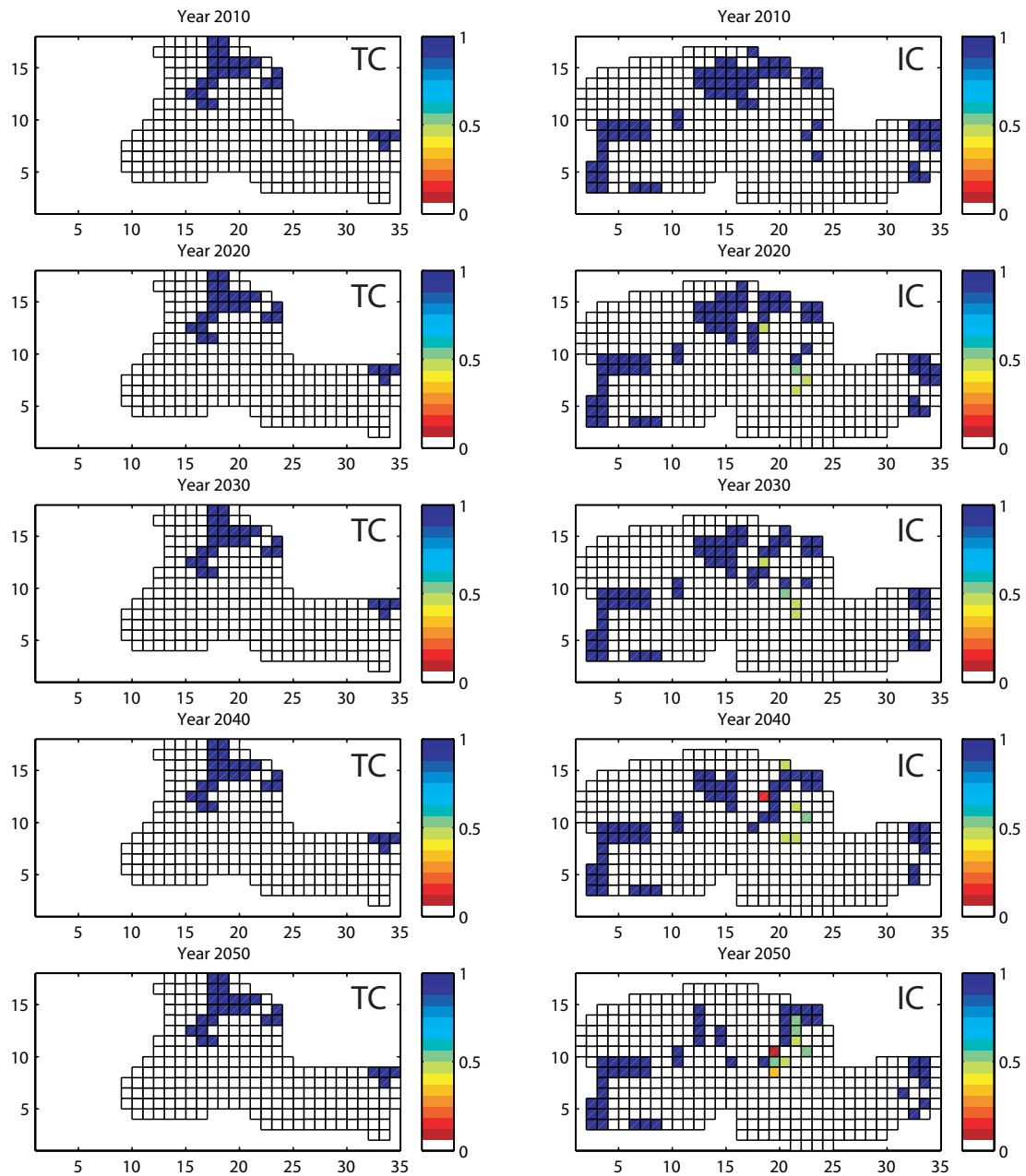


Figure 5.10: Density plot of the well locations as proposed by the last generation individuals. The dark blue colored cells indicate that all of the non-dominated solutions propose pumping at this location. Contrary to that, reddish to light colors indicate that only parts of the solutions propose pumping at the corresponding FD cells. A shifting in the location of the IC pumping activity over time is visible in the central basin. This shift is induced by deep cones of depressions developing in the confined IC and the restrictions upon maximal drawdown.

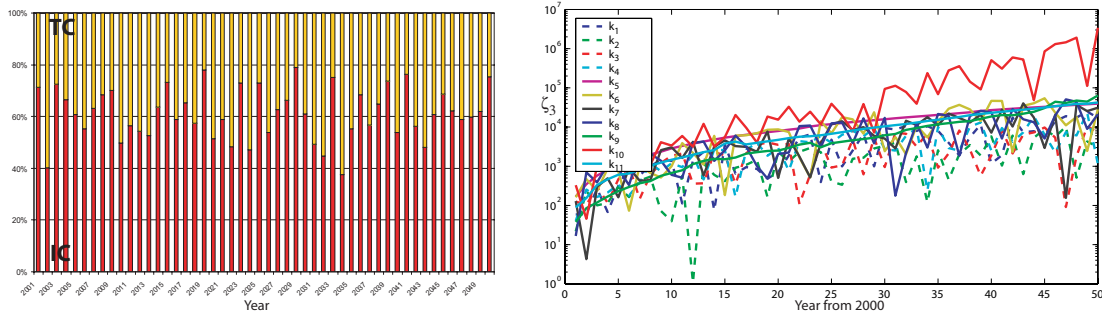


Figure 5.11: Scheduling of pumping shows oscillation within clusters and between the two aquifers, TC and IC. The lower peak of ζ_3 for network cluster k_2 (light green color) vanishes in period $t = 12$ which indicates collapse of pumping within one FD cell.

Policy Implications

For each of the decision-makers, intelligent scheduling of pumping apparently pays, as shown in the case of the *Perpetuation*-strategies. So far, however, it has not been stated more precisely whether transboundary cooperation is a necessary prerequisite for the achievement of these benefits as was suggested by the results of the simplistic linear optimization model in Chapter 3 suggested. Remember that cooperation in our case implies the notion of a transboundary institution that determines basin-wide allocation, irrespective of national boundaries. Due to the considerable size of the resource, it is conceivable that the cost savings can be realized entirely by the optimal location-allocation of pumping within each national territory without the need for further transnational cooperation – at least over the optimization time horizon of 50 years.

The Figure 5.12 shows for each country how much of the demand it should cover from foreign territory according to the *Pareto*-optimal *Perpetuation*-strategies. Algeria has no incentive to pump in Libya due to the great distances of its demand centers from the Libyan territory. The commonly shared Chott region between Algeria and Tunisia (see Figure 1.1 in Chapter 1 for a map overview) is critical with regard to Chott induced salination. The gradient criteria present there require Tunisia to shift part of its TC pumping to the nearby Algerian side. Clearly, Tunisia could provide its demand from the IC. However, it appears to be more cost efficient to convey water from the nearby Algerian infrastructure than to invest in IC boreholes, at least in the beginning. Remember that the IC in Tunisia is more than 1000 m deep and boreholes therefore expensive to drill. Furthermore, optimization proposes that Tunisia gets part of its water to supply the Nefzawa oases from the southern Ghadames wellfield in Libya where the three countries join near the oasis of Ghadames. The Ghadames wellfield serves the western branch of the *Great Man Made River* with groundwater from the IC. Libya finally should spread pumping of the Ghadames wellfield over a greater area than initially planned. Yet, we do believe that the Libyan authorities planned the wellfield in the Ghadames region based on

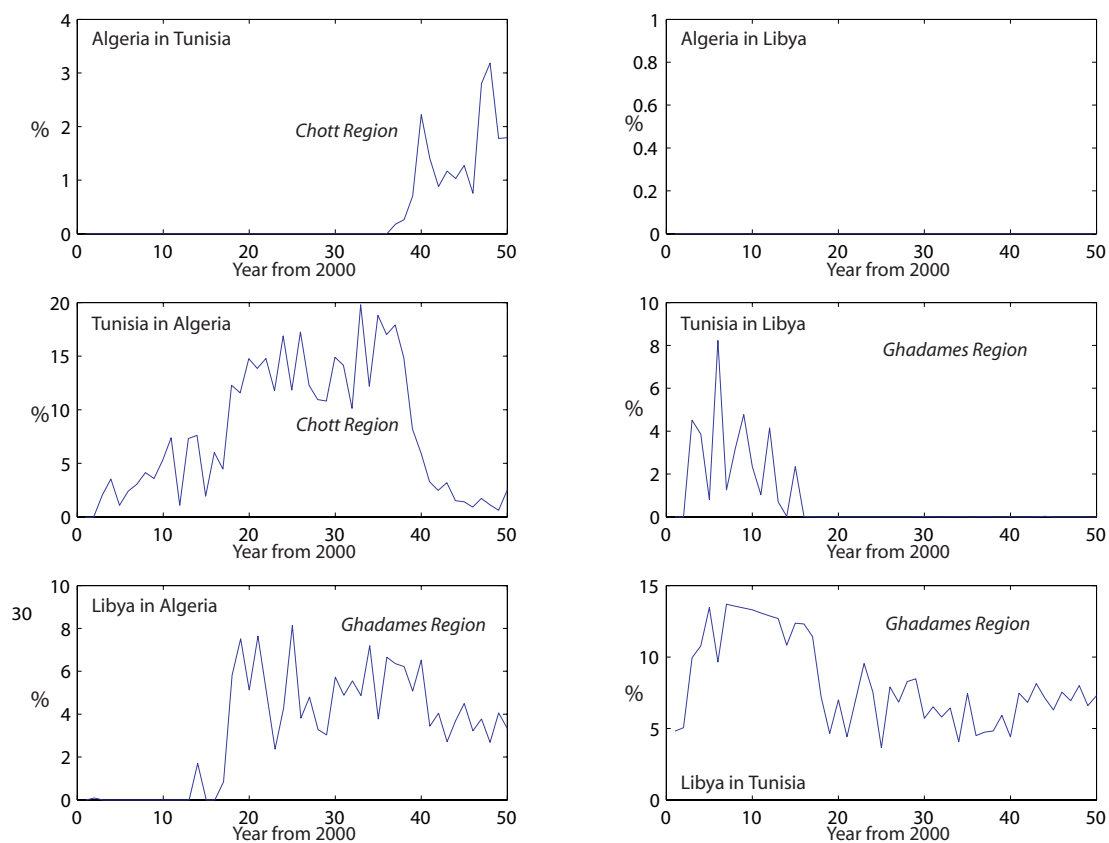


Figure 5.12: For each country, percentage of pumping in foreign countries compared to total country demand is shown. The proposed values for Libya might be an artefact from a wrong FD NWSAS model conceptualization in the Ghadames area and have to be reviewed (see text).

detailed knowledge about the resource and its properties. It is not conceivable that a wellfield installation of this size with an estimated maximum yield of 20 m³/s would require relocation after that short a time of less than 20 years in operation (see IC graphics in Figure 5.10). In fact, a lifetime of approximately 40 years of the Libyan wellfield infrastructure has been assumed by Libyan authorities (oral communication O. Salem and L. Madi, 2002). The borehole dynamics in that region proposed by our modeling results might be related to a wrong conceptualization of our FD NWSAS model in the Ghadames region. Certainly, a more detailed FD model of the Libyan Ghadames area could improve model results there.

Based on this, the results from the linear simulation–optimization in Chapter 3 have to be refuted. Since that overly simplistic linear model was not capable of binary scheduling, i.e. switching on and off of pumping locations, it proposed an optimal allocation that has not necessarily anything to do with optimal real–world strategies.

Compared to the overall quantity pumped, the share of transboundary water transfer is marginal as proposed by the optimized location–allocation schemes. In other words, benefits result mostly from intelligent pumping scheduling within the countries. This is mainly because of the immense resource size and the transnational distances between the demand centers. As optimization results show, only the Chott region could profit from transboundary management and it seems beneficiary to establish a transnational institution that would regulate resource allocation in this area. For this, the establishment of the trinational SASS programm within the non–governmental OSS has laid a promising foundation.

This finding does not discard the necessity for transboundary management. In contrary, any strategy deemed optimal for one country is only optimal as long as the others follow their optimal strategies due to the transboundary feedback given by the aquifers piezometry. This becomes even more true over the long horizon. Dispersive forces will start to dominate due to the regional lowering of the piezometric level which might render transboundary management a necessity under the pursuit of cost minimizing strategies. Optimization runs over a longer time horizon – say 100 years or more – might very well reproduce actual future location–allocation behavior. Yet, one has to keep in mind, that it would be extraordinarily difficult to determine technical change and its implications on prices and technology over such a time horizon. Why this is of importance shows the following example. When Libya started to plan the *Great Man Made River* in the late seventies, the cost of 1 m³ of desalinated seawater was approximately 5.5 US\$. At that time, the per meter cube cost figures resulting from the *Great Man Made River*–project were by large competitive with less than 1 US\$ (Alghariani, 2004). Due to technical progress in the development of new membranes, the average price of desalinated seawater nowadays has fallen to less than 0.5 US\$. The role of desalinated seawater in substituting the increasingly expensive fossil groundwater will therefore increase in the foreseeable future. If the oases agriculture were to be preserved by the governments over the long run, it can be sustained with this infinite resource and the capital saved by

pursuing intelligent groundwater management strategies can be used to invest in the necessary desalination infrastructure.

5.3 Areas of Future Research

Two salient issues need further attention. First, due to the complexity of the search space, the quality of the optimization cannot be easily assessed. That is, we do not know how *good*, i.e. how close to the optimum, the calculated *Pareto*-front is. The development of a benchmark problem would certainly be welcome. The sole measure at hand for doing so is critically reviewing whether the trade-off solutions are reasonable. Clearly, this can only be established with appropriate feedback from the local decision-makers. Second, of the many simulation-optimization model enhancements and applications that are possible, the following require future attention with high priority:

- A vigorous sensitivity analysis with regard to population and mating pool size as determinants of the diversity of *Pareto*-optimal solutions has to be carried out. A bigger population size than the one utilized would generally be preferable. However, computational limitations are restrictive. On average, optimization convergence was achieved after one week of computing. A more time-efficient implementation of the conjugate gradient solver would greatly improve speed and flexibility with regard to future calculations. Furthermore, the evolutionary algorithm optimization method is inherently parallel. The benefits of parallel, distributed computing should be exploited in the future in order to reduce computation time.
- Different multi-objective evolutionary algorithms have to be compared with regard to their performance and their capability of approximating the set of *Pareto*-optimal solutions. The strict modularity between the problem dependent *Variator* and the problem independent *Selector* framework will allow a straight forward implementation of the different optimization algorithms.
- Of utmost importance is the improvement of the quality of the input price data – infrastructural as well as energy prices. As shown in Section 4.2 of Chapter 4, their spatial distribution, magnitude and ratio relative to each other critically determine optimal solutions.
- Sensitivity to technical progress has to be determined. Furthermore, it would be desirable to include the second backstop technology option of pumping desalinated water from the coast to the inland in the model. With that, the gradual transition from the consumptive use of fossil groundwater to the tapping of the infinite resource of desalinated seawater could be reproduced.
- In theory, the method utilized can be coupled with any groundwater system within which optimal scheduling according to some quantifiable criteria is to

be determined. It would be interesting to couple it with smaller scale FD models such as the Nefzawa model to determine optimal pumping strategies on a local scale.

- The quantification of agricultural benefits could be included in the simulation–optimization approach so as to maximize individual current net benefits instead of minimizing individual current costs. The endogenous determination of water supply might render altogether different location–allocation strategies optimal since some agricultural centers simply do not produce at the *Pareto*–frontier. However, it is doubtful whether the necessary systematic knowledge about agricultural productivity will ever be available at the basin scale. Nevertheless, such a model extension could be tested at the oasis level.
- Options of demand management have not been investigated in this study. Over the course of time, farmers adapt to changing environmental as well as economic conditions. Hence, the demand sensitivity of irrigation water to its price might be utilized by decision makers to steer future agriculture production towards a desired direction. The economic system of desert agriculture could be modeled by means of a decentralized agent approach with endogenic demand. The evolving patterns of groundwater utilization under optimizing behavior could then be studied.

Chapter 6

Conclusions

The major findings are:

- Using the Nefzawa oases in Southern Tunisia as an example, typical problems with regard to desert agriculture are discussed. Considerable technical inefficiencies of agricultural production are shown to exist. Private producers compared to governmentally supported ones are generally more efficient with regard to their input to output ratio of production. Nevertheless, a further promotion of the unregulated private groundwater utilization should be discouraged within the present legal framework. Due to the invisible nature of the groundwater resource, a knowledgeable planner aware of regional resource characteristics in the Nefzawa is better able to secure the productive potential of groundwater and soil and devise strategies against ongoing groundwater and soil salination than a large number of individuals which are ignorant of regional resource aspects.
- Over the last 20 years, TC groundwater over parts of the Nefzawa oases has been affected by quality deterioration. Three potential salination sources have been identified, i.e. pollution by brine from the nearby salt lake Chott El Djerid, upwelling from saline Turonian resp. IC water as well as backflow from highly charged agricultural drainage water. The relevance of the corresponding sources in the affected areas was assessed by environmental tracer analysis. It could be shown that the fingerprint of both, Turonian / IC as well as drainage water was visible in the TC. A finite difference flow and transport model was constructed to confirm the basic understanding of the salination processes and their time scales. Subsequently, scenario analysis was carried out. Results show that neither, continued present nor increased pumping in the region are sustainable because of the ongoing salinity increase. Pumped TC / IC water for irrigation purposes, however, could be conveyed from more distant places to the Nefzawa.
- The local threat of salination as well as the increasing depth from which groundwater has to be pumped are the two major restrictions with regard to future groundwater management options. The increasing demand therefore has to be covered by intelligent strategies. A simplistic linear simulation–optimization model is presented which allows the quantification of cost savings under optimal, that is cost–minimal, strategies subject to the above restrictions. Optimization is carried out over 50 years. Under the assumption that groundwater provision costs are proportional to pumping depth, it was shown that a simple redistribution of the fixed, demanded quantity over the existing

network can reduce costs by 15% compared to a reference *Status Quo*-strategy, under which each country simply covers its demand as envisaged.

- Traditional, gradient-based optimization techniques overly restrict the allowed complexity of the optimization problem. The development of recent multi-objective evolutionary optimization algorithms and their capability of successfully handling complex simulation-optimization models motivated the development of a multi-objective groundwater management tool. Under the assumption of given time-varying demand for each country and agricultural center, this tool is capable to identify *Pareto*-optimal location-allocation strategies with regard to the groundwater provision costs for each country. The model calculates nonlinear installation as well as running costs incurring due to pumping and the conveyance of groundwater. From a given set of pumping locations and for each agricultural demand center, it identifies a conveyance network by which the pumped water is transported to the final demand destination. Furthermore, it incorporates a heuristics that relocates boreholes once a constraint at a certain location is no longer fulfilled. Already installed boreholes can be activated again after a certain head recovery. The genetic optimization algorithm operates on a set resp. population of different pumping strategies. Mutation and variation operators are presented so as to preserve population diversity. Due to program modularity, the optimization model can be coupled with any finite difference groundwater model.
- The simulation-optimization model is tested on a synthetic supply problem where three countries have to decide upon their distribution of pumping over a given time-horizon so as to minimize their corresponding costs. It is shown how the model can be used as a descriptive as well as prescriptive tool. Under the assumption of national territories, optimization results for the chosen problem setup suggest the following: a) Optimal, i.e. individually cost minimal strategies, require each national decision-maker to locate his wells so that the drawdown effect caused by his own on the others is substantial; b) each of the decision-makers could be made better off if territorial restrictions were not present. In other words, although each decision-maker is inclined to harm his neighbors while minimizing his own costs, transboundary cooperation pays.
- Two different location-allocation strategies in the context of the NWSAS are finally ranked against the non-cooperative *Status Quo*-strategy. The *Perpetuation*-strategy is one where the decision-makers cooperate on freely distributing demand over existing infrastructure, irrespective of national borders. The *Imaginary future*-strategy is one where existing water provision infrastructure is refuted and optimal location-allocation patterns are sought from scratch. Model results show that the latter strategies cause excessive costs compared to the former two. Furthermore, average per unit water provision prices in the year 2050 are 7 times smaller for the *Perpetuation*-strategy compared with the

Status Quo–strategy. Therefore, it appears to be individually rational for the Northern African decision–makers to implement optimal *Perpetuation* strategies. They are characterized by intelligent scheduling, i.e. oscillating pumping stress between boreholes and aquifers, upon the existing and required future infrastructure. Over the optimization time horizon of 50 years, demand can be covered without the large–scale renewal of groundwater provision infrastructure. Due to the threat of salination in the Chott region of the central NWSAS basin, transboundary cooperation between Algeria and Tunisia would be beneficiary. Due to the size of the resource however, large volume transboundary water transfers do not result from optimization and each country has enough options to cover its demand under cost–minimizing behavior on its own territory during the next 50 years.

Appendix A

Stochastic Frontier Production Function Estimation

A.1 FRONTIER 4.1c Input Data File

Table A.1: Input file listing

#	t	ln(Y)	ln(q)	ln(A)	ln(l)	ln(f)	S	Exp	Org	Edu	Fam
1	1	8.37	13.02	3.91	5.36	19.93	1.8	12	1	3	10
2	1	9.37	13.18	4.61	5.25	20.03	1.8	12	1	2	7
3	1	8.02	12.65	4.61	4.79	19.56	1.8	12	1	3	13
4	1	8.68	12.83	4.61	5.89	19.74	1.8	12	1	1	10
5	1	6.21	12.54	4.32	5.97	19.45	1.8	12	1	5	7
6	1	8.49	11.95	4.01	2.71	18.86	1.8	12	1	2	6
7	1	8.88	13.34	5.01	5.97	20.25	1.8	12	1	3	6
8	1	8.23	13.12	4.61	5.30	20.03	1.8	12	1	3	8
9	1	8.75	12.65	5.30	6.15	19.56	1.8	42	1	2	7
10	1	8.92	12.83	5.30	6.15	19.74	1.8	30	1	2	8
11	1	6.62	11.73	3.22	4.50	18.64	1.8	12	1	5	4
12	1	9.45	12.83	5.12	4.62	19.74	1.8	30	1	2	4
13	1	7.60	11.73	3.57	4.93	18.64	1.8	12	1	3	3
14	1	7.17	10.63	3.22	3.22	17.54	4.2	40	1	5	5
15	1	7.65	11.33	3.91	4.09	18.23	4.2	22	1	5	8
16	1	4.61	9.94	2.53	3.40	16.85	4.2	30	1	3	13
17	1	6.62	10.63	3.22	3.74	17.54	4.2	21	1	2	14
18	1	4.94	9.94	2.53	2.77	16.85	4.2	15	1	3	4
19	1	4.79	10.63	3.22	3.81	17.54	4.2	27	1	2	10
20	1	5.70	9.94	2.53	4.50	16.85	4.2	25	1	1	6
21	1	7.00	11.33	3.91	4.36	18.23	4.2	17	1	4	8
22	1	7.60	12.14	5.30	3.40	19.04	4.2	55	1	5	7
23	1	2.30	9.25	1.83	2.71	16.15	4.2	24	1	3	9
24	1	8.83	11.73	4.32	4.50	18.64	4.2	12	1	2	9
25	1	5.74	9.94	2.12	3.61	16.85	4.2	60	1	2	2
26	1	7.67	11.89	4.47	3.74	18.79	4.2	32	1	5	8
27	1	6.72	9.94	2.53	4.09	16.85	4.2	22	1	1	8
28	1	8.88	12.42	5.01	5.35	19.33	4.2	46	1	2	8
29	1	9.34	13.31	5.99	5.74	20.21	4.2	32	1	1	23
30	1	8.34	12.71	5.30	5.48	19.62	4.2	40	1	2	7
31	1	6.72	11.33	3.91	4.73	18.23	4.2	37	1	1	12

Stochastic Frontier Production Function Estimation

#	t	ln(Y)	ln(q)	ln(A)	ln(l)	ln(f)	S	Exp	Org	Edu	Fam
32	1	6.69	9.94	2.53	3.95	16.85	4.2	10	1	2	9
33	1	6.40	9.94	2.53	3.85	16.85	4.2	10	1	6	4
34	1	5.52	9.65	2.08	4.61	16.56	4.2	42	1	2	4
35	1	6.19	9.94	2.53	4.41	16.85	4.2	17	1	5	5
36	1	6.40	11.64	4.32	4.50	18.55	4.2	25	1	4	10
37	1	6.52	9.94	2.53	4.25	16.85	4.2	31	1	3	10
38	1	6.54	10.63	3.22	3.83	17.54	4.2	22	1	5	10
39	1	7.05	11.04	3.62	4.14	17.95	4.2	50	1	1	6
40	1	7.31	11.73	4.32	4.01	18.64	4.2	8	1	6	9
41	1	7.07	9.94	2.53	3.50	16.85	4.2	25	1	3	11
42	1	5.70	9.94	2.53	3.09	16.85	4.2	31	1	1	7
43	1	6.40	9.94	3.22	4.33	16.85	4.2	52	1	1	4
44	1	7.17	12.02	4.61	4.91	18.93	7	32	1	1	8
45	1	5.63	9.94	2.53	3.40	16.85	7	29	1	5	9
46	1	6.35	11.33	3.78	4.94	18.23	7	45	1	2	7
47	1	8.13	12.02	4.61	5.35	18.93	7	50	1	2	2
48	1	7.41	11.44	4.03	4.74	18.35	7	17	1	5	8
49	1	6.96	11.44	4.14	4.09	18.35	7	50	1	2	4
50	1	6.48	11.04	3.62	4.62	17.95	7	38	1	2	12
51	1	7.05	12.02	4.61	4.52	18.93	7	12	1	5	9
52	1	8.81	12.58	4.83	4.50	19.49	7	52	1	2	7
53	1	7.44	11.95	4.54	4.77	18.86	7	40	1	1	4
54	1	7.31	12.50	5.08	5.01	19.41	7	49	1	2	5
55	1	8.15	12.65	5.93	6.25	19.56	7	9	1	6	4
56	1	5.70	10.35	2.77	3.91	17.25	7	50	1	2	5
57	1	7.31	12.02	4.61	5.42	18.93	7	7	1	2	7
58	1	5.30	9.94	2.53	3.56	16.85	7	50	1	1	7
59	1	6.23	11.33	3.91	4.53	18.23	7	15	1	2	7
60	1	3.91	9.94	2.53	3.76	16.85	7	48	1	2	5
61	1	6.91	12.02	4.61	3.40	18.93	7	15	1	2	8
62	1	5.44	9.94	2.53	5.31	16.85	7	37	1	1	8
63	1	7.00	12.24	4.83	5.30	19.15	7	40	1	2	10
64	1	7.09	11.33	3.91	4.68	18.23	7	30	1	5	6
65	1	7.00	11.33	3.91	5.48	18.23	7	23	1	2	6
66	1	6.19	10.63	3.22	2.48	17.54	7	42	1	1	4
67	1	7.13	11.73	4.32	4.96	18.64	7	8	1	1	9
68	1	6.55	10.63	3.22	4.09	17.54	7	42	1	1	9
69	1	6.58	11.33	3.91	4.75	18.23	7	48	1	1	4
70	1	7.06	11.55	4.14	4.82	18.46	7	40	1	1	10
71	1	5.56	9.94	2.53	4.20	16.85	7	12	1	1	7
72	1	6.31	11.33	3.91	4.41	18.23	7	10	1	4	7
73	1	6.09	9.94	2.90	3.40	16.85	7	40	1	2	6

#	t	ln(Y)	ln(q)	ln(A)	ln(l)	ln(f)	S	Exp	Org	Edu	Fam
74	1	5.52	11.33	3.91	3.40	18.23	7	20	1	1	6
75	1	6.48	11.33	3.91	4.09	18.23	7	41	1	1	12
76	1	4.32	7.13	-1.90	2.71	14.03	3.6	42	1	1	8
77	1	6.81	11.26	3.44	3.58	18.17	3.6	16	1	6	6
78	1	6.75	11.67	4.32	5.70	18.57	3.6	54	1	2	7
79	1	7.09	10.35	3.00	4.09	17.25	3.6	11	1	4	7
80	1	6.55	11.26	4.32	5.08	18.17	3.6	20	1	3	6
81	1	6.43	10.66	4.25	3.11	17.57	3.6	31	1	4	9
82	1	7.16	11.04	3.91	3.40	17.95	3.6	13	1	3	6
83	1	8.78	12.65	5.30	5.35	19.56	3.6	32	1	2	11
84	1	6.48	10.90	3.50	5.10	17.81	3.6	40	1	2	8
85	1	7.15	10.21	3.22	4.17	17.12	3.6	45	1	4	10
86	1	7.70	11.60	4.61	5.04	18.51	3.6	37	1	4	8
87	1	7.65	12.29	5.01	4.03	19.20	3.6	33	1	1	7
88	1	3.91	9.36	2.08	4.50	16.27	3.6	53	1	4	5
89	1	6.76	11.04	3.91	4.65	17.95	3.6	60	1	2	7
90	1	5.01	9.65	2.53	3.50	16.56	3.6	4	1	5	4
91	1	10.22	13.54	6.31	7.47	20.45	3.6	20	1	3	15
92	1	8.00	11.26	4.16	4.84	18.17	3.6	26	1	6	6
93	1	6.25	10.57	2.53	3.69	17.48	3.6	17	1	1	7
94	1	8.47	12.54	5.16	5.36	19.45	3.6	28	1	2	12
95	1	7.17	11.04	3.91	3.74	17.95	3.6	5	1	5	6
96	1	7.84	11.60	5.01	5.91	18.51	3.6	32	1	1	3
97	1	5.70	11.04	3.91	4.53	17.95	3.6	17	1	3	7
98	1	6.98	10.35	3.22	4.39	17.25	3.6	1	1	3	7
99	1	5.30	0.00	3.91	1.39	0.00	3.6	14	1	1	6
100	1	6.21	9.05	1.61	4.09	15.96	3.6	25	1	3	1
101	1	5.86	10.21	3.91	3.40	17.12	3.6	20	1	5	11
102	1	6.57	10.35	3.22	3.83	17.25	3.6	33	1	2	4
103	1	7.14	11.95	4.32	3.89	18.86	3.6	40	1	2	8
104	1	8.74	11.90	4.72	3.61	18.81	3.6	55	1	1	2
105	1	6.04	9.88	2.53	3.22	16.78	3.6	19	1	3	6
106	1	5.63	9.65	2.30	5.14	16.56	3.6	20	1	5	2
107	1	7.43	10.86	3.91	4.01	17.76	2.6	7	1	3	6
108	1	8.16	12.69	5.52	4.88	19.60	2.6	42	1	2	14
109	1	7.47	11.55	4.32	3.89	18.46	2.6	30	1	2	10
110	1	6.63	9.88	3.22	4.29	16.78	2.6	12	1	2	8
111	1	5.14	8.78	2.30	0.69	15.68	2.6	17	1	2	10
112	1	7.65	11.08	3.91	4.09	17.99	2.6	14	1	2	8
113	1	8.13	12.18	5.30	4.68	19.09	2.6	22	1	2	4
114	1	8.24	11.77	4.61	4.50	18.68	2.6	31	1	2	8
115	1	9.62	13.85	5.70	4.79	20.76	2.6	26	1	3	7

Stochastic Frontier Production Function Estimation

#	t	ln(Y)	ln(q)	ln(A)	ln(l)	ln(f)	S	Exp	Org	Edu	Fam
116	1	6.70	10.77	5.01	4.96	17.68	2.6	17	1	2	5
117	1	8.13	12.51	5.30	5.02	19.42	2.6	42	1	2	4
118	1	8.64	12.65	6.21	4.79	19.56	2.6	23	1	3	13
119	1	7.00	10.86	3.22	4.95	17.76	2.6	35	1	2	8
120	1	7.05	11.77	3.91	6.06	18.68	2.6	56	1	2	3
121	1	6.36	11.08	3.91	4.42	17.99	2.6	6	1	3	-
122	1	5.16	10.57	3.22	3.66	17.48	2.6	22	1	4	6
123	1	6.02	8.78	-0.92	4.09	15.68	2.6	45	1	2	2
124	1	5.70	9.69	2.89	3.81	16.60	2.6	50	1	1	7
125	1	7.44	12.87	5.52	5.87	19.78	2.6	30	1	3	8
126	1	10.76	14.26	6.91	6.19	21.16	2.6	52	1	1	8
127	1	9.56	12.30	5.30	5.19	19.21	2.6	50	1	2	8
128	1	7.03	11.42	4.09	4.85	18.32	2.6	70	1	2	8
129	1	5.37	9.47	3.22	5.91	16.38	2.6	60	1	1	8
130	1	8.32	11.08	5.01	5.99	17.99	2.6	60	1	2	5
131	1	5.86	9.47	3.22	2.48	16.38	2.6	40	1	1	6
132	1	8.22	12.24	4.61	5.14	19.15	2.6	32	1	5	8
133	1	7.67	11.34	4.32	4.17	18.25	2.6	13	1	3	7
134	1	7.38	11.26	5.30	4.50	18.17	2.6	30	1	4	9
135	1	6.11	9.69	3.22	4.57	16.60	2.6	52	1	1	3
136	1	6.62	10.97	5.01	3.40	17.88	2.6	37	1	2	7
137	1	7.09	11.95	5.52	4.79	18.86	2.6	36	1	2	10
138	1	7.29	10.82	3.91	4.50	8.02	3	10	2	1	6
139	1	7.96	10.12	4.83	5.19	6.91	3	18	2	2	3
140	1	6.55	10.63	3.91	4.23	7.63	3	18	2	1	8
141	1	9.25	11.55	5.30	5.78	9.22	3	12	2	5	6
142	1	5.19	7.64	2.77	3.50	7.60	4	6	2	5	8
143	1	7.78	9.02	3.91	4.80	8.04	3.5	16	2	2	8
144	1	8.34	11.04	5.70	6.17	8.01	3.5	19	2	3	6
145	1	6.51	8.04	3.91	4.16	6.91	4	18	2	3	7
146	1	8.34	9.94	5.30	5.90	8.02	4	3	2	1	7
147	1	7.00	8.55	3.91	4.39	6.91	4	21	2	3	9
148	1	6.31	8.20	3.22	4.09	6.96	4	28	2	1	5
149	1	7.17	9.45	5.01	4.19	6.91	3.5	12	2	2	4
150	1	6.72	8.84	3.91	4.50	7.60	3.5	18	2	5	8
151	1	6.25	7.79	3.22	4.55	6.96	3.5	18	2	5	6
152	1	6.51	9.70	3.22	3.95	8.02	3	13	2	2	6
153	1	9.46	10.63	5.70	6.13	9.22	3	12	2	5	8
154	1	9.06	9.83	5.30	6.23	9.90	3.5	17	2	1	5
155	1	8.72	11.89	4.61	4.50	8.59	3.5	18	2	3	8
156	1	7.84	9.81	4.61	4.83	8.43	3.5	18	2	6	8
157	1	9.49	11.95	5.99	6.90	10.86	3.5	2	2	3	6

#	t	ln(Y)	ln(q)	ln(A)	ln(l)	ln(f)	S	Exp	Org	Edu	Fam
158	1	5.99	8.04	2.53	3.40	6.22	4	18	2	1	8
159	1	8.58	11.22	4.61	4.50	8.32	3.5	10	2	1	5
160	1	7.65	9.72	3.69	4.50	7.67	2.5	13	2	1	9
161	1	8.32	10.41	4.61	5.19	9.23	2.5	22	2	3	4
162	1	6.75	9.62	3.91	4.58	8.53	2.5	10	2	3	6
163	1	7.88	9.53	4.61	5.19	8.99	2.5	14	2	3	8
164	1	8.48	10.63	4.83	5.69	3.93	2.5	18	2	2	7
165	1	7.38	8.55	3.91	4.19	7.65	2.5	5	2	5	11
166	1	8.85	11.51	4.83	4.91	8.53	2.5	16	2	3	7
167	1	8.06	10.15	4.32	4.38	8.61	2.5	13	2	1	7
168	1	6.80	9.51	3.91	4.37	7.67	2.5	10	2	3	7
169	1	7.31	9.65	3.91	4.52	7.63	2.5	12	2	5	6
170	1	10.11	12.07	5.70	6.54	10.84	2.5	22	2	1	8
171	1	7.74	9.72	3.91	4.50	8.57	2.5	12	2	5	4
172	1	8.26	9.87	4.61	4.79	7.65	2.5	13	2	2	5
173	1	8.15	10.24	4.14	4.01	8.55	2.5	13	2	2	6
174	1	8.58	10.65	5.01	6.27	8.46	2.5	12	2	5	5
175	1	8.46	10.75	4.83	4.89	8.20	2.5	12	2	2	6
176	1	6.77	8.74	3.91	4.09	7.65	3	13	2	3	3
177	1	7.82	10.12	4.61	4.83	8.32	3	13	2	5	8
178	1	7.47	8.74	3.22	4.44	8.06	2.5	23	2	5	7
179	1	9.83	12.11	6.91	8.37	11.17	2.5	16	2	5	2
180	1	7.44	10.28	3.91	3.97	8.29	3.2	18	2	1	6
181	1	7.50	9.74	3.91	4.09	8.58	2.5	13	2	4	4
182	1	7.97	10.12	3.91	4.79	8.02	2	13	2	1	7
183	1	8.84	11.63	5.70	5.60	6.91	2	13	2	2	9
184	1	8.04	10.16	4.16	4.22	7.60	2	15	2	3	6
185	1	9.12	11.04	5.01	4.74	9.41	2	19	2	1	8
186	1	8.26	10.79	5.01	5.57	8.56	2	13	2	5	5
187	1	8.67	10.82	4.61	4.89	8.72	2	12	2	6	6
188	1	7.88	10.57	4.61	4.72	7.65	2	11	2	4	4
189	1	8.65	11.16	5.01	5.27	8.09	2	12	2	3	11
190	1	9.49	11.77	5.86	5.65	10.02	2	17	2	1	14
191	1	8.29	11.26	5.70	5.89	8.78	2	8	2	5	5
192	1	8.76	11.73	5.01	6.12	8.37	2	15	2	3	10
193	1	6.68	10.41	4.91	4.50	7.35	3	9	2	3	7
194	1	6.04	10.35	4.09	4.14	8.32	2	12	2	3	8
195	1	7.43	13.27	4.83	5.48	8.56	2	10	2	5	3
196	1	6.31	11.22	4.61	4.52	7.65	2.5	11	2	3	16
197	1	6.31	10.41	4.61	3.40	8.58	2.5	8	2	1	8
198	1	6.40	11.04	3.22	4.50	7.63	2.5	10	2	3	8
199	1	6.71	8.62	4.32	4.09	6.91	2	2	2	2	8

Stochastic Frontier Production Function Estimation

#	t	ln(Y)	ln(q)	ln(A)	ln(l)	ln(f)	S	Exp	Org	Edu	Fam
200	1	7.74	11.04	5.30	6.11	8.29	2.5	13	2	5	6
201	1	8.28	10.41	4.61	5.03	8.52	3	13	2	2	7
202	1	5.39	9.02	3.91	4.38	8.02	2.5	13	2	2	5
203	1	4.79	0.00	4.61	3.40	7.60	2.5	10	2	5	7
204	1	10.50	0.00	5.70	7.71	9.47	3	17	2	5	4
205	1	8.57	11.08	5.30	5.98	8.19	3	8	2	1	8
206	1	9.24	11.16	5.86	6.04	8.61	2	21	2	3	11
207	1	8.80	10.41	4.61	5.52	8.73	1	21	2	3	6
208	1	10.38	14.95	7.09	6.88	9.39	3	19	2	2	7
209	1	7.74	11.10	5.30	6.09	7.78	2	21	2	2	7
210	1	9.14	10.92	5.30	6.41	9.64	2	21	2	2	10
211	1	12.35	14.73	8.85	8.94	13.82	1	10	2	1	10
212	1	8.56	11.26	5.70	6.74	8.27	2	21	2	1	4
213	1	9.78	11.55	6.40	6.64	9.55	2	21	2	1	6
214	1	8.56	9.14	4.83	6.14	7.82	2	20	2	1	12
215	1	7.84	10.53	5.70	6.42	8.29	2	16	2	3	6
216	1	9.56	11.33	5.99	6.60	9.47	2	15	2	2	6
217	1	7.58	9.83	4.61	3.81	6.96	2	21	2	5	9
218	1	9.13	10.82	6.40	6.84	8.61	2	21	2	6	5
219	1	9.55	11.26	5.99	6.89	9.24	2	13	2	3	9
220	1	6.11	10.82	3.91	4.09	6.96	2	16	2	1	5
221	1	6.96	11.51	4.32	3.76	8.05	2	19	2	1	3
222	1	8.73	10.45	5.70	5.90	9.71	1.5	17	2	1	9
223	1	9.02	10.57	5.30	6.36	8.41	1.5	20	2	2	10
224	1	6.75	9.76	4.61	4.91	6.91	1.5	18	2	3	12
225	1	6.75	9.83	3.91	4.09	8.37	1.5	6	2	3	6
226	1	6.48	9.40	3.22	4.01	7.63	1.5	18	2	5	2
227	1	5.83	10.41	3.91	4.09	7.65	1.5	20	2	1	5
228	1	8.28	10.23	4.61	4.44	8.52	1.5	18	2	1	4
229	1	7.60	9.25	3.91	4.32	7.63	1.5	18	2	2	3
230	1	7.35	9.94	3.91	4.36	8.54	1.5	18	2	5	6
231	1	7.84	10.82	3.91	4.09	7.70	1.5	18	2	1	6
232	1	6.40	10.82	3.91	3.93	7.35	1.5	19	2	5	4
233	1	7.55	11.04	4.61	4.09	7.90	1.5	19	2	3	10
234	1	7.38	10.68	4.61	4.32	8.06	1.5	16	2	2	9
235	1	6.96	9.72	4.61	3.74	6.96	1.5	12	2	2	4
236	1	8.06	10.53	3.91	4.47	7.65	1	20	2	3	7
237	1	9.24	9.94	5.30	6.10	8.92	1	12	2	1	9
238	1	6.40	10.23	5.01	3.74	8.71	1	13	2	1	12
239	1	8.89	9.72	5.70	6.51	8.70	1	19	2	2	6
240	1	7.50	9.53	4.83	5.98	7.60	1	18	2	1	4
241	1	6.75	9.53	4.14	4.52	6.91	1	18	2	1	8

#	t	ln(Y)	ln(q)	ln(A)	ln(l)	ln(f)	S	Exp	Org	Edu	Fam
242	1	8.54	10.53	4.61	4.79	8.32	1	15	2	3	4
243	1	8.38	10.35	6.11	6.11	8.70	1	8	2	5	12
244	1	6.68	10.82	2.81	4.09	7.60	1	18	2	3	6
245	1	7.79	10.35	3.91	4.36	8.02	1	18	2	5	2
246	1	8.79	10.53	4.61	5.19	8.33	1	18	2	5	12
247	1	7.47	10.82	4.32	4.38	8.02	1	6	2	1	6
248	1	6.86	9.94	4.47	4.30	8.02	1	20	2	3	7
249	1	6.21	9.25	3.22	3.40	0.00	1	16	2	1	6
250	1	9.05	10.75	5.30	6.35	8.72	1	18	2	1	7
251	1	9.01	10.82	5.30	5.48	8.55	2	11	2	5	6
252	1	8.31	10.35	5.30	5.16	7.63	2	13	2	1	11
253	1	7.44	10.41	4.61	4.67	7.65	2	5	2	1	12
254	1	7.52	10.12	4.32	5.01	6.96	2	18	2	1	3
255	1	6.91	10.16	3.91	4.70	7.65	2	14	2	3	6
256	1	7.24	9.94	4.61	4.57	7.65	2	9	2	3	7
257	1	8.14	10.53	4.61	5.55	8.53	2	12	2	3	3
258	1	6.28	8.55	3.22	3.40	6.22	2	13	2	3	7
259	1	9.24	10.35	5.30	5.35	9.23	2	12	2	1	11
260	1	8.07	10.82	4.61	4.55	8.01	2	21	2	5	3
261	1	8.74	11.01	4.61	4.75	7.61	2	11	2	6	4

A.2 FRONTIER 4.1c Output File

Output from the program FRONTIER (Version 4.1c)

instruction file = bothM4.ins

data file = bothM4.txt

Tech. Eff. Effects Frontier. The model is a production function. The dependent variable is logged.

the ols estimates are :

	coefficient	standard-error	t-ratio
β_0	0.25974630E+01	0.32157123E+00	0.80774111E+01
β_1	0.11069507E+00	0.36228682E-01	0.30554540E+01
β_2	0.56312979E+00	0.56929453E-01	0.98917126E+01
β_3	0.35719401E+00	0.58138433E-01	0.61438535E+01
β_4	-0.46931855E-02	0.12173963E-01	-0.38551006E+00
β_5	-0.12047427E+00	0.32257876E-01	-0.37347241E+01
σ^2	0.50901530E+00		

log likelihood function = -0.27918425E+03

the estimates after the grid search were :

β_0	0.31977745E+01
-----------	----------------

Stochastic Frontier Production Function Estimation

β_1	0.11069507E+00
β_2	0.56312979E+00
β_3	0.35719401E+00
β_4	-0.46931855E-02
β_5	-0.12047427E+00
δ_1	0.00000000E+00
δ_2	0.00000000E+00
δ_3	0.00000000E+00
δ_4	0.00000000E+00
σ^2	0.85768760E+00
γ	0.66000000E+00

iteration = 0 func evals = 20 llf = -0.27738074E+03
0.31977745E+01 0.11069507E+00 0.56312979E+00 0.35719401E+00-0.46931855E-02
-0.12047427E+00 0.00000000E+00 0.00000000E+00 0.00000000E+00 0.00000000E+00
0.85768760E+00 0.66000000E+00

gradient step

iteration = 5 func evals = 41 llf = -0.27592502E+03
0.32122976E+01 0.79459368E-01 0.53948404E+00 0.41245180E+00 0.13996815E-01
-0.13578368E+00 0.10349570E-01-0.53267614E-01 0.97124908E-02-0.78655164E-02
0.83820334E+00 0.68012998E+00

iteration = 10 func evals = 59 llf = -0.27404267E+03
0.33387421E+01 0.60724208E-01 0.52367913E+00 0.39249010E+00 0.30724426E-01
-0.14040596E+00 0.14497710E-01-0.50982573E+00 0.93143877E-01 0.85635289E-02
0.93184295E+00 0.72245163E+00

iteration = 15 func evals = 113 llf = -0.27316727E+03
0.32997083E+01 0.60789714E-01 0.52512698E+00 0.39448871E+00 0.32159531E-01
-0.14219930E+00 0.16630032E-01-0.10747870E+01 0.12523102E+00 0.13301172E-01
0.12416709E+01 0.80072767E+00

iteration = 20 func evals = 217 llf = -0.27308127E+03
0.32246288E+01 0.64337326E-01 0.52531712E+00 0.39255489E+00 0.31886815E-01
-0.14200128E+00 0.17772029E-01-0.14932558E+01 0.13927200E+00 0.45947232E-02
0.14588927E+01 0.81558809E+00

iteration = 25 func evals = 323 llf = -0.27308058E+03
0.32147419E+01 0.64716152E-01 0.52503272E+00 0.39257921E+00 0.32021008E-01
-0.14200292E+00 0.18158594E-01-0.15434887E+01 0.14227855E+00 0.49444837E-02
0.14716277E+01 0.81581765E+00

iteration = 29 func evals = 370 llf = -0.27308056E+03
0.32140740E+01 0.64786540E-01 0.52501530E+00 0.39255711E+00 0.31972100E-01
-0.14194959E+00 0.18156218E-01-0.15457058E+01 0.14237986E+00 0.47701763E-02
0.14721429E+01 0.81571762E+00

the final mle estimates are :

β_0	0.32140740E+01	0.44222703E+00	0.72679276E+01
-----------	----------------	----------------	----------------

β_1	0.64786540E-01	0.36542182E-01	0.17729248E+01
β_2	0.52501530E+00	0.55665603E-01	0.94315929E+01
β_3	0.39255711E+00	0.57166233E-01	0.68669403E+01
β_4	0.31972100E-01	0.14085639E-01	0.22698366E+01
β_5	-0.14194959E+00	0.34354467E-01	-0.41319108E+01
δ_1	0.18156218E-01	0.13217712E-01	0.13736279E+01
δ_2	-0.15457058E+01	0.18559898E+01	-0.83282017E+00
δ_3	0.14237986E+00	0.11104470E+00	0.12821851E+01
δ_4	0.47701763E-02	0.53355017E-01	0.89404457E-01
σ^2	0.14721429E+01	0.89986696E+00	0.16359561E+01
γ	0.81571762E+00	0.10879942E+00	0.74974448E+01

log likelihood function = -0.27308056E+03

LR test of the one-sided error = 0.12207381E+02

with number of restrictions = 5
note that this statistic has a mixed chi-square distribution

number of iterations = 29

(maximum number of iterations set at : 100)

number of cross-sections = 261

number of time periods = 1

total number of observations = 261

thus there are: 0 obsns not in the panel

covariance matrix :

0.19556474E+00 -0.10687188E-01 0.41771892E-02 -0.71797037E-02 0.83063025E-03
-0.71342638E-02 -0.28681359E-02 0.42182321E+00 -0.23881405E-01 -0.11587778E-02
-0.89939501E-01 0.60746174E-02
-0.10687188E-01 0.13353311E-02 -0.74207469E-03 -0.77247325E-04 -0.28439650E-03
0.35629547E-03 0.72498461E-04 -0.14826881E-01 0.70399852E-03 -0.89525691E-04
0.25247044E-02 -0.58154871E-03
0.41771892E-02 -0.74207469E-03 0.30986593E-02 -0.20114019E-02 0.12378591E-03
0.47752014E-04 -0.14571165E-03 0.22822592E-01 -0.11221443E-02 0.39675435E-03
-0.10121137E-01 -0.84101455E-03
-0.71797037E-02 -0.77247325E-04 -0.20114019E-02 0.32679782E-02 0.25714081E-04
0.98390319E-04 0.80836887E-04 -0.10019366E-01 0.42494836E-03 -0.28284430E-03
0.54548022E-02 0.63775487E-03
0.83063025E-03 -0.28439650E-03 0.12378591E-03 0.25714081E-04 0.19840524E-03
-0.20184430E-03 0.53954960E-04 -0.20187765E-02 0.32934573E-03 0.24700093E-03
0.16704751E-03 0.15223796E-03
-0.71342638E-02 0.35629547E-03 0.47752014E-04 0.98390319E-04 -0.20184430E-03
0.11802294E-02 0.80506321E-04 -0.80900727E-02 0.57888996E-03 0.19890037E-03

Stochastic Frontier Production Function Estimation

-0.10610501E-02 -0.75212883E-03
-0.28681359E-02 0.72498461E-04 -0.14571165E-03 0.80836887E-04 0.53954960E-04
0.80506321E-04 0.17470790E-03 -0.17523000E-01 0.97356935E-03 0.55516956E-04
0.50436432E-02 0.22164612E-03
0.42182321E+00 -0.14826881E-01 0.22822592E-01 -0.10019366E-01 -0.20187765E-02
-0.80900727E-02 -0.17523000E-01 0.34446982E+01 -0.14729223E+00 0.15067605E-01
-0.14493406E+01 -0.11236420E+00
-0.23881405E-01 0.70399852E-03 -0.11221443E-02 0.42494836E-03 0.32934573E-03
0.57888996E-03 0.97356935E-03 -0.14729223E+00 0.12330926E-01 0.11069263E-03
0.40717954E-01 0.14085822E-02
-0.11587778E-02 -0.89525691E-04 0.39675435E-03 -0.28284430E-03 0.24700093E-03
0.19890037E-03 0.55516956E-04 0.15067605E-01 0.11069263E-03 0.28467578E-02
-0.17789729E-01 -0.19856509E-02
-0.89939501E-01 0.25247044E-02 -0.10121137E-01 0.54548022E-02 0.16704751E-03
-0.10610501E-02 0.50436432E-02 -0.14493406E+01 0.40717954E-01 -0.17789729E-01
0.80976055E+00 0.84222139E-01
0.60746174E-02 -0.58154871E-03 -0.84101455E-03 0.63775487E-03 0.15223796E-03
-0.75212883E-03 0.22164612E-03 -0.11236420E+00 0.14085822E-02 -0.19856509E-02
0.84222139E-01 0.11837313E-01

mean efficiency = 0.63829636E+00

Table A.2: Individual, farm-specific technical efficiency estimates

Firm ID	Eff.-est.	Firm ID	Eff.-est.	Firm ID	Eff.-est.	Firm ID	Eff.-est.
1	0.71	66	0.75	131	0.56	196	0.41
2	0.81	67	0.63	132	0.62	197	0.57
3	0.61	68	0.70	133	0.67	198	0.64
4	0.67	69	0.53	134	0.39	199	0.66
5	0.13	70	0.62	135	0.38	200	0.52
6	0.85	71	0.59	136	0.36	201	0.81
7	0.64	72	0.51	137	0.26	202	0.32
8	0.60	73	0.70	138	0.77	203	0.31
9	0.54	74	0.41	139	0.76	204	0.89
10	0.59	75	0.58	140	0.65	205	0.76
11	0.46	76	0.82	141	0.82	206	0.77
12	0.81	77	0.64	142	0.60	207	0.81
13	0.65	78	0.27	143	0.82	208	0.78
14	0.77	79	0.74	144	0.66	209	0.52
15	0.74	80	0.31	145	0.70	210	0.78
16	0.27	81	0.49	146	0.77	211	0.77
17	0.67	82	0.71	147	0.76	212	0.62
18	0.44	83	0.69	148	0.74	213	0.78
19	0.20	84	0.40	149	0.70	214	0.78
20	0.47	85	0.70	150	0.68	215	0.46
21	0.59	86	0.55	151	0.67	216	0.78
22	0.58	87	0.60	152	0.74	217	0.76
23	0.13	88	0.12	153	0.82	218	0.62
24	0.84	89	0.44	154	0.82	219	0.76
25	0.59	90	0.36	155	0.86	220	0.52
26	0.70	91	0.69	156	0.77	221	0.69
27	0.75	92	0.70	157	0.77	222	0.72
28	0.75	93	0.67	158	0.79	223	0.77
29	0.71	94	0.65	159	0.86	224	0.48
30	0.59	95	0.68	160	0.82	225	0.66
31	0.47	96	0.47	161	0.79	226	0.68
32	0.75	97	0.23	162	0.65	227	0.41
33	0.69	98	0.69	163	0.75	228	0.82
34	0.45	99	0.75	164	0.80	229	0.80
35	0.59	100	0.73	165	0.79	230	0.73
36	0.33	101	0.36	166	0.84	231	0.82
37	0.68	102	0.63	167	0.83	232	0.55
38	0.62	103	0.57	168	0.69	233	0.73
39	0.65	104	0.83	169	0.75	234	0.69
40	0.63	105	0.66	170	0.85	235	0.67
41	0.81	106	0.37	171	0.80	236	0.82
42	0.61	107	0.69	172	0.82	237	0.81
43	0.55	108	0.51	173	0.85	238	0.43
44	0.58	109	0.64	174	0.74	239	0.69
45	0.63	110	0.59	175	0.82	240	0.54
46	0.46	111	0.70	176	0.72	241	0.59
47	0.73	112	0.73	177	0.76	242	0.82
48	0.71	113	0.59	178	0.82	243	0.53
49	0.65	114	0.71	179	0.57	244	0.73
50	0.57	115	0.79	180	0.81	245	0.79
51	0.57	116	0.26	181	0.80	246	0.82
52	0.83	117	0.52	182	0.82	247	0.73
53	0.66	118	0.56	183	0.76	248	0.56
54	0.49	119	0.57	184	0.83	249	0.73
55	0.47	120	0.32	185	0.86	250	0.76
56	0.56	121	0.37	186	0.72	251	0.81
57	0.58	122	0.23	187	0.83	252	0.75
58	0.54	123	0.84	188	0.76	253	0.71
59	0.49	124	0.40	189	0.80	254	0.73
60	0.18	125	0.23	190	0.82	255	0.65
61	0.67	126	0.77	191	0.61	256	0.67
62	0.40	127	0.79	192	0.76	257	0.75
63	0.43	128	0.40	193	0.52	258	0.73
64	0.66	129	0.14	194	0.45	259	0.84
65	0.59	130	0.53	195	0.51	260	0.78
						261	0.84

Bibliography

- ABEGGLEN, C., BECK, L., HAAG, S., RUTZ, D. & SCHOCH, C. 2001a Grundwassernutzung im nördlichen Afrika. Anhang. Master's thesis, Institute of Hydromechanics and Water Resources Management, Swiss Federal Institute of Technology, ETH Zurich.
- ABEGGLEN, C., BECK, L., HAAG, S., RUTZ, D. & SCHOCH, C. 2001b Grundwassernutzung im nördlichen Afrika. Technischer Bericht. Master's thesis, Institute of Hydromechanics and Water Resources Management, Swiss Federal Institute of Technology, ETH Zurich.
- ADOUM, A. 1996 Législation et réglementation des eaux en Algérie. *Tech. Rep.*. Agence National des Ressources Hydrauliques, Algier.
- AHLFELD, D. & RIEFLER, R. 2003 Documentation for MODOFC: A program for solving optimal flow control problems. *Tech. Rep.*. Amherst.
- AHLFELD, D. P. & MULLIGAN, A. E. 2000 *Optimal management of flow in groundwater systems*. San Diego: Academic Press.
- AIGNER, D., LOVELL, C. & SCHMIDT, P. 1977 Formulation and estimation of stochastic frontier production function models. *Journal of Econometrics* **6**, 21–37.
- ALGHARIANI, S. A. 2004 Water transfer versus desalination in North Africa: sustainability and cost comparison. Comments by: The Center of Data, Studies & Researches Great Man-Made River Authority Libyan Arab Jamahiriya.
- ARMINES–ENIT 1984 Modèle mathématique du Complexe Terminal Nefzawa–Djérid. *Tech. Rep.*. Ministère de l'Agriculture, Tunis, armines / Tunis.
- BALAND, J.-M. & PLATTEAU, J.-P. 1996 *Halting Degradation of Natural Resources*. Food and Agriculture Organization of the United Nations and Oxford University Press.
- BARTH, H. 1866 *Die grosse Reise Forschungen und Abenteuer in Nord- und Zentralafrika 1849-1855*, [aufl. 2] edn. Stuttgart; Wien: Thienemann Ed. Erdmann.
- BATTESE, G. E. 1992 Frontier production functions and technical efficiency: a survey of empirical applications in agricultural economics. *Agricultural Economics* **7**, 185–208.

- BATTESE, G. E. & COELLI, T. 1995 A model for technical inefficiency effects in a stochastic frontier production function for panel data. *Empirical Economics* **20**, 325–332.
- BATTESE, G. E. & COELLI, T. J. 1993 A stochastic frontier production function incorporating a model for technical inefficiency effects. *Tech. Rep.*. Armidale, working Papers in Econometrics and Applied Statistics.
- BEAR, J. 1979 *Hydraulics of groundwater*. New York a.o.: McGraw-Hill, mcGraw-Hill series in water resources and environmental engineering.
- BECK, L. 2002 Grundwassernutzung im nördlichen Afrika. Modellierung und Optimierung der aktuellen Bewirtschaftung. Master's thesis, Institute of Hydro-mechanics and Water Resources Management, Swiss Federal Institute of Technology, ETH Zurich.
- BINMORE, K. 1994 *Game theory and the social contract*. Cambridge, Massachusetts [etc.]: MIT Press.
- BLEULER, S., LAUMANN, M., THIELE, L. & ZITZLER, E. 2003 PISA - a platform and programming language independent interface for search algorithms. *Evolutionary Multi-Criterion Optimization, Proceedings* **2632**, 494–508.
- BRILL, T. C. & BURNES, H. S. 1994 Planning versus competitive rates of groundwater pumping. *Water Resources Research* **30** (6), 1873–1880.
- BRL 1999 Etude du plan directeur général de développement des régions sahariennes. *Tech. Rep.*. Ouargla, bRL Ingénierie.
- BROWN, L. R., GARDNER, G., HALWEIL, B. & STARKE, L. 1998 *Beyond Malthus sixteen dimensions of the population problem*. Washington, DC: Worldwatch Institute.
- BROZOVIC, N. 2002 Optimal extraction of a path-dependent, spatially heterogeneous resource or why aquifers are not bathtubs. Department of Agricultural and Resource Economics, University of California, Berkeley, CA 94720.
- CHIANG, W.-H. & KINZELBACH, W. 2001 *3D-groundwater modeling with PMWIN a simulation system for modeling groundwater flow and pollution*. Berlin: Springer.
- CIA 2003 *The world factbook*. United States Central Intelligence Agency.
- DASKIN, M. S. 1995 *Network and discrete location models, algorithms and applications*. New York [etc.]: Wiley.
- DEB, K. 2001 *Multi-objective optimization using evolutionary algorithms*. Chichester: John Wiley & Sons.

-
- DGRE 2000 Annuaire de la piézométrie des nappes de Tunisie. *Tech. Rep.*. Rep. Min. Agr. / DGRE, Tunis, general Direction of Water Resources.
- DOCKNER, E. 2000 *Differential games in economics and management science*. Cambridge: University Press.
- DOLLÉ, V. & TOUTAIN, G. 1990 Les systèmes agricoles oasiens. *Tech. Rep.*. Montpellier, options Méditerranéennes : Série A. Séminaires Méditerranéens.
- DOUGHERTY, D. E. & MARRYOTT, R. A. 1991 Optimal groundwater-management by simulated annealing. *Water Resources Research* **27** (10), 2493–2508.
- EDMUNDS, W., SHAND, P., GUENDOUZ, A., MOULLA, A., MAMOU, A. & ZOUARI, K. 1997 Recharge characteristics and groundwater quality of the Grand Erg oriental basin. *Tech. Rep.* Rep. WD/97/46R. British Geological Survey, Nottingham.
- EDMUNDS, W. M. & GAYE, C. B. 1997 Naturally high nitrate concentrations in groundwaters from the Sahel. *Journal of Environmental Quality* **26** (5), 1231–1239.
- EL-FAHEM, T. 2003 Salinisation of groundwater in the Nefzaoua Oases - South Tunisia. Master's thesis, Institute of Hydromechanics and Water Resources Management, Swiss Federal Institute of Technology, ETH Zurich and RWTH, Aachen.
- ELBATTI, D. 1996 Inventaire et analyse de la législation sur les eaux souterraines en Tunisie. *Tech. Rep.*. Direction Générale des Ressources en Eaux, Tunis.
- ERICKSON, M., MAYER, A. & HORN, J. 2001 The niched pareto genetic algorithm 2 applied to the design of groundwater remediation systems. In *Evolutionary multi-criterion optimization first international conference proceedings* (ed. E. Zitzler). Zurich, Switzerland.
- FAO 2003 *Groundwater management the search for practical approaches*. Rome: Food and Agriculture Organization of the United Nations, a joint publ. of the FAO Land and Water Development Division ... [et al.].
- FAO 2004a Agricultural statistical database. Food and Agricultural Organisation of the United Nations.
- FAO 2004b Aquastat, FAO information system on water and agriculture. FAO-STAT, Food and Agricultural Organisation of the United Nations.
- FAOSTAT 2004 Agricultural Statistical Database.
- FARRELL, M. J. 1957 The measurement of productive efficiency. *Journal of Royal Statistical Society* pp. 253–281, a 120.

- FEINERMAN, E. & KNAPP, K. C. 1983 Benefits from groundwater-management - magnitude, sensitivity, and distribution. *American Journal of Agricultural Economics* **65** (4), 703–710.
- FREESTONE, D. & HEY, E. 1996 *The Precautionary Principle and International Law: The Challenge of Implementation*, chap. Origins and Development of the Precautionary Principle, pp. 3–15. Kluwer Law International.
- GISSER, M. & SANCHEZ, D. A. 1980 Competition versus optimal-control in groundwater pumping. *Water Resources Research* **16** (4), 638–642.
- GLEICK, P. H. 2002 *The world's water 2002-2003 the biennial report on freshwater resources*. Washington, D.C.: Island Press.
- GLOVER, F., KLINGMAN, D. & PHILLIPS, N. V. 1992 *Network models in optimization and their applications in practice*. New York [etc.]: Wiley.
- GUEDDARI, M. 1980 Géochimie des sels et des saumures du Chott el Djérid (Sud Tunisien). PhD thesis, Univ. de Paul Sabatier, Toulouse, thèse 3ème cycle.
- HAIMES, Y. Y. 1977 *Hierarchical analyses of water resources systems modeling and optimization of large-scale systems*. New York a.o.: McGraw-Hill, McGraw-Hill series in water resources and environmental engineering.
- HARBAUGH, A. & McDONALD, M. 1996 Programmer's documentation for MODFLOW-96, an update to the U.S. Geological Survey modular finite-difference ground-water flow model. *Tech. Rep.*. U.S. Geological Survey Open-File Report 96-486.
- HEAL, G. 1998 *Valuing the Future: Economic Theory and Sustainability*. Columbia University Press.
- HEATON, T. H. E. 1984 Sources of the nitrate in phreatic groundwater in the western Kalahari. *Journal of Hydrology* **67** (1-4), 249–259.
- HEXEM, R. W. & HEADY, E. O. 1978 *Water production functions for irrigated agriculture*. Ames - Io.: The Iowa State University Press, Roger W. Hexem, Earl Orel Heady.
- HILLEL, D. 1994 *Rivers of Eden the struggle for water and the quest for peace in the Middle East*. New York [etc.]: Oxford University Press.
- KOUNDOURI, P. 2004 Potential for groundwater management: Gisser-sanchez effect reconsidered. *Water Resources Research* **Vol. 40** (6).
- KRIAA, S. 2003 Contribution à l'étude de la qualité des eaux de la nappe du Complexe Terminal dans la Nefzaoua. Master's thesis, ENIT, Tunis.

-
- KRUGMAN, P. R. 1996 *The Self-Organizing Economy*. Cambridge, MA [etc.]: Blackwell Publishers.
- KRUSMAN, G. P. 1997 *Recharge of phreatic aquifers in (semi-) arid areas*, chap. Recharge from intermittent flow, pp. 145–184. Balkema A.A / Rotterdam Publ.
- LEE, K. C., SHORT, C. & HEADY, E. O. 1981 Optimal groundwater mining in the Ogallala aquifer - estimation of economic-loss and excessive depletion due to commonality. *American Journal of Agricultural Economics* **63** (5), 1039–1039.
- MAMOU, A. 1990 Caractéristiques et évaluation des ressources en eau du sud Tunisien. PhD thesis, Université de Paris-Sud, Centre DOrsay.
- MAMOU, A. & HLAIMI, A. 1999 Les nappes phréatiques de la nefzaoua. caractéristiques et exploitation. *Tech. Rep.*. Rep. Min. Agr. / DGRE, Tunis, general Direction of Water Resources, Ministry of Agriculture.
- MATHWORKSINC. 2003a *Optimization Toolbox Version 2.3*. Natick, MA.
- MATHWORKSINC. 2003b *Statistics Toolbox Version 4.1*. Natick, MA.
- MCKINNEY, D. C. & LIN, M. D. 1994 Genetic algorithm solution of groundwater-management models. *Water Resources Research* **30** (6), 1897–1906.
- MECKELEIN, W. E. 1977 Geographische Untersuchungen am Nordrand der tunesischen Sahara. *Stuttgarter Geographische Schriften* **91** (1), 247–301, wissenschaftliche Ergebnisse der Arbeitsexkursion 1975 des Geographischen Instituts der Universität Stuttgart.
- MEDDEB, M.-F. 2003 Field investigation in the sustainable production of the Nezfauoa Oases. Master's thesis, Chalmers University of Technology, Göteborg.
- MEEUSEN, V. D. B. J. 1977 Efficiency estimation from Cobb-Douglas production functions with composed error. *International Economic review* **18**, 435–444.
- MEYBECK, M. & SYSTEM, G. E. M. 1989 *Global freshwater quality a first assessment*. Oxford [etc.]: Blackwell Reference, ed. by Michel Meybeck, Deborah V. Chapman, Richard Helmer, Published on behalf of the World Health Organization and the United Nations Environment Programme. First published in USA 1990.
- NAIR, A., NAVADA, S., KULKARNI, K., KULKARNI, U. & JOSPEH, T. 2001 Environmental isotope studies in the arid regions of western Rajasthan, India. *Tech. Rep.* IAEA-TECDOC-1207. IAEA, Isotope Techniques in Water Resource Investigations in Arid and Semi-Arid Regions.
- NEGRI, D. H. 1989 The common property aquifer as a differential game. *Water Resources Research* **25** (1), 9–15.

- NEUMANN, J. v. & MORGENSTERN, O. 1966 *Theory of games and economic behavior*, [third , ninth printing] edn. Princeton: Princeton University Press.
- NIESWIADOMY, M. 1985 The demand for irrigation water in the High-Plains of Texas, 1957-80. *American Journal of Agricultural Economics* **67** (3), 619–626.
- NOEL, J. E., GARDNER, B. D. & MOORE, C. V. 1980 Optimal regional conjunctive water management. *American Journal of Agricultural Economics* **62** (3), 489–498.
- OSS 2003 The north western sahara aquifer system: Joint management of a trans-border basin. *Tech. Rep.*. Observatoire du Sahara et du Sahel, Tunis.
- PALLAS, P. & SALEM, O. 2000 Regional aquifer systems in arid zones – managing non-renewable resources. Paris: UNESCO, water Resources Utilization and Management of the Socialist People Arab Jamahiriya.
- PÉRENNÈS, J.-J. 1993 *L'eau et les hommes au Maghreb*. Paris: Editions Karthala, contribution à une politique de l'eau en Méditerranée.
- POSTEL, S. 1999 *Der Kampf ums Wasser die Chancen einer bedarfsorientierten Verteilungspolitik*. Schwalbach/Ts.: Wochenschau Verlag.
- POUGET, M. 1966 Etude pédologique des oasis de la PIK et du groupe Mansoura. *Tech. Rep.*. Rep. Min. Agr. / DGRE, Tunis, general Direction of Water Resources, Ministry of Agriculture.
- PRICKETT, T. A. & LONNQUIST, C. 1971 Selected digital computer techniques for groundwater resource evaluation. *Tech. Rep.*. Urbana, Bulletin 55.
- PROVENCHER, B. & BURT, O. 1993 The externalities associated with the common property exploitation of groundwater. *Journal of Environmental Economics and Management* **24** (1), 139–158.
- PURI, S., APPELGREN, B., ARNOLD, G., AURELI, A., BURCHI, S., BURKE, J., MARGAT, J. & PALLAS, P. 2000 Internationally shared (transboundary) aquifer resources management. *Tech. Rep.*. UNESCO, International Hydrological Programme.
- ROGERS, L. L. & DOWLA, F. U. 1994 Optimization of groundwater remediation using artificial neural networks with parallel solute transport modeling. *Water Resources Research* **30** (2), 457–481.
- RUBIO, S. & CASINO, B. 2003 Strategic behaviour and efficiency in the common property extraction of groundwater. *Environmental and Resource Economics* **26** (1), 73–87.

-
- SAHARA AND SAHEL OBSERVATORY 2000 Système aquifère du sahara septentrional. *Tech. Rep.*. Observatoire du Sahara et du Sahel, Tunis, analyse Globale des Données Hydrogéologiques du SASS.
- SAHARA AND SAHEL OBSERVATORY 2001 Acquisition, organization and analysis of the SASS hydrological data. *Tech. Rep.*. Observatoire du Sahara et du Sahel, Tunis.
- SAHARA AND SAHEL OBSERVATORY 2002 SASS: Modèle mathématique. *Tech. Rep.*. Observatoire du Sahara et du Sahel, Tunis.
- SALEM, O. 1996 Groundwater legislation in Libya. *Tech. Rep.*. General Water Authority, Tripolis.
- SAMPAT, P. & PETERSON, J. A. 2000 *Deep trouble: The hidden threat of groundwater pollution*. Washington: Worldwatch Institute, Payal Sampat ; Jane Peterson ed.
- SCHLIEPHAKE, K. 1995 Water - a scarce resource in Libya. An analysis of the situation from a geographical and economic standpoint. *Natural Resources and Development* **49/50**, 128–140.
- STIGLITZ, J. 1974 Growth with exhaustible natural resources: The competitive economy. *Review of Economic Studies* (41), 123–138, symposium on the Economics of Exhaustible Resources.
- TSUR, Y. & ZEMEL, A. 1995 Uncertainty and irreversibility in groundwater resource-management. *Journal of Environmental Economics and Management* **29** (2), 149–161.
- UNESCO 1972 Etude des Ressources en Eau du Sahara Septentrional. *Tech. Rep.*. Paris, rapport sur les résultats du Project, Conclusions et Recommandations; Appendices.
- UNITED NATIONS 1960 Large scale groundwater development. *Tech. Rep.*. United Nations, Water Resources Development Center, United Nations, New York.
- UNITED NATIONS 1977 Report on the united nations water conference, Mar del Plata 1977. *Tech. Rep.*. United Nations.
- US FEDERAL RESEARCH DIVISION, L. O. C. 1986 *Libya, A Country Study*. Library of Congress Publications.
- US FEDERAL RESEARCH DIVISION, LIBRARY OF CONGRESS 1993 *Algeria, A Country Study*. Library of Congress Publications.
- USGS 2001 Gtopo30 Global Digital Elevation Model. Website, uS Geological Survey, Land Processes Distributed Activity Archive Center.

- WANG, M. & ZHENG, C. 1997 Optimal remediation policy selection under general conditions. *Ground Water* **35** (5), 757–764.
- WANG, W. & AHLFELD, D. P. 1994 Optimal groundwater remediation with well location as a decision variable - model development. *Water Resources Research* **30** (5), 1605–1618.
- WORLD BANK 1998 Groundwater in urban development: Assessing management needs and formulating policy strategies. *Tech. Rep.* 390. World Bank, Washington, DC.
- WORLD BANK 1999 Groundwater in rural development: Facing the challenges of supply and resource sustainability. *Tech. Rep.* 463. World Bank, Washington, DC.
- WORLD BANK 2002 *World Development Indicators*. Development Data Center, The World Bank.
- WORTHINGTON, V. E., BURT, O. R. & BRUSTKERN, R. L. 1985 Optimal management of a confined groundwater system. *Journal of Environmental Economics and Management* **12** (3), 229–245.
- WRIGHT, A. 1991 *Foundations of genetic algorithms*, , vol. 1, chap. Genetic Algorithms for Real Parameter Optimization, pp. 205–218. San Mateo, California: Morgan Kaufmann Publishers.
- ZHENG, C. & BENNETT, G. D. 2002 *Applied contaminant transport modeling*, 2nd edn. New York: Wiley, Chunmiao Zheng, Gordon D. Bennett.
- ZITZLER, E. 1999 Evolutionary algorithms for multiobjective optimization: Methods and applications. PhD thesis, Swiss Federal Institute of Technology, Zurich, TIK-Schriftenreihe, NR. 30.
- ZITZLER, E. 2001 SPEA2: Improving the strength pareto evolutionary algorithm. TIK Report 103. Swiss Federal Institute of Technology, Zurich.
- ZITZLER, E., LAUMANN, M. & THIELE, L. 2002 SPEA2: Improving the strength pareto evolutionary algorithm for multiobjective optimization. In *Evolutionary Methods for Design, Optimization and Control* (ed. K. Giannakoglou, D. Tsahalis, J. Periaux, K. Papailiou & T. Fogarty). CIMNE, Barcelona, Spain.

Curriculum vitae

Name	Tobias Ulrich Siegfried
Date of Birth	16.09.1970
Place of Birth	Aarau
Nationality	Swiss

Education

- 1976 - 1985: Primary and secondary level education
- 1985 - 1990: Senior Grade in Natural Sciences; Kantonsschule Zürcher Unterland, Bülach
- 1992 - 1997: Environmental Sciences, Swiss Federal Institute of Technology, Zürich; *Diplomierter Naturwissenschaftler ETH*
- 1998 - 1999: Theory and History of International Relations, London School of Economics, LSE, London; *Master of Science*

Scholarships and Awards

- 1989: Swiss Winner of a European Space Agency competition on occasion of the 25th Birthday of the agency
- 1998: ETH-Award and Medal for an outstanding diploma thesis
- 1998: Scholarship *Emil Boral-Stiftung für Postgraduierte aus Oesterreich und der Schweiz*

Work Experience

- 1994: Database development on PC Systems
- 1993–1996: Network assistant, Department of Environmental Sciences, ETH Zürich
- 1995–1996: Environmental assessment report in the Lake Ohrid area on behalf of the World Bank, Ernst Basler+Partner, Zürich
- 1996: Quantification and consequences of nitrate pollution in Switzerland, Ernst Basler+Partner, Zürich
- 2002: Groundwater Modeling Expert, Addis Ababa Water Supply Project, Stage III A Groundwater Phase II, Addis Ababa Water and Sewerage Authority, Federal Democratic Republic of Ethiopia

Publications

Journal Papers

- Zammouri, M., Siegfried, T., El Fahem, T., Kriaa, S., Kinzelbach, W., *Salination of Groundwater in the Nefzawa Oases (Tunisia): Results of a Regional-Scale Hydrogeologic Approach*, Journal of Hydrology, submitted
- Kinzelbach, W., Bauer, P., Siegfried, T. And Brunner, P., *Sustainable Groundwater Management Problems and Scientific Tools*, Episodes, Vol. 26, No. 4, December 2003
- Kunstmann H., Kinzelbach W., Siegfried T., *Conditional first-order second-moment method and its application to the quantification of uncertainty in groundwater modeling*, Water Resources Research, Vol. 38, No. 4, 2002
- Schlöpfer D., Siegfried T., *The Lake Ohrid Conservation Project*, World Water and Environmental Engineering, April 1996
- Siegfried T., Benz R., Wachter G., *Astronomie im Weltraum*, Orion, 48. Jahrgang, Nr. 237, April 1990

Congress Papers

- Siegfried T., Kinzelbach W., *Management of Internationally Shared Groundwater Resources in Semiarid and Arid Regions The Northern African Aquifer System*, In: Hydrology of Mediterranean and Semiarid Regions, IAHS Publication, no. 278, 2002
- Kinzelbach, W., P. Bauer, T. Siegfried, P. Brunner, *Sustainable water management in arid environments*, In: Research Basins and Hydrological Planning. Proceedings of an international conference. Hefei, China, Xi, Gu and Seiler (eds), Taylor&Francis Group, London, p. 27-34

Reports

- Siegfried T., Schubert R., *Umweltorientierte Entwicklungspolitik*, Centre for Economic Research, Swiss Federal Institute of Technology, Zürich, August 1995
- Siegfried, T. and W.Kinzelbach, *Modeling of Groundwater Withdrawal and its Consequences to the Aquifer, A Case Study in Semi-Arid Botswana*, Report Inst. of Hydromechanics and Water Res. Management, Swiss Federal Institute of Technology, Zürich, 1997
- Siegfried T., Mock R., *Fuzzifizierung von Schadensindikatoren*, Inst. for Energy Technology, Swiss Federal Institute of Technology, Zürich, 1997

Varia

- Siegfried, T., *Die Wüste wächst*, Gegenworte, Zeitschrift für den Disput ber Wissen, Berlin-Brandenburgische Akademie der Wissenschaften (Hrsg.), 10. Heft, Herbst 2002
- Kinzelbach W., Bauer P., Siegfried T. und Brunner P., *Nachhaltige Grundwasserwirtschaft Probleme und wissenschaftliche Werkzeuge*, Österreichische Wasser- und Abfallwirtschaft, Heft 3/4, März/April 2003, Springer Verlag
- Siegfried T., *Knappe Ressource im Nördlichen Afrika*, Bulletin ETH Zürich, Nr. 289, Mai 2003

- Kinzelbach W., Bauer P. & Siegfried T., *Nachhaltige Wasserwirtschaft in ariden und semi-ariden Regionen*, Warnsignal Klima: Genug Wasser für alle?, Wissenschaftliche Auswertungen, J. L. Lozán et al. (Hrsg.), Hamburg 2004